DEVELOPMENT OF A NEURAL NETWORKS MODEL TO PREDICT THE DIAUXIC LAG LENGTH

By

SANGEETHA SHEKAR

A THESIS PRESENTED TO THE GRADUATE SCHOOL
OF THE UNIVERSITY OF FLORIDA IN PARTIAL FULFILLMENT
OF THE REQUIREMENTS FOR THE DEGREE OF
MASTER OF SCIENCE

UNIVERSITY OF FLORIDA

2001

Dedicated to my Mother and Prashant

ACKNOWLEDGMENTS

I would like to thank my committee members- Professors Spyros A. Svoronos, Ben Koopman, and Thomas E. Bullock-for their academic advisement and guidance on this project.

A special thanks go to my co-advisors and fellow “diauxiers”- Professors Spyros A. Svoronos, Professor Ben Koopman, Keisha Lisbon, Micheal McKean, Anna Casasus Zambrana, and Seung-Yeon Weon-for their help, support, and willingness to discuss their ideas.

I would like to thank the Chemical Engineering Department for the financial support through my course of study.

Finally I would like to thank my mother, Prashant, sister and all my friends for their love, support, and prayers without which it would have been impossible for me to complete this thesis.

TABLE OF CONTENTS

page

Abstract of Thesis Presented to the Graduate School
of the University of Florida in Partial Fulfillment of the
Requirements for the Degree of Master of Science

DEVELOPMENT OF A NEURAL NETWORKS MODEL TO PREDICT THE DIAUXIC LAG LENGTH

By

Sangeetha Shekar

December 2001

Chairman: Dr. Spyros A. Svoronos
Major Department: Chemical Engineering

In wastewater treatment plants nitrogen is removed by passing the wastewater alternatively from aerobic zones to anoxic zones. Nitrification takes place in the aerobic zone and denitrification in the anoxic zone. A diauxic lag might occur when following the switch from oxygen to nitrate as the terminal electron acceptor. The present research attempts to use a neural network in place of the traditional models to predict the duration of the diauxic lag under a given set of conditions.

Experimental data gathered from studies with the culture *Pseudomonas denitrificans* (ATCC 13867) was classified based on dissolved oxygen concentrations in the aerobic phase and the reviving phase of the culture. One neural network was trained to predict the duration of the diauxic lag for experiments with an anoxic reviving phase and low dissolved oxygen concentrations in the aerobic phase. The inputs to this network were initial biomass concentration, dissolved oxygen concentration in the aerobic phase and the length of the aerobic phase in hours. A second neural network was trained to

predict the lag length for experiments where dissolved oxygen concentration was maintained at air saturation in the aerobic phase with the reviving phase (oxic/anoxic) of the culture, initial biomass concentration, length of the aerobic phase in hours and nitrate concentrations in the aeration phase as the input variables. An interleaved simulated annealing and conjugate gradient search algorithm was used to train the networks. The predicted lag length from the networks was compared to the actual experimental data and found to be within reasonable limits of accuracy.

CHAPTER 1
INTRODUCTION

Biological removal of nitrogen has become a common practice in many wastewater treatment facilities ever since the harmful effects of excess levels of nitrogen have been known. This has led to focused research on processes that remove nitrogen from wastewater in an efficient and economical manner. In a typical suspended growth biological nitrogen removal system, activated sludge passes through cycles of aerobic and anoxic zones where nitrification and denitrification are achieved respectively. Ammonium is oxidized to nitrate in nitrification and nitrate is reduced to nitrogen gas through several steps in denitrification.

Monod (1942) first described the phenomenon of diauxic lag that can occur when bacteria switch between electron donors (carbon substrates). Diauxie is characterized by a double growth cycle consisting of two exponential phases separated by a phase in which the growth rate is very low or zero. The lag corresponds to the time necessary for bacteria to synthesize and activate the enzymes necessary to metabolize the less preferred substrate (Monod 1942; 1949). Kodama et al. (1969) observed diauxic growth when *Pseudomonas stutzeri* switched from nitrate to nitrite as terminal electron acceptor.

Diauxic lag caused by changing between carbon sources has been successfully modeled using a cybernetic model (Komapala et al. 1986). "Industry Standard" IAWQ Activated Sludge Models No. 1 and 2 (Henze et al., 1987; 1995) do not account for any diauxic lag when bacteria switch between oxygen to nitrate as electron acceptor. Liu et al. (1996) developed a cybernetic model to predict lags for an activated sludge. This model

however could not capture the observed longer lags of a pure culture. A new model accounting for enzyme synthesis and activity in response to culture conditions and enzyme specific levels was then developed (Liu et al. 1998). It could predict length of lags corresponding to the growth pattern.

This manuscript reviews the literature on the models developed to predict diauxic lags and also develops a neural network model to predict the length of the diauxic lag. The neural network was trained with experimental data. The network can successfully predict the lag length in hours as a function of inputs such as biomass in terms of absorbance at time zero, length of aerobic phase in hours, reviving phase of the culture, dissolved oxygen concentrations and nitrate concentrations in the aerobic phase.

CHAPTER 2
LITERATURE REVIEW

Monod first observed the phenomenon of diauxie. Diauxic lag is defined as the phase that separates two exponential growth phases in which the growth rate is very low or zero (Monod, 1942). In diauxic growth the second substrate is not utilized until after the first substrate is exhausted and the enzymes required by the bacteria to utilize the second are not synthesized until then (Monod, 1942). Hamilton and Dawes (1945) also observed the diauxic growth phenomenon in *Pseudomonas aeruginosa* in a medium of glucose and organic acid. They observed that organic acid is preferentially used over glucose. Standing et al. (1972) observed that *E. coli* exhibits a diauxic behavior in a mixture of glucose and xylose. They also observed that when *E. coli* was in an initial medium of glucose and galactose, glucose and galactose were utilized sequentially and there was no lag period between the two exponential growth phases. Therefore, it can no longer be assumed that diauxie is always characterized by a lag period. Sequential utilization of substrates was also observed in *Propionibacterium shermanii* in a mixture of lactate and glucose where lactate was completely consumed before growth on glucose took place (Lee et al., 1974). This pattern of sequential utilization without a lag period is also observed in *Klesbiella pneumoniae* when the nutrient source is switched to xylose from glucose (Baloo and Ramakrishana, 1991). In each case the preferred substrate is the one on which the bacteria grow the fastest. Therefore diauxic growth phenomena may or may not be characterized by a lag period but is directly related to the bacterial preference for consuming the fastest growth supporting substrate (Ramakrishna et al., 1987).

Ramakrishna et al. (1987) and Baloo and Ramakrishna (1991) record the general growth characteristics of bacteria on multiple substrates.

Kodama et al. (1969) were the first to perform experiments of diauxic behavior between different electron acceptors. Their studies showed a biphasic growth pattern of *Pseudomonas stutzeri* between nitrate and nitrite as electron acceptors. The preferred electron acceptor nitrate was fully consumed before any nitrite was consumed. The exponential growth phases were separated by a lag period in which the growth rate was very low. Sequential utilization was also observed by Steinberg et al. (1992) in fresh-water selenate respiring bacteria. In the presence of both nitrate and selenate, nitrate was completely exhausted before selenate consumption began. There was no lag period between growth on nitrate and selenate.

Recently, the phenomena of diauxie when bacteria switch from oxygen to nitrate as electron acceptors was demonstrated for both activated sludge as well as pure culture (Liu et al. 1998a). For the pure culture *Pseudonmonas dentrificans* it was observed that lags up to 7 hours could take place before the second exponential growth phase on nitrate began.

Diauxic lag caused by change in carbon sources has been successfully modeled using a cybernetic model (Kompala et al. 1986). Activated Sludge Models No. 1 and 2 (Henze et al. 1987; 1995) do not account for any diauxic lag when bacteria switch between oxygen to nitrate as electron acceptor. A cybernetic approach was developed (Liu et al. 1996) which incorporated a simplified version Activated Sludge Model No. 1 (Henze et al. 1987). This cybernetic approach was able to predict lags observed with activated sludge.

2.1 Industry Standard Activated Sludge Model

In the "Industry Standard" models for activated sludge (ASM –1, Henze et al., 1987; ASM-2, Henze et al., 1995), the effect of dissolved oxygen on the rate of growth of heterotrophic biomass under anoxic conditions is represented by the term

$$\frac{K_{O,H}}{S_O + K_{O,H}} \tag{2-1}$$

where as the rate of heterotrophic growth under aerobic conditions is controlled by the term

$$\frac{S_O}{S_O + K_{O,H}} \tag{2-2}$$

where S_O is the dissolved oxygen concentration and $K_{O,H}$ the oxygen half-saturation concentration. The former term approaches zero when the dissolved oxygen concentration is high, and approaches 1.0 when dissolved oxygen concentration is low. The latter term has complementary behavior, approaching 1.0 when DO is high and tending towards zero when DO is low. Together, the two terms sum always to 1.0, thus ensuring that the total rate of growth using both electron acceptors does not exceed that which is possible in a highly aerobic environment. This feature, however, prevents either model from accurately portraying the dramatic decrease or even cessation of growth during the diauxie.

An example of a conventional model of heterotrophic growth under aerobic and anoxic conditions when the carbon source is non-limiting is shown in Table 2.1. The model, which is a simplified model of ASM-1, contains process rate expressions for aerobic growth of heterotrophic biomass. The components include active heterotrophic biomass ($X_{B,H}$), dissolved oxygen (S_O), and the sum of nitrate plus nitrogen expressed as equivalent nitrate (S_{NO}) by the following equation

$$S_{NO} = [NO_3 - N] + \frac{(2.857 - 1.143)}{2.857}[NO_2 - N] \quad (2\text{-}3)$$

Table 2.1 Conventional model for heterotrophic growth under aerobic and anoxic conditions

Component ▶	i	1	2	3	
j	Process ▼	S_O	S_{NO}	$X_{B,H}$	Process rate, ρ_j, $ML^{-3}T^{-1}$
1	Aerobic Growth of heterotrophs	$-\frac{1-Y_{H,O}}{Y_{H,O}}$		1	$\hat{\mu}_{H,O}\left(\frac{S_O}{K_{O,H}+S_O}\right)X_{B,H}$
2	Anoxic Growth of heterotrophs		$-\frac{1-Y_{H,NO}}{2.86Y_{H,NO}}$	1	$\hat{\mu}_{H,NO}\left(\frac{K_{O,H}}{K_{O,H}+S_O}\right)\left(\frac{S_{NO}}{K_{NO}+S_{NO}}\right)X_{B,H}$
3	Decay of heterotrophs			-1	$b_H X_{B,H}$
Observed conversion rate, $ML^{-3}T^{-1}$		$r_i = \sum_j \gamma_{ij}\rho_j$			

Neither of the process rate expressions for growth contains a substrate concentration term, nor is the substrate shown as a component. This is because the carbon source (glucose) is not limiting growth.

For the reason explained above this type of model cannot capture the diauxic lag even though it is able to match the growth rates in aerobic and anoxic conditions. Clearly a new modeling approach is required to successfully portray the diauxic lag.

2.2 Cybernetic Model

Cybernetic modeling (Ramakrishna, 1982; Ramakrishna et al., 1984; Komapala et al., 1986; Straight and Ramakrishna, 1991; Straight and Ramakrishna, 1994; Ramakrishna et al., 1995) has been successful in portraying the diauxic lag observed when the bacteria switch between electron donors. It is based on the premise that bacteria are optimal strategists (Ramakrishna et al., 1987) and that they regulate enzyme synthesis and activity so to maximize their specific growth rate. In the cybernetic model (Liu et al. 1998a), the kinetic expressions of Table 2.1 are modified in a manner analogous to the modifications of Monod kinetic expressions by Kompala et al. (1986).

The diauxic lag is attributed to the fact that appropriate enzymes for alternate electron acceptors must be synthesized. Therefore the Liu et al. (1998a) model adds as components the concentrations of two enzymes, E_O and E_{NO}, to regulate the biomass synthesis in the presence of oxygen and nitrate, respectively. Both the concentrations and activities of these enzymes affect the growth rate of heterotrophic biomass. If e_k denotes the specific level of an enzyme [i.e.. $e_k = E_K/X_{B,H}$ for k=O (oxygen) or NO (equivalent nitrate)] and v_k denotes the relative activity (ranging from 0 to 1) of the respective enzymes, then the effects of enzyme level and activity on biomass growth rate can be expressed by a Monod growth rate expression by the factor $v_k e_k/e_{k,max}$, where $e_{k,max}$ is the enzyme maximum specific level. This gives the following equation for aerobic and anoxic growth

$$\rho_k = \hat{\mu}_{H,k} \frac{e_k v_k}{e_{k,\max}} \left(\frac{S_k}{K_k + S_K} \right) X_{B,H} \qquad (2\text{-}4)$$

where $K_O=K_{O,H}$.

It is postulated that the synthesis rate of each enzyme can be described by the expression

$$\alpha_k u_k \left(\frac{S_k}{K_k + S_k} \right) X_{B,H} \tag{2-5}$$

in which the maximum specific synthesis rate depends on a "cybernetic variable" u_k (ranging from 0 to 1) that controls whether the enzyme is synthesized or not and at what rate, and α_k is a synthesis rate coefficient.

Enzyme decay is assumed to be first order with respect to enzyme concentrations, in a manner analogous to biomass decay; i.e. the decay rate is

$$\beta_k E_k \tag{2-6}$$

In the above formulation the variables u_k and v_k represent the control actions of the cellular regulatory processes of repression-induction and inhibition-activation. In the cybernetic modeling approach it is postulated that the bacteria adjust the values of these variables, as well as of $e_{k,max}$, so as to maximize their instantaneous growth rate. As shown by Komapala et al. (1986), the solution of the optimization problem is

$$u_k = \frac{\rho_k / v_k}{\sum_{k=1} (\rho_k / v_k)} \tag{2-7}$$

$$v_k = \frac{\rho_k / v_k}{\max_k (\rho_k / v_k)} \tag{2-8}$$

$$e_k = \frac{\alpha_k}{\beta_k + \hat{\mu}_{H,k}} \tag{2-9}$$

The complete kinetic model is summarized in Table 2.2. It should be noted that the term $K_{O,H}/(K_{O,H} + S_O)$, which is used in ASM-1 and ASM-2 to switch off growth on nitrate when oxygen is present, is not included, as v_{NO} assumes this function.

To better define the factors that influences the onset and length of diauxic lags as the activated sludge switches from oxygen to nitrate as electron acceptor further refinement of the model was required.

Table 2.2 Process kinetics and stoichiometry of the cybernetic model of Liu et al. (1998a)

Component → i		1	2	3	4	5	
j	Process ↓	S_O	S_{NO}	$X_{B,H}$	E_O	E_{NO}	Process rate, ρ_j, $ML^{-3}T^{-1}$
1	Aerobic growth of heterotrophs	$-\frac{1-Y_{H,O}}{Y_{H,O}}$		1			$\mu_{H,O}\frac{e_o v_o}{e_{o,\max}}\left(\frac{S_O}{K_{O,H}+S_O}\right)X_{B,H}$
2	Anoxic growth of heterotrophs		$-\frac{1-Y_{H,NO}}{2.86Y_{H,NO}}$	1			$\mu_{H,NO}\frac{e_{NO} v_{NO}}{e_{NO,\max}}\left(\frac{S_{NO}}{K_{NO}+S_{NO}}\right)X_{B,H}$
3	Decay of heterotrophs			-1			$b_H X_{B,H}$
4	Synthesis rate of enzyme associated with aerobic growth				1		$\alpha_O\left(\frac{S_O}{K_{O,H}+S_O}\right)X_{B,H}u_O$
5	Synthesis rate of enzyme associated with anoxic growth					1	$\alpha_{NO}\left(\frac{S_{NO}}{K_{NO}+S_{NO}}\right)X_{B,H}u_{NO}$
6	Enzyme decay rate				-1		$\beta_O E_O$
7	Enzyme decay rate					-1	$\beta_{NO} E_{NO}$
Observed conversion rate, $ML^{-3}T^{-1}$		$r_i = \sum_j \gamma_{ij}\rho_j$					

Model Relationships

$$v_i = \frac{\rho_i / v_i}{\max_i (\rho_i / v_i)} \qquad u_i = \frac{\rho_i / v_i}{\sum_{i=1}^{2} (\rho_i / v_i)} \qquad e_i = \frac{E_i}{X_{B,H}} \qquad e_{i,\max} = \frac{\alpha_i}{\mu_{\max,i} + \beta_i}$$

where i = O or NO,
$\rho_O = \rho_1$,
$\rho_{NO} = \rho_2$

2.3 Modeling of Diauxic Lag in Pseudomonas Dentrificans

The model proposed by Liu et al. (1998a) is based on the hypothesis that the diauxic lag occurs due to the lack of enzymes needed for electron acceptor utilization (nitrate reductase in this case). The lag is the period when the enzyme builds up and when it reaches a certain level becomes activated and exponential growth resumes.

Liu et al. revised their cybernetic model (1998b). One modification is that the co-efficients of the enzyme synthesis rates are not constant but an increasing function of enzyme specific level. At low enzyme specific levels, low amount of energy will be available for bio -synthesis. Increasing enzyme level would increase the energy available and thereby the potential enzyme synthesis rate. Furthermore, at higher the enzyme specific levels, more metabolic machinery will be available for utilizing this energy, therefore increasing the efficiency of enzyme synthesis.

The expression for enzyme activity, v_{NO} also differs from the one used in the cybernetic models. It provides for a sharper transition from inactive to active enzyme by utilizing a logistic function $e_{NO}/e_{NO,max}$

$$v_{NO} = \frac{1}{1 + e^{4s\left(r_{c,NO} - \frac{e_{NO}}{e_{No,amx}}\right)}} \tag{2-10}$$

For larger values of the parameter s, v_{NO} is close to zero (inactive enzyme) for ratio $e_{NO}/e_{NO,max} = 0$ and close to one (full activation) for $e_{NO}/e_{NO,max} = 1$. The parameter

$r_{c,NO}$ (critical ratio) sets the value of the ratio for which enzyme activity reaches 50%. The parameter s (sharpness parameter) is the slope of the curve at $e_{NO}/e_{NO,max} = r_{c,NO}$.

Table 2.3 Process kinetics and stoichiometry of the model proposed by Liu et al. (1998b)

Component →	i	1	2	3	4	5	
j	Process ↓	S_O	S_{NO}	$X_{B,H}$	E_O	E_{NO}	Process rate, ρ_j, $ML^{-3}T^{-1}$
1	Aerobic growth	$-\frac{1-Y_{H,O}}{Y_{H,O}}$		1			$\mu_{H,O}\frac{e_o v_o}{e_{o,\max}}\left(\frac{S_O}{K_{O,H}+S_O}\right)X_B$
2	Anoxic growth		$-\frac{1-Y_{H,NO}}{2.86Y_{H,NO}}$	1			$\mu_{H,NO}\frac{e_{NO}v_{NO}}{e_{NO,\max}}\left(\frac{S_{NO}}{K_{NO}+S_{NO}}\right)X_B$
3	Decay			-1			$b_H X_B$
4	Synthesis rate of enzyme associated with aerobic growth				1		$\left[\alpha_{O,1}+\alpha_{O,2}\frac{e_O}{e_{O,\max}}\right]\left(\frac{S_O}{K_{O,H}+S_O}\right)X_B u_O$
5	Synthesis rate of enzyme associated with anoxic growth					1	$\left[\alpha_{NO,1}+\alpha_{NO,2}\frac{e_{NO}}{e_{NO,\max}}\right]\left(\frac{S_{NO}}{K_{NO}+S_{NO}}\right)X_B u_{NO}$
6	Enzyme decay rate				-1		$\beta_O E_O$
7	Enzyme decay rate					-1	$\beta_{NO} E_{NO}$
Observed conversion rate, $ML^{-3}T^{-1}$		$r_i = \sum_j \gamma_{ij}\rho_j$					

Model Relationships

$$v_i = \frac{1}{1+e^{4s\left(r_{c,i}-\frac{e_i}{e_{i,\max}}\right)}} \qquad u_i = \frac{\rho_i/v_i}{\sum_{i=1}^{2}(\rho_i/v_i)} \qquad e_i = \frac{E_i}{X_B} \qquad e_{i,\max} = \frac{\alpha_{i,1}+\alpha_{i,2}}{\mu_{\max,i}+\beta_i - b_H}$$

where i = O or NO,
$\rho_O=\rho_1$,
$\rho_{NO}=\rho_2$

The revised kinetic model is presented in Table 2.3. Different yield coefficients are used for aerobic and anoxic growth.

The above mechanistic model could fit quite well the experimental data of Liu et al. (1998a, 1998b), in which all aerobic growths were with high dissolved oxygen concentrations (near saturation). However, it was considerably less successful in fitting more recent experimental data obtained in our lab, in which diauxic growth with low dissolved oxygen concentrations were investigated.

2.4 Hybrid Models

Neural network models were introduced into the activated sludge modeling by Liu et al. (1995). Liu et al. (1995) combined a material balance model with artificial neural networks for the reaction rates. The inputs were the standard inputs of ASM-1. This model performed very well with simulated data but poorly with experimental data. Clearly some important inputs to the neural network were missing. Zhao et al. (1999) used a simplified version of the Activated Sludge Model No. 2 (SPM) and neural networks to model accurately the process dynamics of nitrogen and phosphorous (nutrients) in a sequencing batch reactor (SBR). The SPM provided a preliminary prediction of the process behavior based on a smaller set of inputs such as measurements of influent ammonia and phosphate, COD, and timer control signals. The neural network was fed with the above inputs and additional parameters that could influence the process. The network was trained to predict the difference between the actual process output data and SPM predictions. In order words the network learned to bias the SPM. It was found that the above hybrid model was more suitable for on-line prediction and control than the SPM model. The hybrid model for anaerobic wastewater treatment systems developed by

Kamara et al. (2000) combines a feed forward network, describing bacterial kinetics and a priori knowledge based on the mass balances of the process components. The model's architecture consists of a static model of unmeasured process parameters (kinetic growth rate) integrated with a dynamic representation of the process, using a set of dynamic differential equations. The performance of this approach was evaluated using experimental data. Tay and Zhang (1999) developed a conceptual adaptive model for anaerobic wastewater systems using advanced neural fuzzy systems in place of the conventional kinetic models. The conceptual neural fuzzy model had the robustness of fuzzy systems, the learning ability of neural networks and could adapt to various situations. The conceptual model was used to simulate the daily performance of two high-rate anaerobic wastewater treatment systems. Häck and Köhne (1999) tried to devise a new method to estimate wastewater process parameters (e.g. COD) based on on-line measurements of auxiliary parameters. They used neural networks to enable detection of non-linear static/dynamic correlation between the auxiliary and process parameters based on measured values of the auxiliary parameters. The network was trained using experimental data.

Among the entire set of hybrid or neural network models that have been developed so far, none of the models can predict the diauxic growth pattern.

CHAPTER 3
PURPOSE

The purpose of this study is to develop a neural network model that predicts the length of the diauxic lag when bacterial cultures switch electron acceptors (oxygen to nitrate) in a synthetic wastewater medium. In a previous study performed by Liu et al. (1996) it was shown that diauxic lags occur between aerobic growth and anoxic growth in a nitrification- denitrification system. The diauxic lag is generally attributed to time required to synthesize and activate inducible enzymes for utilizing alternate electron acceptors. The model proposed by Liu et al (1998a, 1998b) suggests that there is a decrease in enzyme specific levels under aerobic conditions. In experiments in which *Pseudomonas denitrificans* was revived from agar plates and then grown in batch reactors first under aerobic conditions and then under anoxic conditions it was observed that the length of the lag depends on the concentrations of nitrate it was exposed to both in the reviving phase and the aerobic phase. The length of the lag is also observed to increase with increase in length of time of the aerobic phase. Also experimental studies showed that bacterial cultures under lower dissolved oxygen concentrations during the aerobic phase have a shorter diauxic lag in comparison to cultures at air saturation during the aerobic phase. The explanation is that lower dissolved oxygen should have a less inhibitory effect on the denitrifying enzymes hence shortening the length of the diauxic lag.

The present research makes an attempt to use a neural network in place of the traditional model to predict the duration of the diauxic lag under a given set of conditions. The aerobic and anoxic phase growth curves can be captured by the traditional Monod (1942) expressions. If these were integrated with a neural network for predicting the lag the resulting hybrid model should be able to describe the complete diauxic growth.

The experimental data was categorized based on the reviving phase (aerobic/anoxic) and dissolved oxygen concentrations. The neural network was first trained with experimental data for which the reviving phase was always anoxic and concentrations of nitrate were very low (almost zero) in the aerobic phase. In this case the inputs to the neural network were biomass concentration in terms of absorbance at the start of the experiment, dissolved oxygen concentrations through the aerobic phase and the duration of the aerobic phase in hours. The neural network had only one output node, that being the time in hours of the diauxic lag. There was a single hidden layer of neurons and the number of nodes in the hidden layer was varied and the performance was compared. The network architecture that gave the lowest root mean squared error was chosen and the corresponding weights saved. The neural network was then tested with experimental data different from the training data and the results compared with the desired output. A second neural network was trained with additional inputs such as the status of the reviving phase of the culture and the varying concentrations of nitrate in the aerobic phase. In this case the dissolved oxygen concentration was maintained at 8.7 mg/L. The network was then tested and the predicted diauxic lag length from the neural network compared to the actual experimental results.

Efforts were also made to devise a standard nitrate reductase enzyme assay for *Pseudomonas denitrificans*. Cultures of *Pseudomonas denitrificans* (ATCC 13867) were pre-cultured in both aerobic and anoxic environments. This would provide cases of both absence and presence of denitrifying enzymes when the cultures were introduced into the bioreactor. The reactor was always held at air saturation (8.7 mg/L) in the aerobic phase, which typically lasted 2-3 hours. Samples for the enzyme assay were withdrawn from the bioreactor at different points in the entire experiment and stored on ice. The samples were then assayed and the enzyme activities recorded.

CHAPTER 4
EXPERIMENTAL METHODS AND RESULTS

Three kinds of experiments performed through the course of this study: High biomass experiments to measure the activities of enzyme, growth experiments to study the effect of dissolved oxygen, on the diauxic lag and growth experiments to study the effect of reviving phase on the length of the diauxic lag.

4.1 Nitrate Reductase Enzyme Assay

4.1.1 Experimental Methods

The denitrifying bacterium used in this study was *Pseudomonas denitrificans* – ATCC 13867. The freeze-dried bacteria were revived in flasks of 125ml of Nutrient Broth (#0003-17-8) supplied from Sigma Chemical Company. The denitrifying bacteria were placed in a shaker and allowed to grow in the medium for two days. Subsequently, the microbial mixture was transferred, using 10µl sterile inoculating loops, onto tryptic soy agar plates using the streak technique. *Pseudomonas denitrificans* were grown on the agar plates at 35^0C in a Fisher Model Isotemp 303 incubator for two days and stored at 4^0C. Agar plates were kept for two weeks for use in experiments before fresh plates were made. De-ionized water was used for preparing agar and liquid media.

Cultures were grown in synthetic liquid medium modified from (Table 4.1) Kornaros et al. (1996) with or with out without nitrate depending on what kind of preculture conditions were required for that experiment. The pH of the medium was adjusted to 7.0 using 2N NaOH before autoclaving and the addition of nitrate-nitrogen (if

required). Culture medium in 250ml flasks (125 ml liquid volume) was inoculated from agar plates. For *oxic* preculture conditions the flasks were agitated in a shaker bath for two days at approximately 25^{o} C. For a*noxic* preculture conditions, the cultures were grown in a nitrate limited synthetic liquid medium (4mg/L NO_3- N) modified from Table 4.1 and allowed to sit under a sterile laminar hood for two days.

Table 4.1. Composition of the synthetic medium

Chemicals		De-ionized water, g/L
Inorganic Salts	NaCl	1
	NH_4Cl	1
	$MgSO_4.7H_2O$	0.2
	$CaCl_2.7H_2O$	0.0264
	Trace Metals	A drop[a]
Phosphates	K_2HPO_4	5
	KH_2PO_4	1.5
Carbon Source	L-Glutamic Acid	5
Nitrogen Source	KNO_3	28.9

[a]Trace metal solution containing .5% (w/v) each of $CuSO_4$, $FeCl_3$, $MnCl_2$, and $Na_2MoO_4.2H_2O$.

4.1.2 Growth Experiments

A MultiGen bench-top bio-reactor, model F-2000 (New Brunswick Scientific) was used for the experiments. The culture was continuously stirred at 30 ± 2^{0}C. The pH ranged from 7.0 in the aerobic phase and increased to 7.2 during the anoxic phase. Dissolved oxygen was monitored using Model DO-40 (New Brunswick Scientific) analyzers with galvanic electrodes. The experimental setup was as shown in Figure 4.1. Each experiment consisted of an aeration period of 3-5 hours during which the reactor was maintained at air saturation (8.7 mg/L). Aeration was then stopped and reactor was sparged with nitrogen gas to remove any residual dissolved oxygen. Thus followed by a

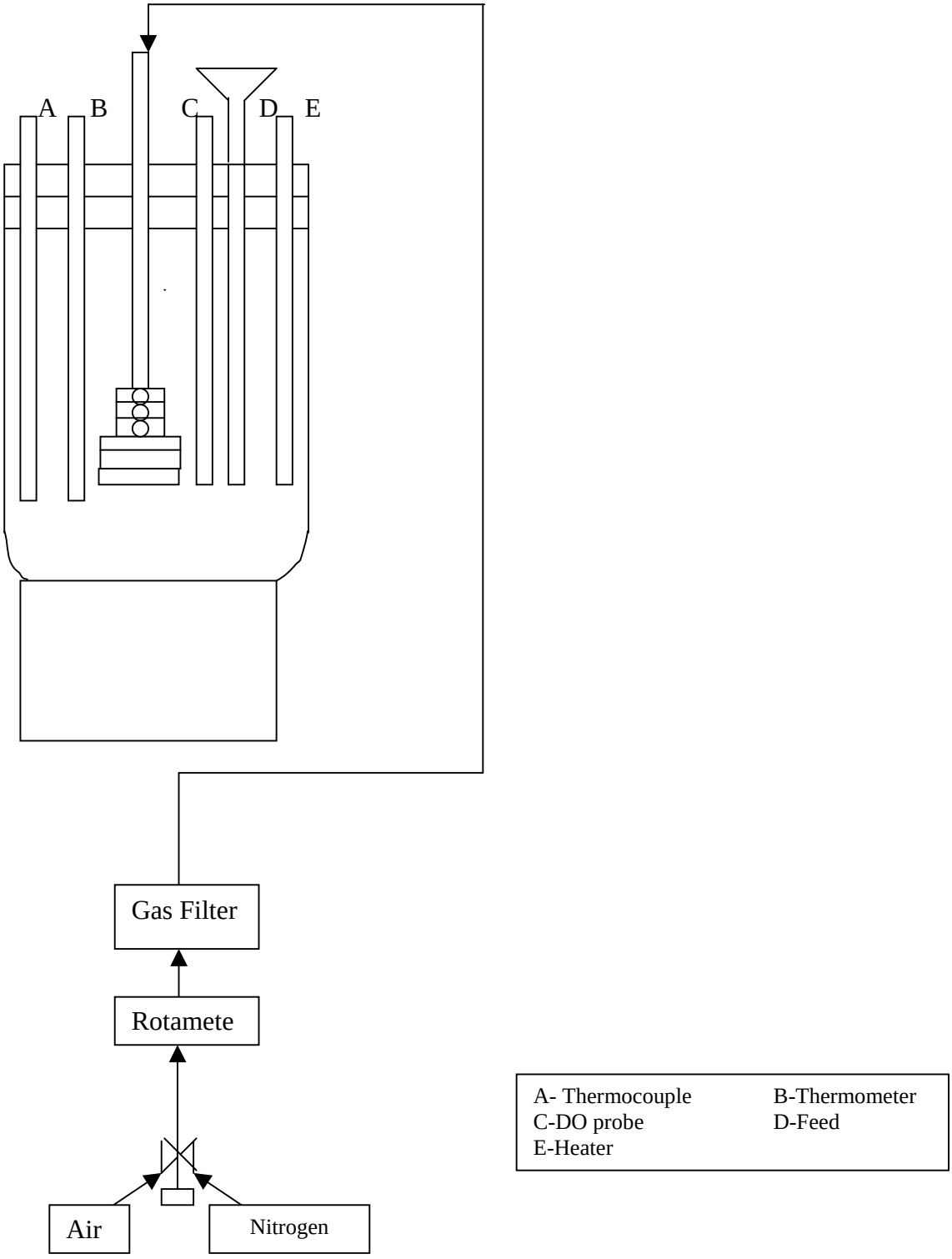

Figure 4.1: Experimental setup for nitrate reductase experiment

period when nitrate was the terminal electron acceptor. Nitrogen gas flooded through the head space of the culture bottle during the period when there was no aeration. The variables monitored include biomass in terms of absorbance, dissolved oxygen, temperature and pH.

4.1.3 Experimental Protocol

Experiments were carried out in order to investigate specific enzyme levels through the course of a diauxic growth. Each experiment consisted of a single reactor with initial biomass concentrations of about 0.3 in terms of absorbance. The first set of experiments was carried out with oxic preculture conditions. Potassium nitrate (400 mg/L) was added to the reactor in the anoxic phase of the experiment. The second set of experiments was carried out under anoxic preculture conditions. Potassium nitrate (400 mg/L) was added to the reactor in the oxic phase of the experiment.

4.1.4 Analytic Methods

Samples were withdrawn from the reactor using a syringe connected to a plastic tube that extended through the cap to the bottom of the reactor. The sample line was flushed several times, then 210 mL was withdrawn. A portion (10 mL) of each sample was used to measure absorbance. Absorbance of the culture was measured using a spectrophotometer (Milton Roy Spectronic 21D) at 550 nm using a 1.25 cm path length. The rest of the withdrawn sample (200 mL) was immediately placed on ice and stored at 0^{o} C. The samples were then analyzed the next day for nitrate reductase enzyme activity. The samples were first degassed for two minutes to create and oxygen free atmosphere, washed with 1M phosphate buffer KPO_4 (pH=7.0) and ice centrifuged at 8000 rpm for 5

minutes at 2 degrees centigrade. The supernatant was drained and 7mL of 1M phosphate buffer KPO_4 (pH=7.0) was added. The bio mass pellet was re-suspended by vortexing and degassed with nitrogen gas for two minutes. The samples were cold centrifuged at 10000 rpm for 5 minutes at 2 degrees centigrade. The supernatant was drained and 1mL of 1M Phosphate buffer KPO_4 (pH=7.0) was added and the biomass pellet re-suspended by vortexing. The sample was then transferred to 1.5 mL tubes and placed in a beaker of ice. Oxygen free conditions were maintained by sparging the container in which the beaker was placed with nitrogen. Each sample was then sonicated for two 15 second periods with an interval of 15 seconds and placed back on the ice bath. A portion of the sample was then pipetted out in a test-tube to which 0.1mL of 50mM $NaNO_3$, 0.03mL of 1M Phosphate buffer KPO_4 (pH = 7.0) buffer, and 0.07 mL of 1mM benzylviologen was added. Next, 0.05ml sodium-diathionide $Na_2S_2O_4^{2-}$ was added and was allowed to react for 30 seconds. The reaction was stopped by vortexing the sample. The nitrite was estimated by adding 0.5 mL - 1 % sulfanilamide in 2.5 N HCl and 0.5mL N-1-Napthylene -diamine dihydrochloride (0.02 % in water) and the sample vortexted. 5mL of deionized water was added the test-tube and vortexed again. The samples were then centrifuged at 3300rpm for 15 minutes. The nitrate reductase activity was measured in terms of absorbance using a spectrophotometer (Milton Roy Spectronic 21D) at 540 nm using a 1.25 cm path length.

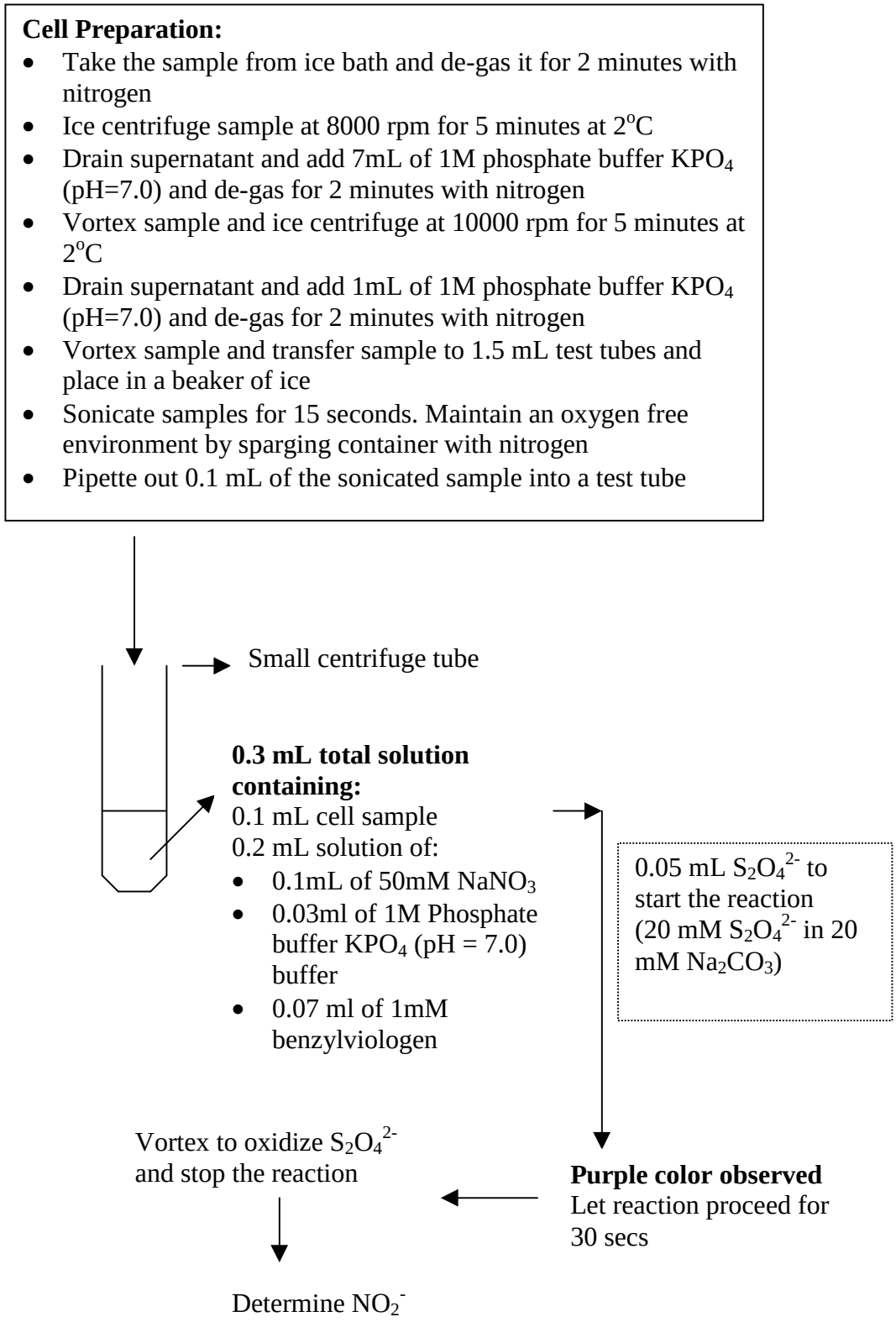

Figure 4.2. Nitrate reductase enzyme procedure

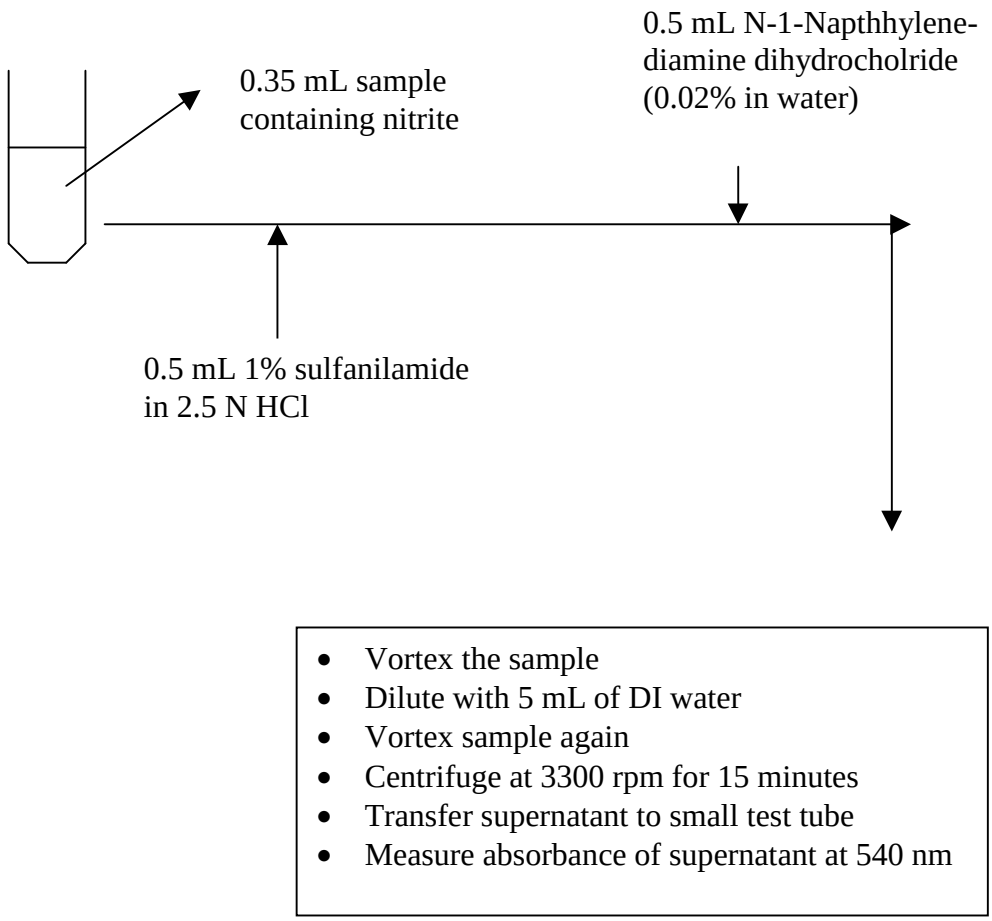

Figure 4.3. Nitrate reductase enzyme procedure (nitrite determination)

4.1.5 Experimental Results

The model proposed by Liu et al. (1998 a, b) attributed the diauxic lag to the low concentrations of nitrate reductase enzyme and in turn activity of the enzyme in the aerobic phase. The shorter lags that occurred when culture had been revived under anoxic conditions and exposed to nitrate in the aerobic phase were attributed to the synthesis of nitrate reductase during the aerobic phase although the enzyme was still inactive. The experimental results (Figure 4.4) of measured enzyme activity versus time when the culture was revived under anoxic conditions and exposed to nitrate in the aerobic phase of the experiment do not agree with the proposed hypothesis. The nitrate reductase enzyme levels were found to increase at a rate faster than biomass and drop after the oxygen supply was turned off. On the other hand, the levels of enzyme activity through an experiment where the culture was revived under oxic preculture conditions and exposed to nitrate only when the oxygen was turned off (Figures 4.5) were found to agree closely with the hypothesis proposed.

The nitrate reductase enzyme assay for *Pseudomonas denitrificans* is far from being standardized. Literature gives us a wealth of information on nitrate reductase assays developed for different strains of bacteria. Krul et al. (1977) devised enzyme assays for nitrate reductase enzyme isolated from several denitrifying bacteria. In their nitrate reductase enzyme assay chloramphenicol was added to stop protein synthesis in the cells just after washing with phosphate buffer and the cells were lysed by first using a French Press at 20,000 psi and then treated with an ultrasonic (MSE) for 2 minutes. They observed that the synthesis of dissimilatory nitrate reductase was only partially repressed by oxygen in some strains of bacteria. However if the oxygen concentration was increased beyond air saturation then significant repression of enzyme synthesis occurred.

Simpkin and Boyle (1988) emphasized the importance of sparging the cell free extracts with nitrogen to create an oxygen free environment and maintained all their samples in a constant temperature water bath. They also preserved the whole cell samples that were withdrawn from the reactor in liquid nitrogen inorder to stop cell activity. They based their conclusions that nitrate reductase synthesis was not repressed fully by oxygen by evaluating the ratio of 'expressed denitrifying enzyme activities' (samples that were sonified and assayed immediately) and 'potential denitrifying enzyme activities' (samples that were in an anoxic environment for a period of three hours, then sonified and assayed). It remains to be investigated if incorporation of these steps to our enzyme assay would give more meaningful results.

4.2 Effects of Dissolved Oxygen Levels

4.2.1 Experimental Methods

Cultures were grown in nitrate limited synthetic liquid medium (4mg/L NO_3- N) modified from (Table 4-1) Kornaros et al. (1996). The pH of the medium was adjusted to 7.0 using 2N NaOH before autoclaving and the addition of nitrate-nitrogen. Culture medium in 250mL flasks (125 mL liquid volume) was inoculated from agar plates (prepared as discussed in section 4.1.1) and allowed to sit under a sterile laminar hood for two days. A procedure termed 'splitting' was then performed on the culture medium. Approximately 250 mL of the culture medium was added to a liter of liquid medium and allowed to mix to prevent flocculation. The culture was then split into two 500 mL volumes, transferred to each bioreactor simultaneously and diluted with liquid medium to an absorbance (λ=550 nm, 1.25 path length) of 0.02- 0.09 for use in experiments.

E-1

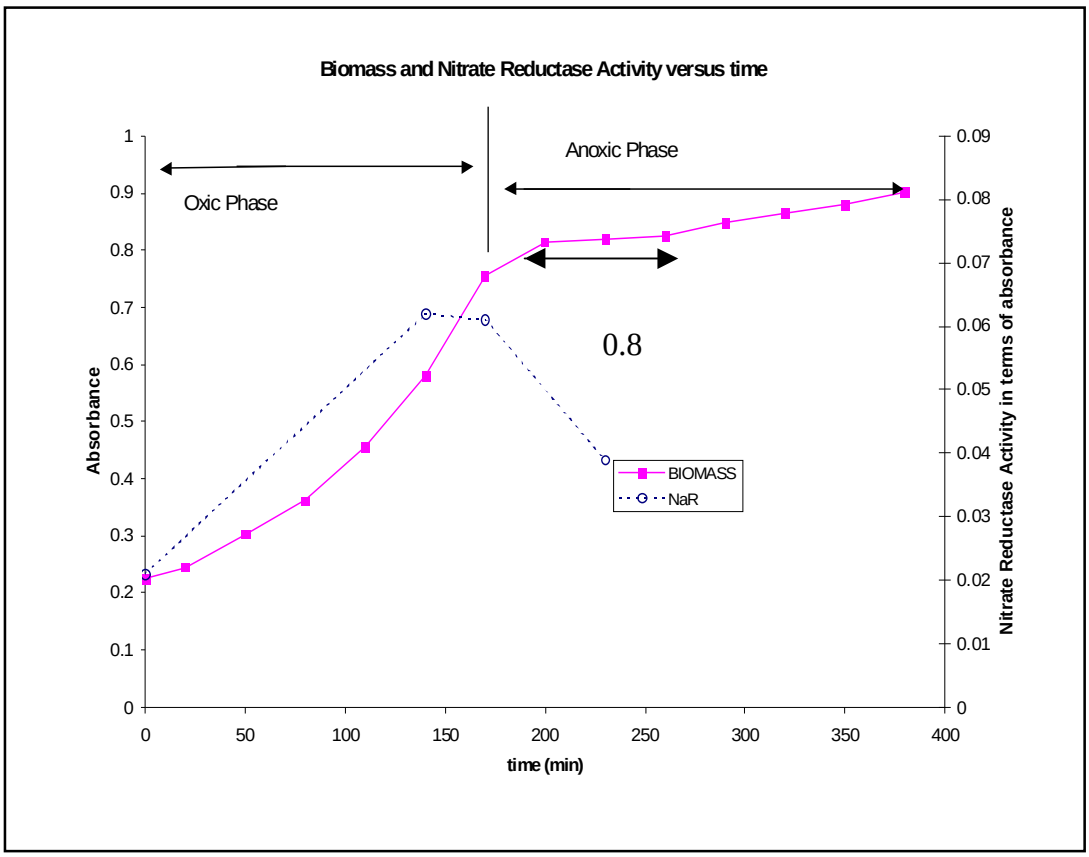

Figure 4.4. Experiment E-1. Experiment with anoxic reviving phase to measure nitrate reductase enzyme activity. Data points show experimental results: biomass and nitrate reductase activity as shown by absorbance

E-2

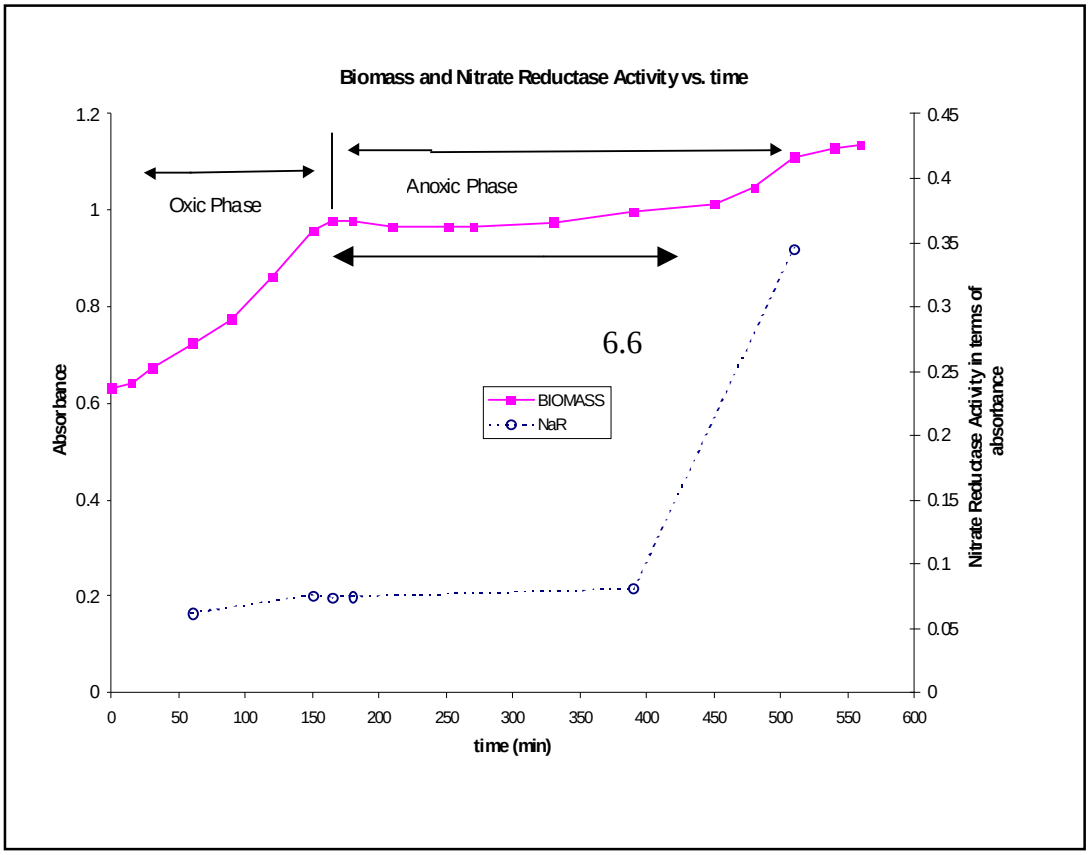

Figure 4.5. Experiment E-2. Experiment with oxic reviving phase to measure nitrate reductase enzyme activity. Data points show experimental results: biomass and nitrate reductase activity as shown by absorbance

E-3

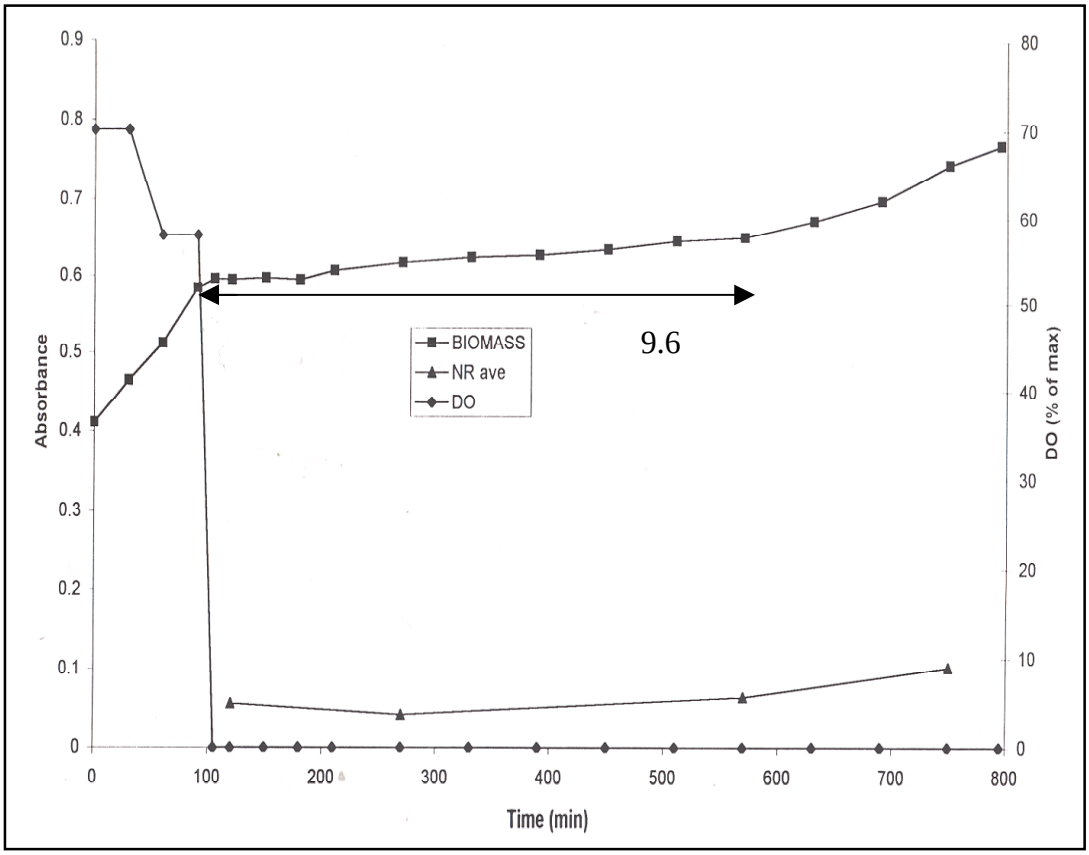

Figure 4.6. Experiment E-3. Experiment with oxic reviving phase to measure nitrate reductase enzyme activity. Data points show experimental results: biomass and nitrate reductase activity as shown by absorbance

E-4

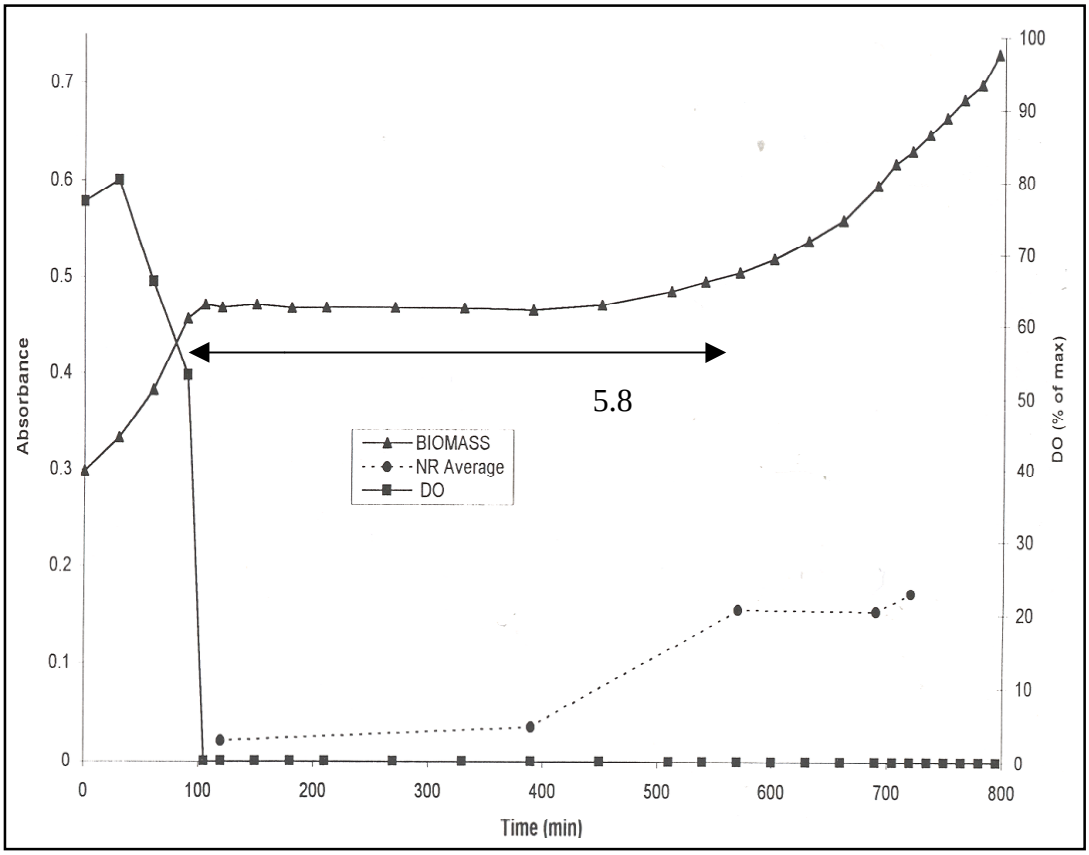

Figure 4.7. Experiment E-4. Experiment with oxic reviving phase to measure nitrate reductase enzyme activity. Data points show experimental results: biomass and nitrate reductase activity as shown by absorbance

E-5

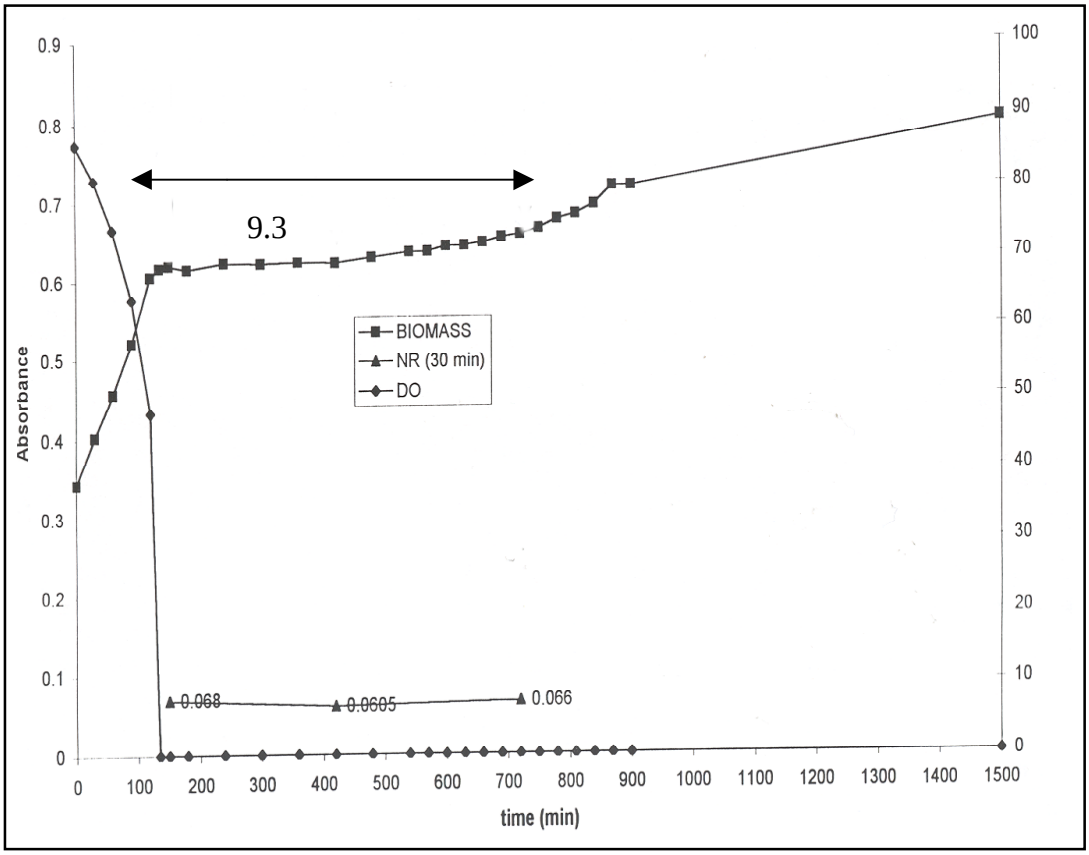

Figure 4.8. Experiment E-5. Experiment with oxic reviving phase to measure nitrate reductase enzyme activity. Data points show experimental results: biomass and nitrate reductase activity as shown by absorbance

E-6

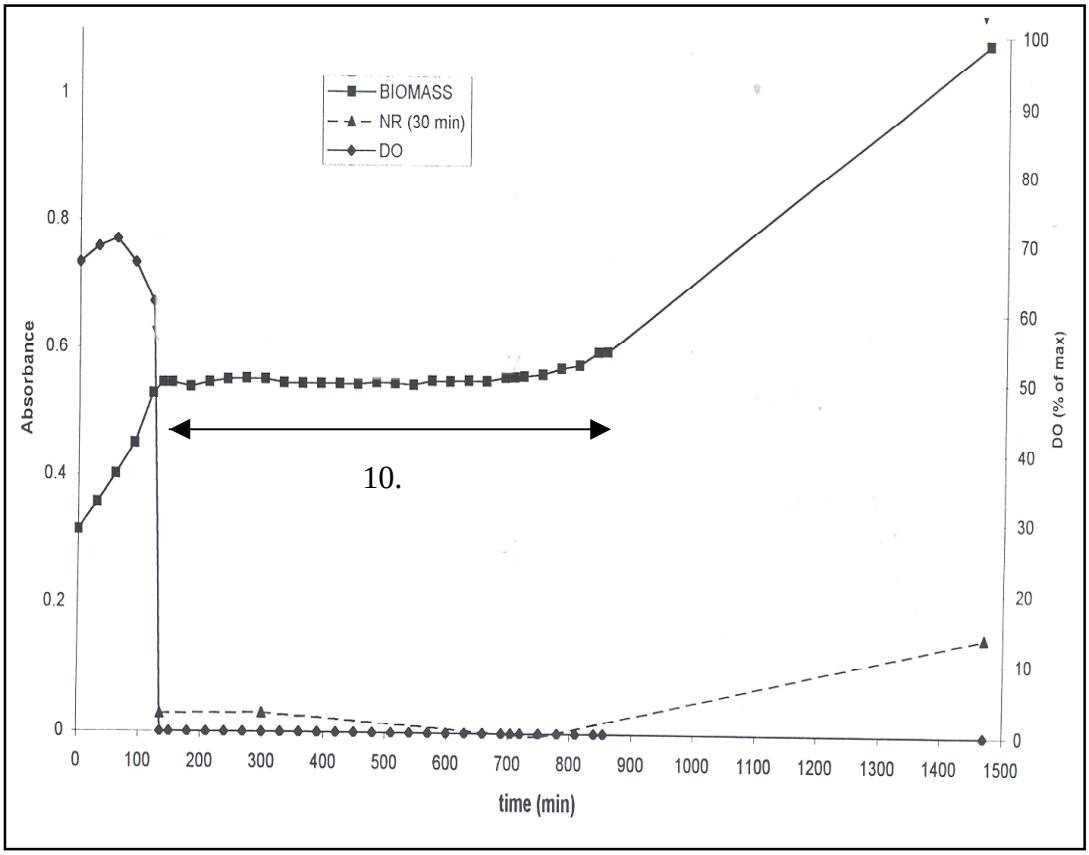

Figure 4.9. Experiment E-6. Experiment with oxic reviving phase to measure nitrate reductase enzyme activity. Data points show experimental results: biomass and nitrate reductase activity as shown by absorbance

4.2.2 Growth Experiments

Two mutiGen bench-top bio-reactors in parallel (models F-1000 and F-2000, New Brunswick Scientific) were used for the experiments. The culture was continuously stirred at 30 ± 2^0C. The pH ranged from 7.0 in the aerobic phase and increased to 7.2 during the anoxic phase. Dissolved oxygen was monitored using Model DO-40 (New Brunswick Scientific) analyzers with galvanic electrodes. The effect of various levels of dissolved oxygen concentration on diauxic lag were compared and contrasted to a high dissolved oxygen concentration of 8.7 mg/L (air saturation). The experimental setup was as shown in Figure 4.10. Each experiment consisted of an aeration period of 3-5 hours during which one reactor was maintained at 100 % air saturation and the other at the respective low DO concentration. To maintain 100% air saturation, a stage dilution was used in which primarily air was fed through a Y-connector, gas filter, and into the bio-reactor. Oxygen was fed into the bioreactor as needed to maintain 100% air saturation. Low dissolved oxygen concentrations (<0.09 mg/L) were maintained by feeding pure nitrogen through a rotameter which mixed with air-nitrogen mixture in which pure air was fed thorough a second rotameter. Low dissolved oxygen concentrations ranging from 0.18 to 0.70 mg/L were achieved by manually controlling the airflow valve on the air tank based on the reading of the DO meter. The dissolved oxygen analyzer, however, could not measure accurately concentrations below 0.15 mg/L. An alternative method was developed to maintain dissolved oxygen control. It was observed that in such low dissolved oxygen experiments the airflow rate correlated closely to the biomass absorbance (K. Lisbon, 2000). The air flow rate was given by the linear equation:

Air Flow Rate = Initial setting + 105.97(Absorbance – Beginning Absorbance).

To begin the anoxic phase, aeration was stopped and reactor was sparged with nitrogen gas to remove any residual dissolved oxygen. 400 mg/L of nitrate-nitrogen was then added to each reactor simultaneously, thus starting a period when nitrate was the terminal electron acceptor. Nitrogen gas flooded through the head-space of the reactors during the period when there was no aeration. The variables monitored included biomass in terms of absorbance, dissolved oxygen, temperature and pH.

4.2.3 Experimental Protocol

Experiments were carried out in order to investigate the effect of various dissolved oxygen concentrations on the duration of diauxic lags. Each experiment consisted of two parallel trials with the same initial culture conditions. To ensure that the parallel cultures had the same initial biomass concentrations, the original cultures was well mixed and divided between the two bioreactors. The first set of set of experiments were carried out a 0.35 mg/L concentration of dissolved oxygen in one bioreactor with dissolved oxygen being maintained over 8.7 mg/L in the other. Potassium nitrate (400 mg/L) was added in the anoxic phase to both reactors. These experiments were repeated at lower dissolved oxygen concentrations ranging from 0.01 to 0.07mg/L.

4.2.4 Analytic Methods

Samples were withdrawn from the reactor using a syringe connected to a plastic tube that extended through the cap to the bottom of the reactor. The sample line was flushed several times, then 30 mL was withdrawn. A portion (10 mL) of each sample was used to measure absorbance. Absorbance of the culture was measured using a spectrophotometer (Milton Roy Spectronic 21D) at 550 nm using a 1.25 cm path length.

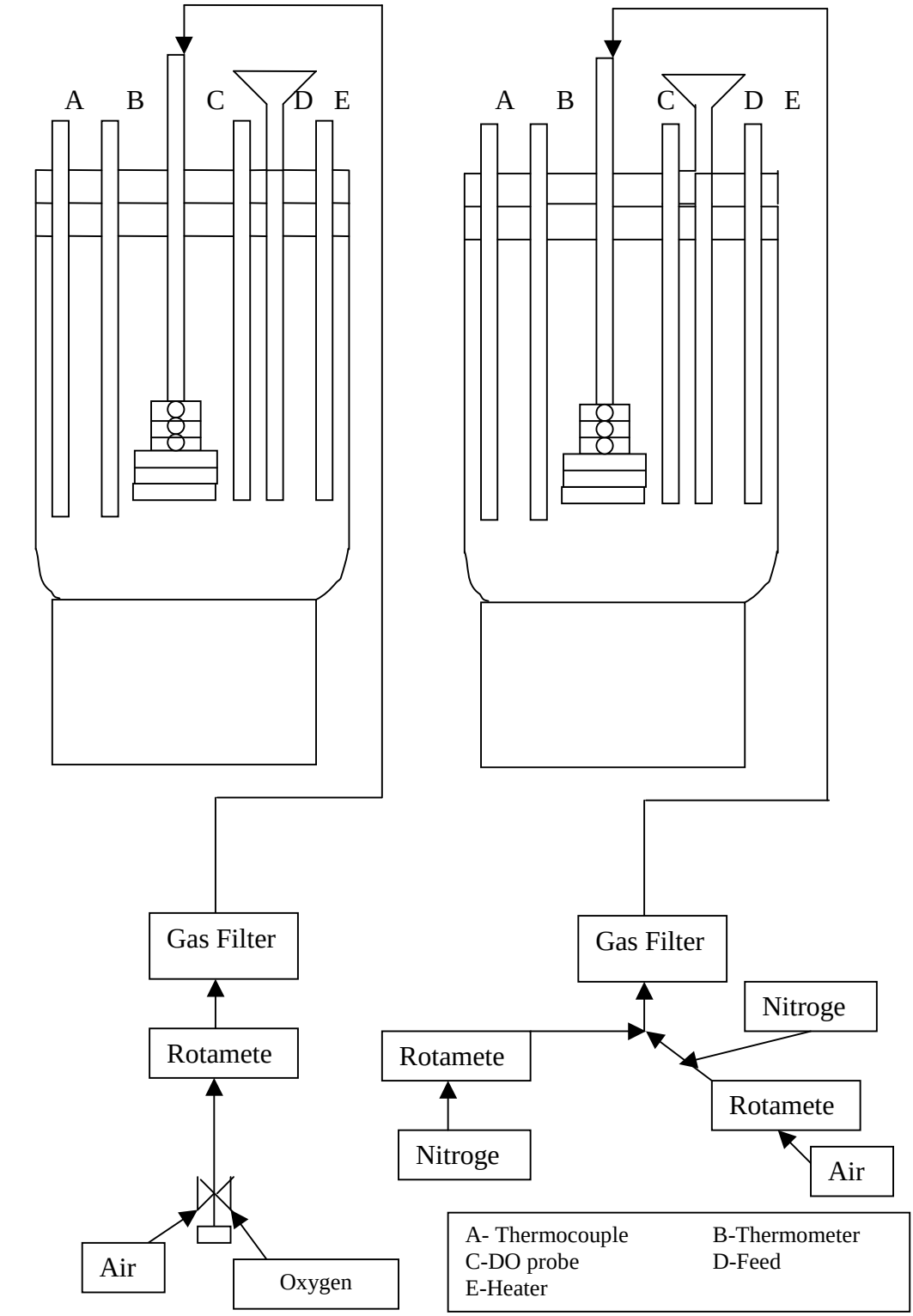

Figure 4.10. Experimental setup for the low DO experiments

4.2.5 Experimental Results

Figure 4.11 shows the results of the runs with low dissolved concentrations < 0.7 mg/L. In these experiments the aerobic growth rate of the reactor at high DO was higher than the low DO reactor. Also the diauxic lag of the high DO reactor was significantly longer. The specific anoxic growth rates were higher in the Low DO reactor. Figure 4.20 shows the results of the runs with low dissolved concentrations > 0.7 mg/L. In these experiments a significant difference in the growth rates in the aerobic phase was not recorded suggesting that *Pseudomonas denitrificans* could be microaerophilic. But a significant difference in length of lag and anoxic specific growth rates was observed. Therefore not only did dissolved oxygen have an effect on the length of the diauxic lag but it also affected the specific growth rates in the aerobic and anoxic phases.

4.3 Preculture Experiments

4.3.1 Experimental Methods

Cultures were grown in synthetic liquid medium modified from (Table 4-1) Koraros et al. (1996) with or with out without nitrate depending on what kind of preculture conditions were required for that experiment. The pH of the medium was adjusted to 7.0 using 2N NaOH before autoclaving and the addition of nitrate-nitrogen (if required). Culture medium in 250mL flasks (125 mL liquid volume) was inoculated from agar plates (prepared as described in section 4.1.1). To maintain *Oxic* preculture conditions the flasks were agitated in a shaker bath for two days at approximately 25^{o} C. If *anoxic* preculture conditions were to be maintained, the cultures were grown in a nitrate limited synthetic liquid medium (4mg/L NO_3- N) modified from Table 4-1 and allowed to sit under a sterile laminar hood for two days. A procedure termed ‘splitting’

E-7

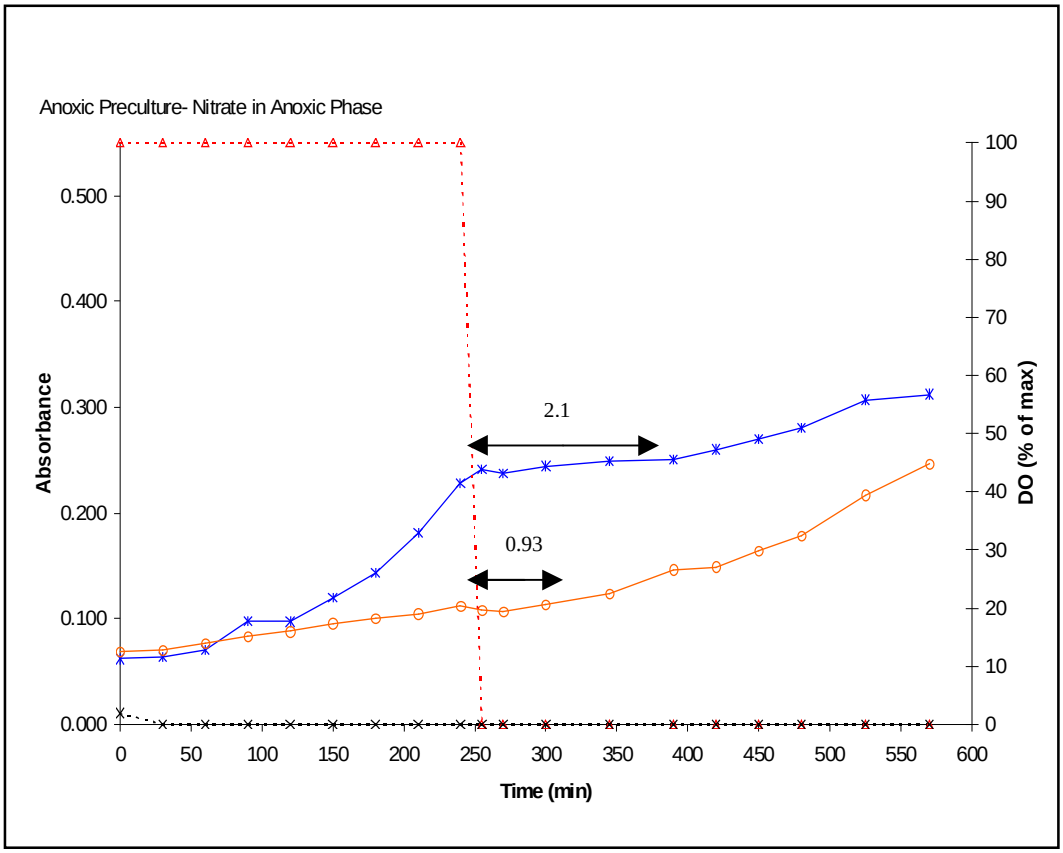

Figure 4.11. Experiment E-7. Comparison of biomass absorbance and dissolved oxygen levels against time. The following symbols represent pure culture absorbance exposed to a specific DO concentration and the levels of dissolved oxygen:

BIOMASS (w/ High DO)
High DO (8.7 mg/l)

BIOMASS (w/ Low DO)
High DO (0.01 mg/l)

E-8

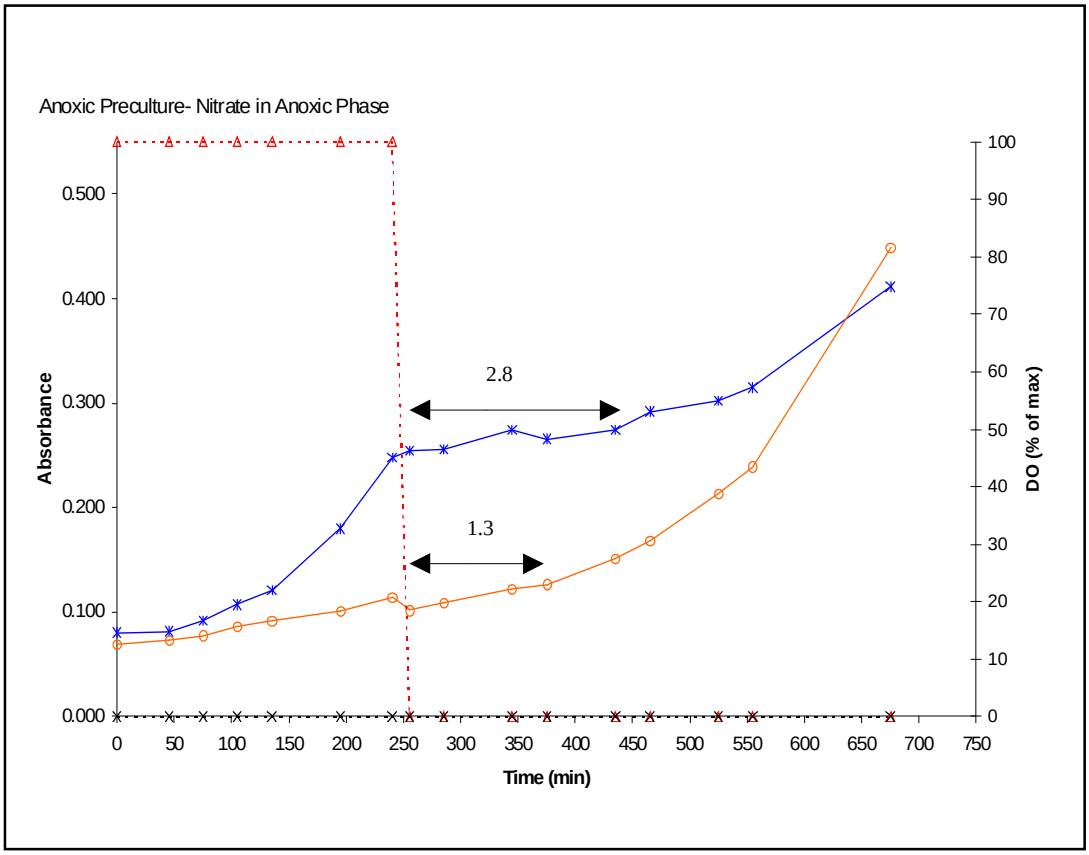

Figure 4.12. Experiment E-8. Comparison of biomass absorbance and dissolved oxygen levels against time. The following symbols represent pure culture absorbance exposed to a specific DO concentration and the levels of dissolved oxygen:

BIOMASS (w/ High DO)
High DO (8.7 mg/l)

BIOMASS (w/ Low DO) 
High DO (0.01 mg/l)

E-9

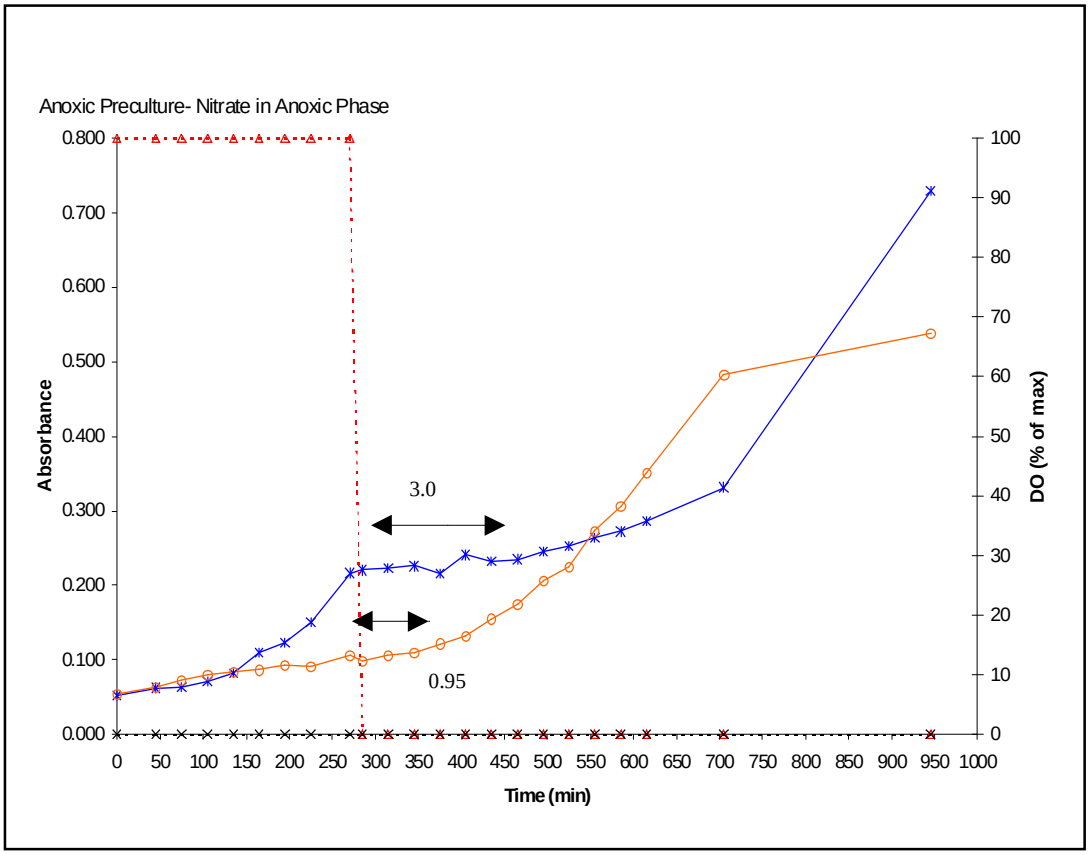

Figure 4.13. Experiment E-9. Comparison of biomass absorbance and dissolved oxygen levels against time. The following symbols represent pure culture absorbance exposed to a specific DO concentration and the levels of dissolved oxygen:

BIOMASS (w/ High DO)
High DO (8.7 mg/l)

BIOMASS (w/ Low DO)
High DO (0.01 mg/l)

E-10

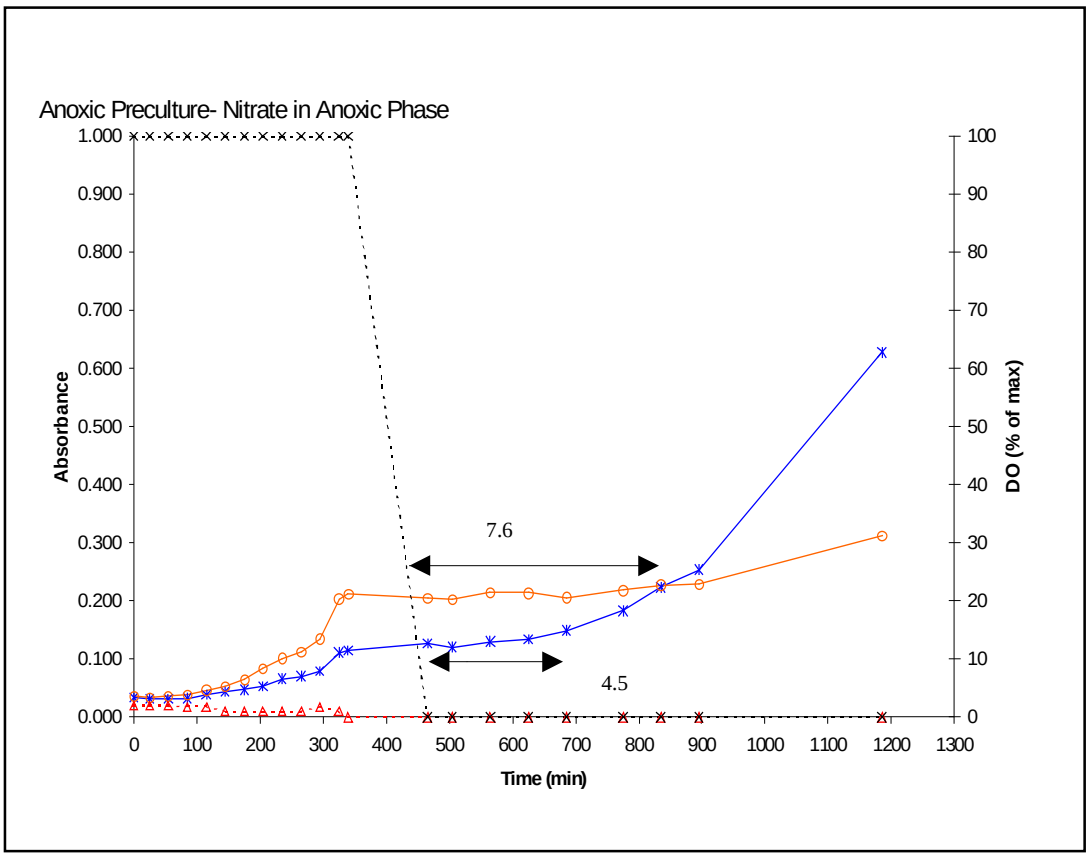

Figure 4.14. Experiment E-10. Comparison of biomass absorbance and dissolved oxygen levels against time. The following symbols represent pure culture absorbance exposed to a specific DO concentration and the levels of dissolved oxygen:

BIOMASS (w/ High DO)
High DO (8.7 mg/l)

BIOMASS (w/ Low DO)
High DO (0.07 mg/l)

E-11

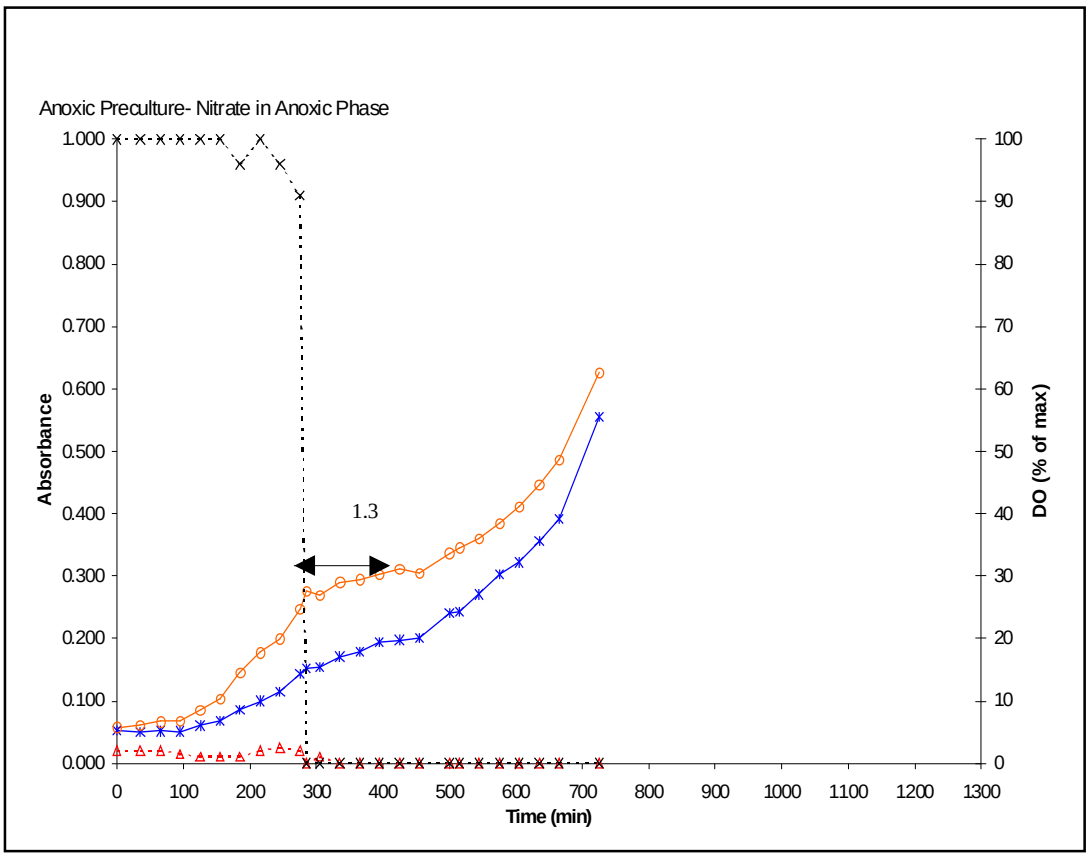

Figure 4.15. Experiment E-11. Comparison of biomass absorbance and dissolved oxygen levels against time. The following symbols represent pure culture absorbance exposed to a specific DO concentration and the levels of dissolved oxygen:

BIOMASS (w/ High DO)
High DO (8.7 mg/l)

BIOMASS (w/ Low DO)
High DO (0.07 mg/l)

E-12

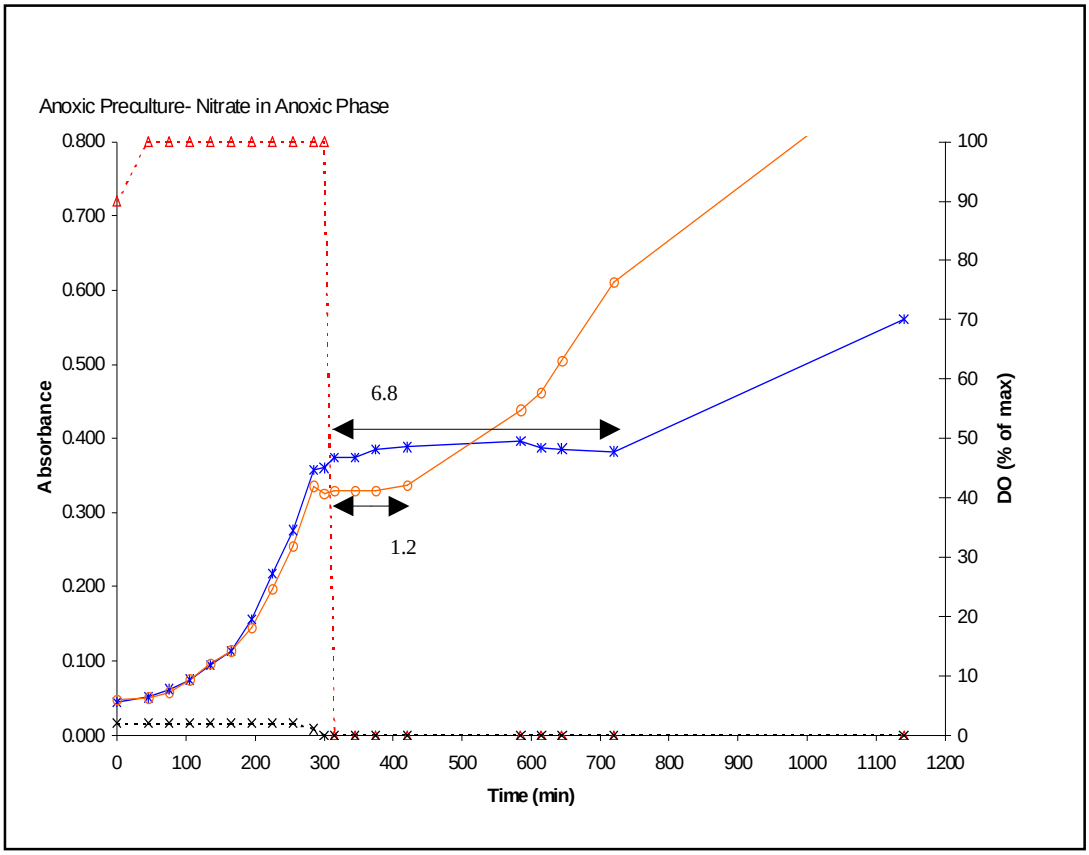

Figure 4.16. Experiment E-12. Comparison of biomass absorbance and dissolved oxygen levels against time. The following symbols represent pure culture absorbance exposed to a specific DO concentration and the levels of dissolved oxygen:

BIOMASS (w/ High DO)
High DO (8.7 mg/l)

BIOMASS (w/ Low DO)
High DO (0.09 mg/l)

E-13

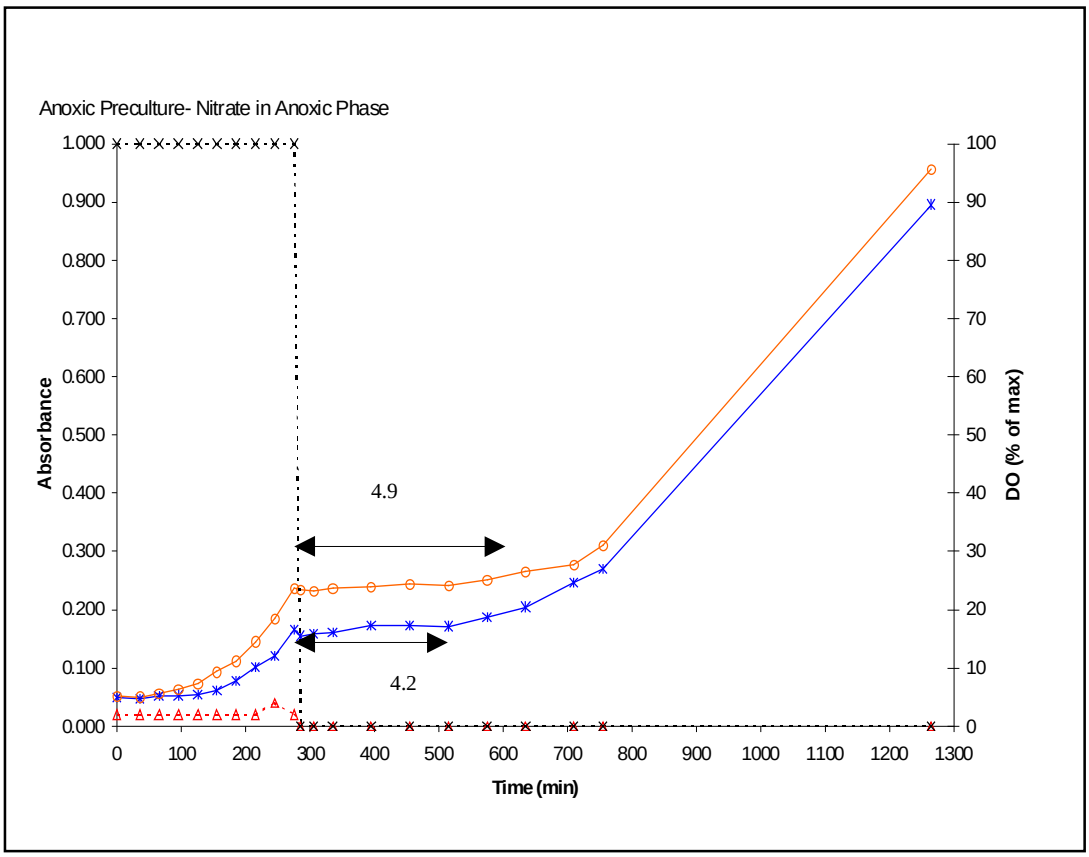

Figure 4.17. Experiment E-13. Comparison of biomass absorbance and dissolved oxygen levels against time. The following symbols represent pure culture absorbance exposed to a specific DO concentration and the levels of dissolved oxygen:

BIOMASS (w/ High DO)
High DO (8.7 mg/l)

BIOMASS (w/ Low DO)
High DO (0.09 mg/l)

E-14

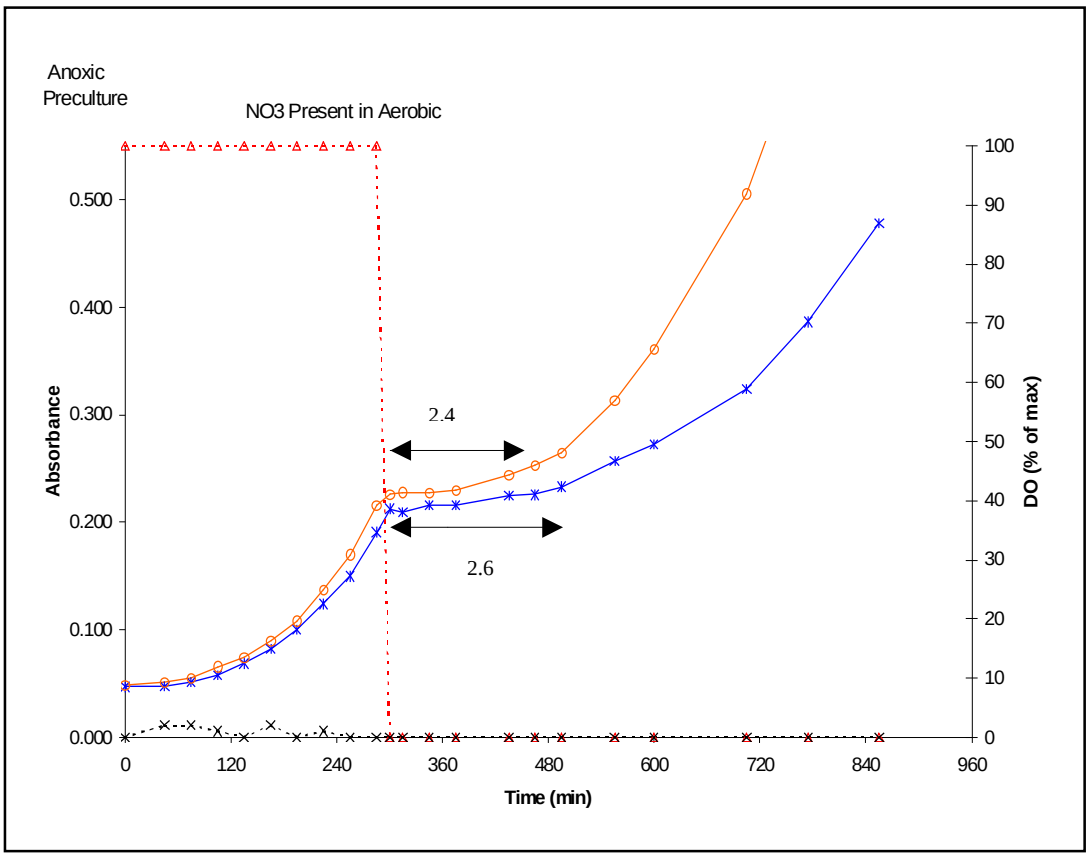

Figure 4.18. Experiment E-14. Comparison of biomass absorbance and dissolved oxygen levels against time. The following symbols represent pure culture absorbance exposed to a specific DO concentration and the levels of dissolved oxygen:

BIOMASS (w/ High DO)
High DO (8.7 mg/l)

BIOMASS (w/ Low DO)
High DO (0.09 mg/l)

E-15

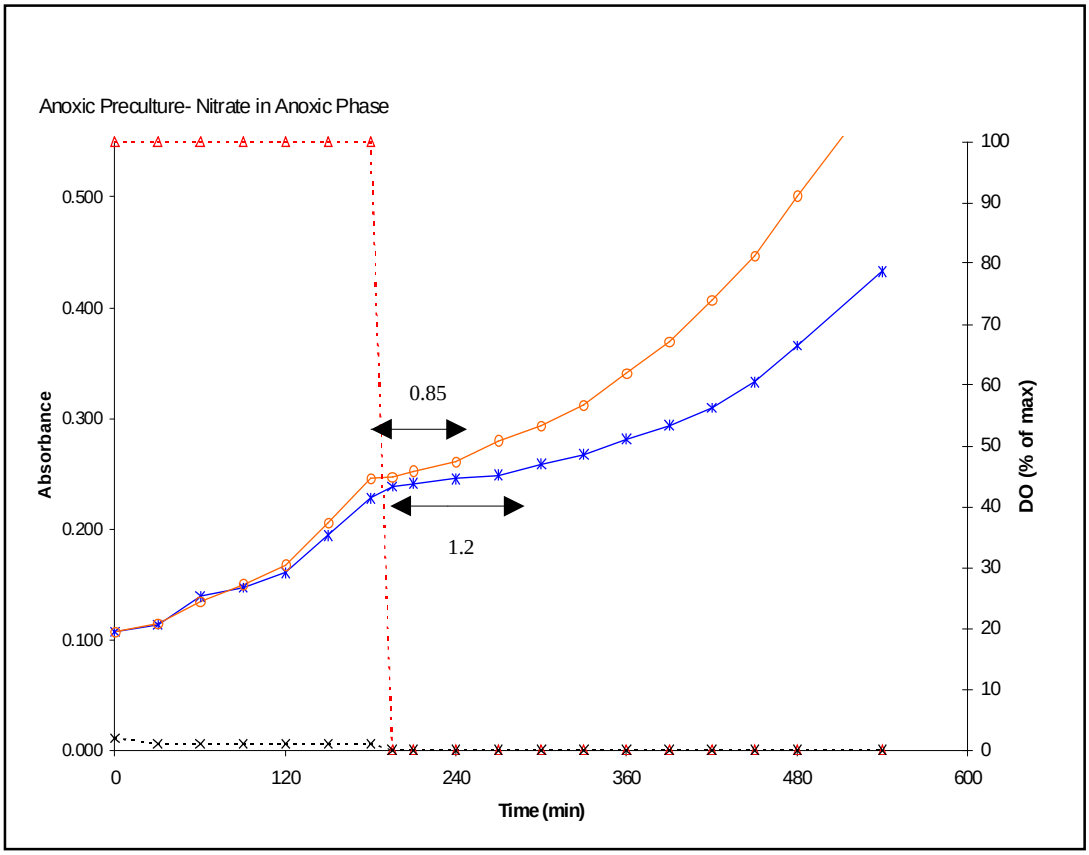

Figure 4.19. Experiment E-15. Comparison of biomass absorbance and dissolved oxygen levels against time. The following symbols represent pure culture absorbance exposed to a specific DO concentration and the levels of dissolved oxygen:

BIOMASS (w/ High DO)
High DO (8.7 mg/l)

BIOMASS (w/ Low DO)
High DO (0.09 mg/l)

E-16

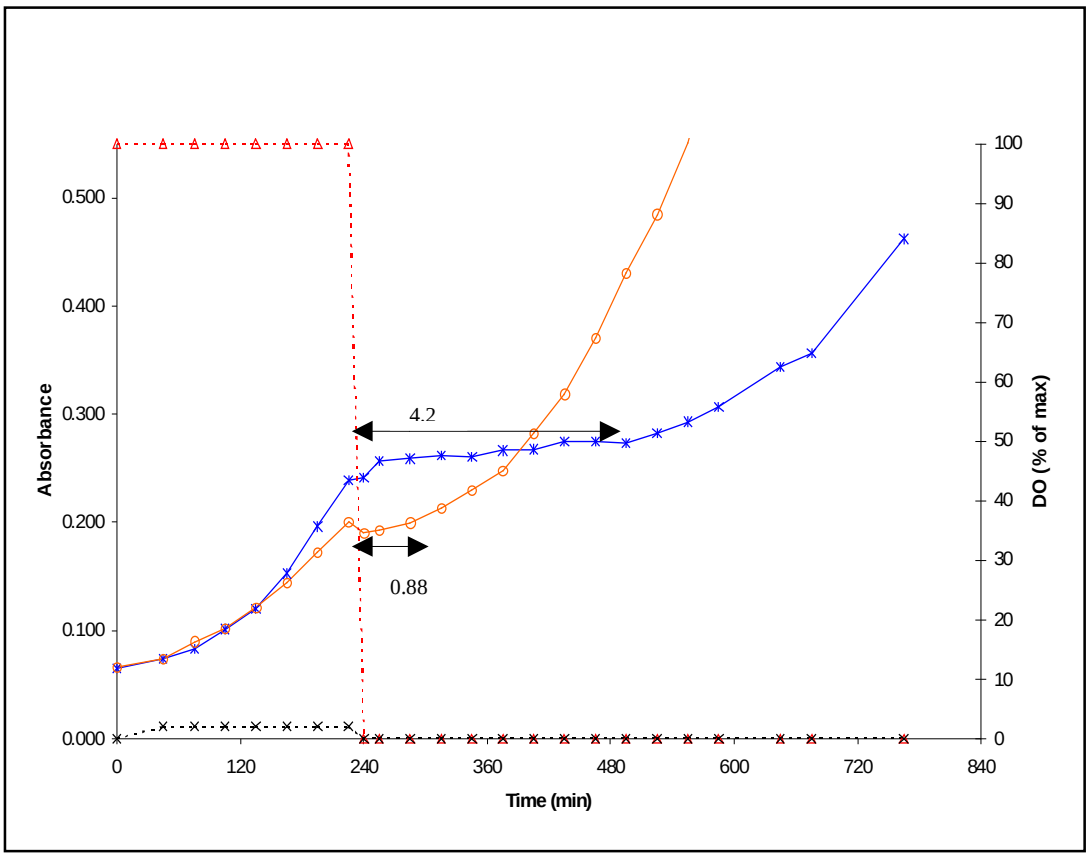

Figure 4.20. Experiment E-16. Comparison of biomass absorbance and dissolved oxygen levels against time. The following symbols represent pure culture absorbance exposed to a specific DO concentration and the levels of dissolved oxygen:

BIOMASS (w/ High DO)
High DO (8.7 mg/l)

BIOMASS (w/ Low DO)
High DO (0.17 mg/l)

E-17

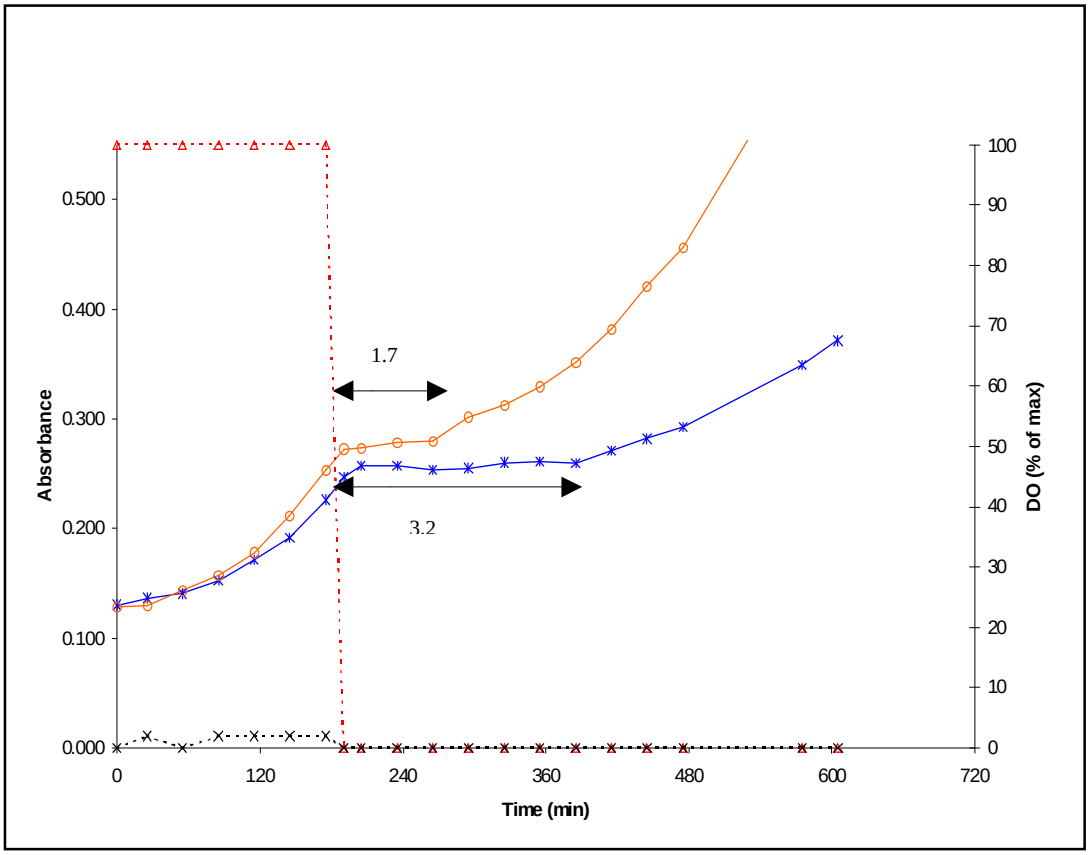

Figure 4.21. Experiment E-17. Comparison of biomass absorbance and dissolved oxygen levels against time. The following symbols represent pure culture absorbance exposed to a specific DO concentration and the levels of dissolved oxygen:

BIOMASS (w/ High DO)
High DO (8.7 mg/l)

BIOMASS (w/ Low DO)
High DO (0.17 mg/l)

E-18

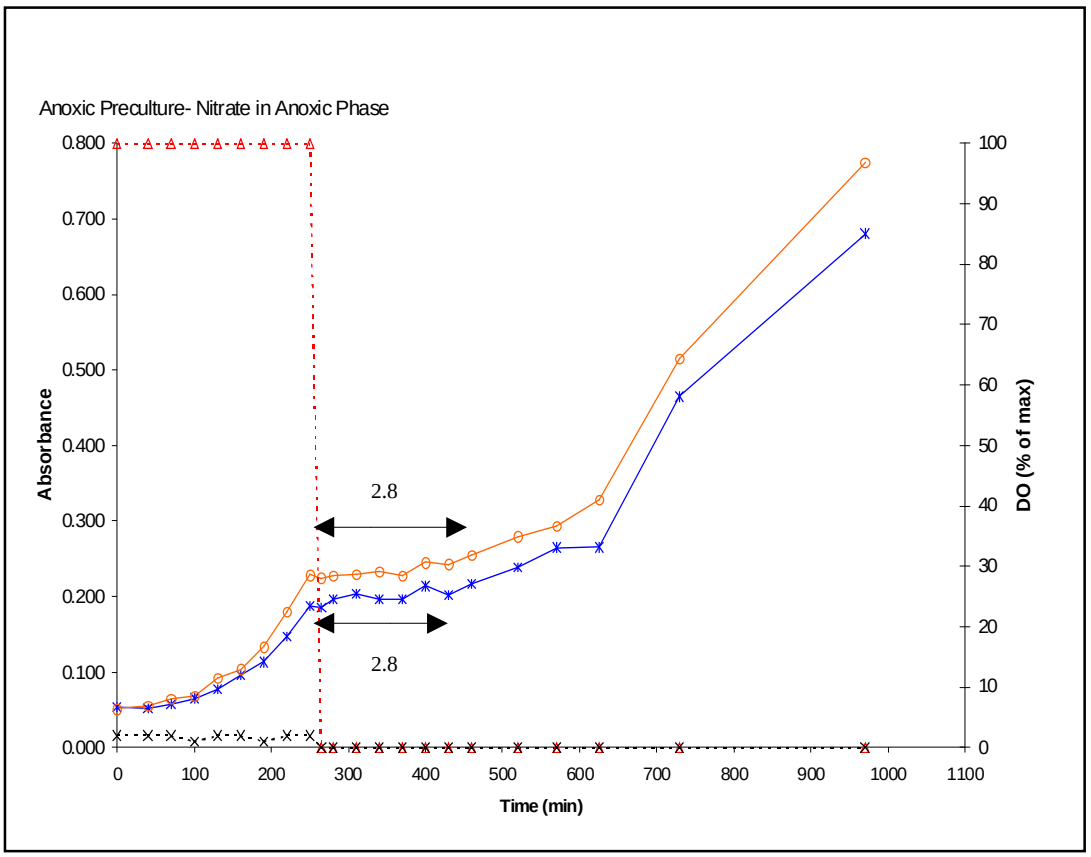

Figure 4.22. Experiment E-18. Comparison of biomass absorbance and dissolved oxygen levels against time. The following symbols represent pure culture absorbance exposed to a specific DO concentration and the levels of dissolved oxygen:

BIOMASS (w/ High DO)
High DO (8.7 mg/l)

BIOMASS (w/ Low DO)
High DO (0.17 mg/l)

E-19

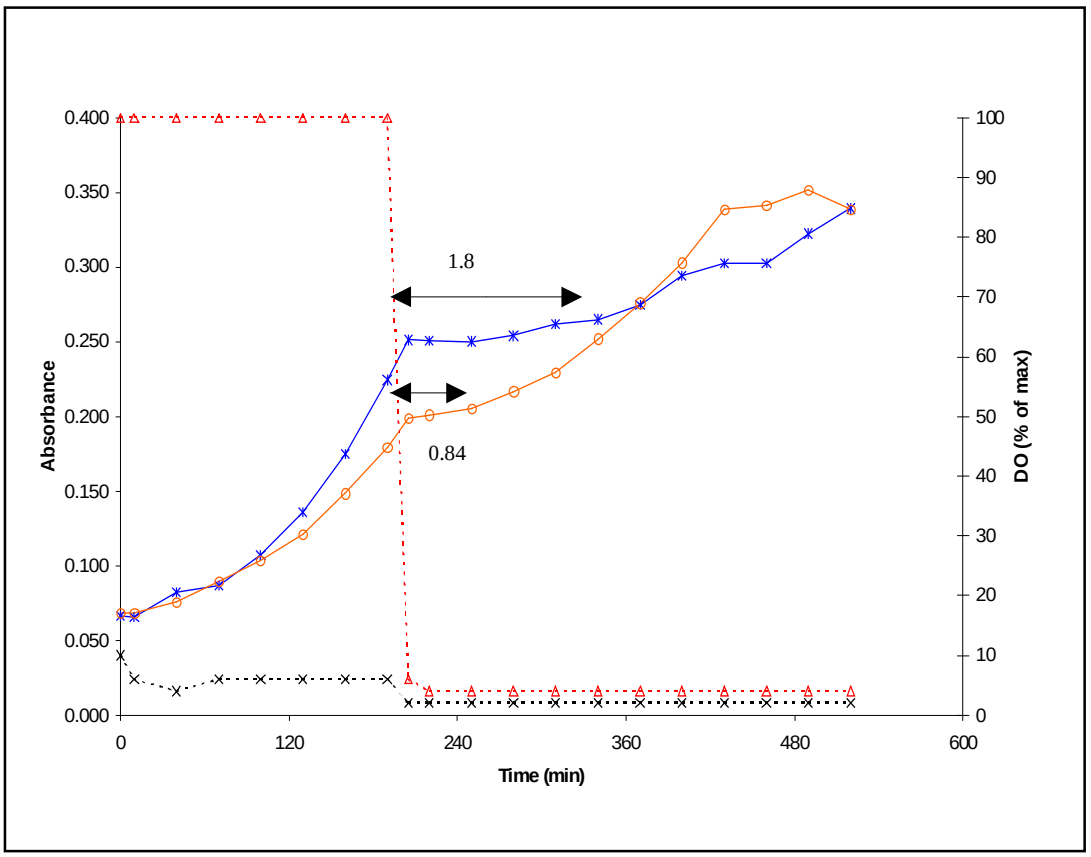

Figure 4.23. Experiment E-19. Comparison of biomass absorbance and dissolved oxygen levels against time. The following symbols represent pure culture absorbance exposed to a specific DO concentration and the levels of dissolved oxygen:

BIOMASS (w/ High DO)
High DO (8.7 mg/l)

BIOMASS (w/ Low DO)
High DO (0.35 mg/l)

E-20

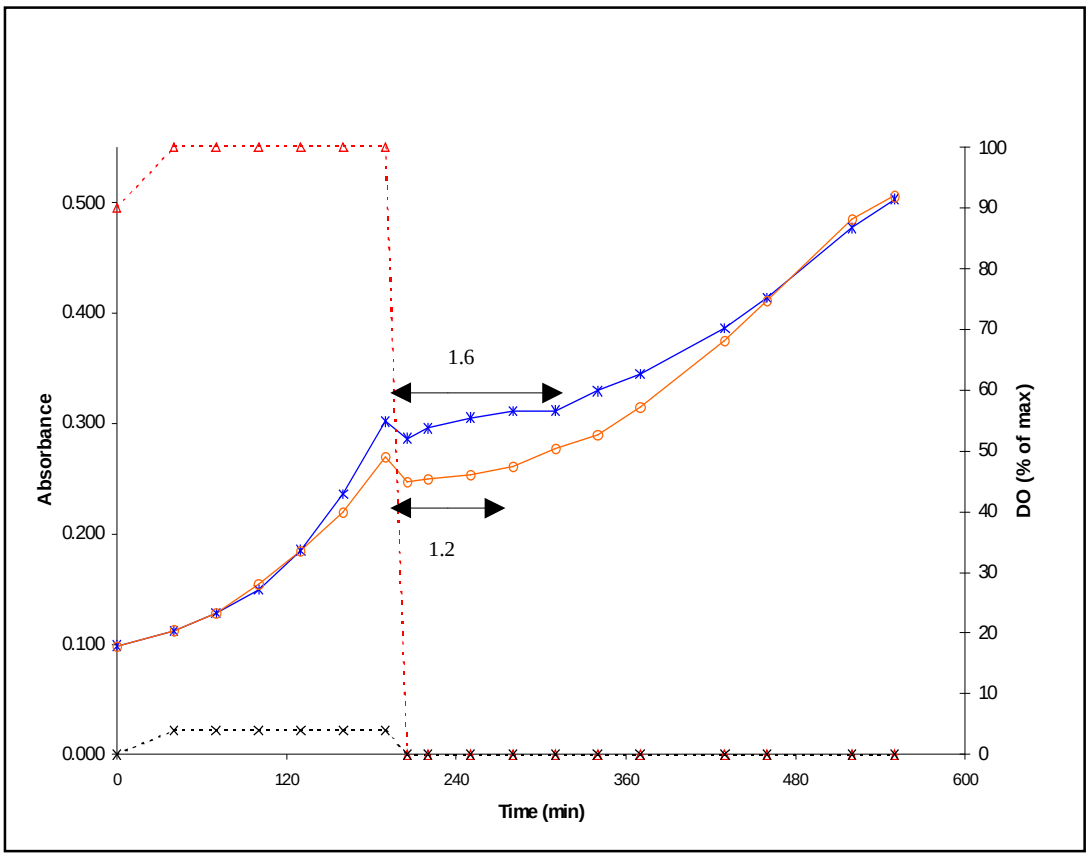

Figure 4.24. Experiment E-20. Comparison of biomass absorbance and dissolved oxygen levels against time. The following symbols represent pure culture absorbance exposed to a specific DO concentration and the levels of dissolved oxygen:

BIOMASS (w/ High DO)
High DO (8.7 mg/l)

BIOMASS (w/ Low DO)
High DO (0.35 mg/l)

E-21

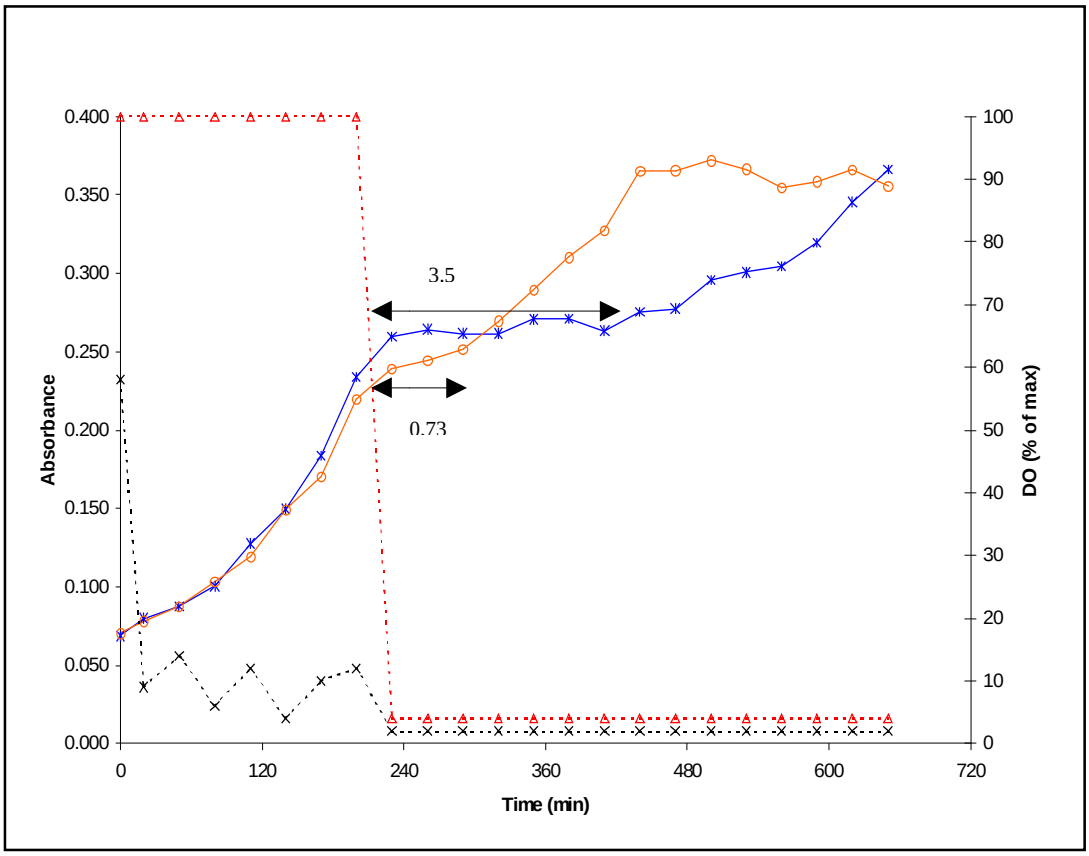

Figure 4.25. Experiment E-21. Comparison of biomass absorbance and dissolved oxygen levels against time. The following symbols represent pure culture absorbance exposed to a specific DO concentration and the levels of dissolved oxygen:

BIOMASS (w/ High DO)
High DO (8.7 mg/l)

BIOMASS (w/ Low DO)
High DO (0.70 mg/l)

E-22

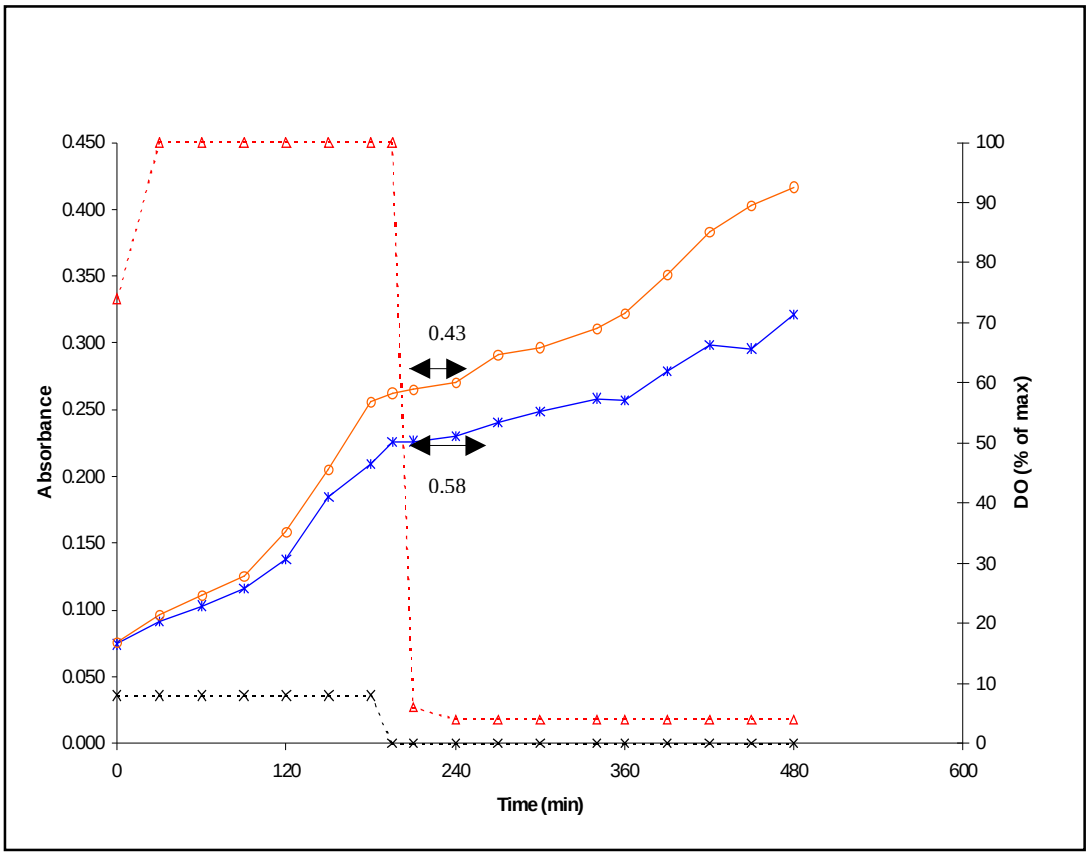

Figure 4.26. Experiment E-22. Comparison of biomass absorbance and dissolved oxygen levels against time. The following symbols represent pure culture absorbance exposed to a specific DO concentration and the levels of dissolved oxygen:

BIOMASS (w/ High DO)
High DO (8.7 mg/l)

BIOMASS (w/ Low DO)
High DO (0.7 mg/l)

E-23

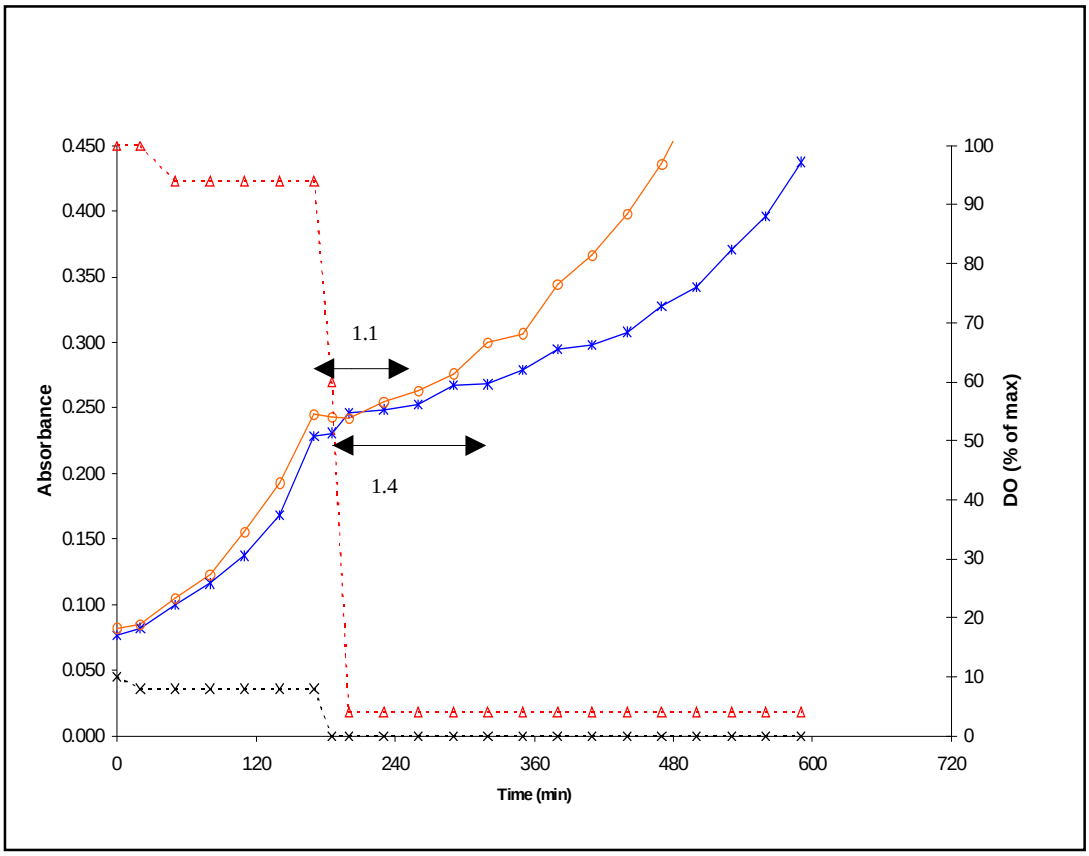

Figure 4.27. Experiment E-23. Comparison of biomass absorbance and dissolved oxygen levels against time. The following symbols represent pure culture absorbance exposed to a specific DO concentration and the levels of dissolved oxygen:

BIOMASS (w/ High DO)
High DO (8.7 mg/l)

BIOMASS (w/ Low DO)
High DO (0.7 mg/l)

was then performed on the culture medium. Approximately 250 mL of the culture medium was added to a liter of liquid medium and allowed to mix to prevent flocculation. The culture was then split into two 500 mL volumes, transferred to each bioreactor simultaneously and diluted with liquid medium to an absorbance (λ=550 nm, 1.25 path length) of 0.02- 0.05 for use in experiments.

4.3.2 Growth Experiments

Two mutiGen bench-top bio-reactors in parallel (models F-1000 and F-2000, New Brunswick Scientific) were used for the experiments. The culture was continuously stirred at 30 ± 2^0C. The pH ranged from 7.0 in the aerobic phase and increased to 7.2 during the anoxic phase. Dissolved oxygen was monitored using Model DO-40 (New Brunswick Scientific) analyzers with galvanic electrodes. The effect of various precultures and presence and absence of nitrate-nitrogen in aerobic phase was compared and contrasted at the dissolved oxygen concentration of 8.7 mg/L through the aerobic phase. The experimental setup was as shown in Figure 4.28. Each experiment consisted of an aeration period of 7-9 hours. 400 mg/L of nitrate-nitrogen was added to one reactor. Once the biomass in the reactors was up to 0.25 in terms of absorbance, a one liter sample was pulled out from the reactors and replaced with fresh synthetic medium at 30^o C. This dilution process was repeated two times. Aeration was then stopped and the reactor was sparged with nitrogen gas to remove any residual dissolved oxygen to mark the beginning of the anoxic phase. Nitrogen gas was flooded through the head space of the reactors during the period when there was no aeration. The variables monitored include biomass in terms of absorbance, dissolved oxygen, temperature and pH.

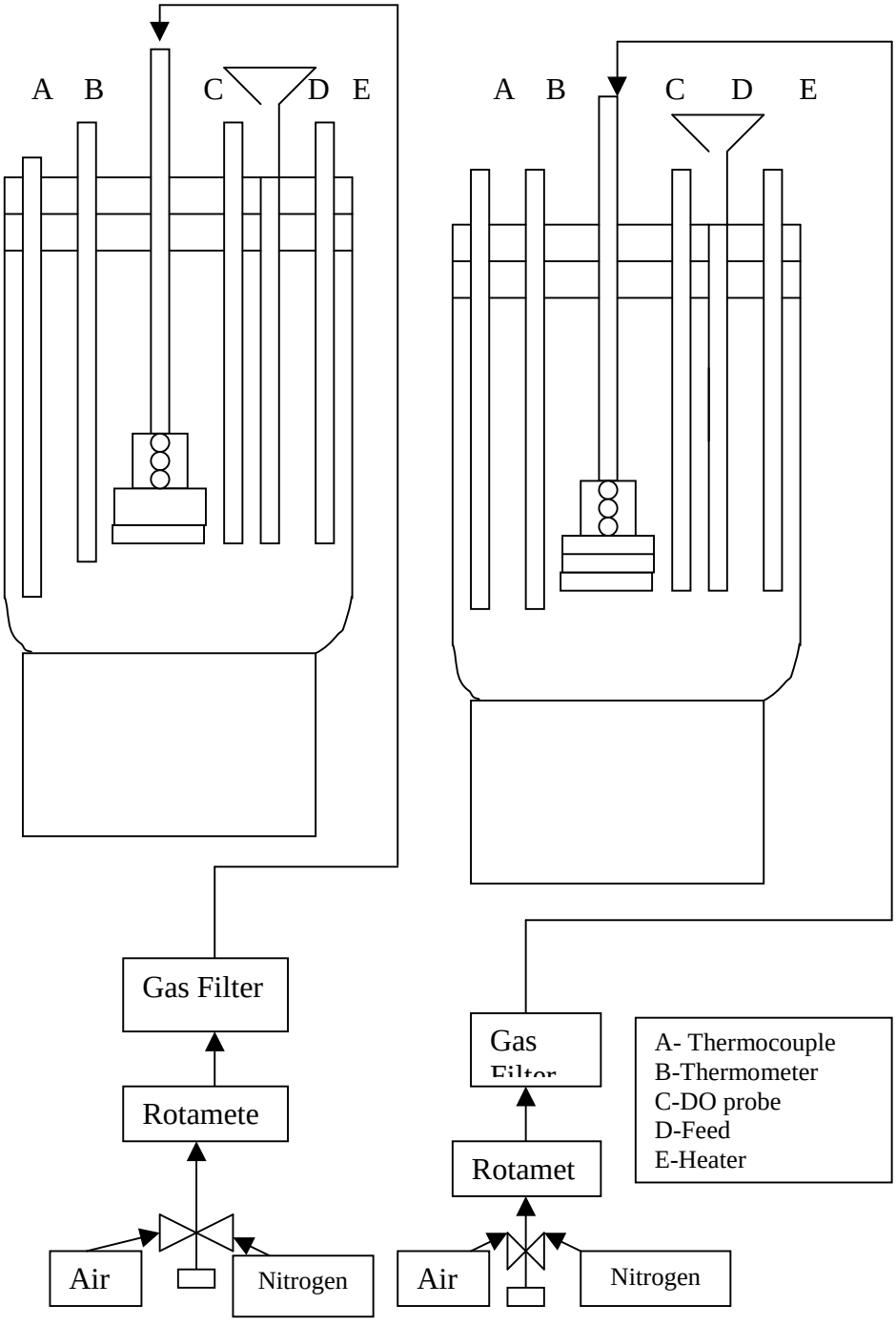

Figure 4.28. Experimental setup for the preculture experiments

4.3.3 Experimental Protocol

Experiments were carried out in order to investigate the effect of various preculture conditions and the nitrate concentrations in the aerobic phase on the duration of diauxic lags. Each experiment consisted of two parallel trials of the same initial culture conditions. To ensure that the parallel cultures had the same initial biomass concentrations, the original culture was well mixed and divided between the two bioreactors. Potassium nitrate (400 mg/L) was added in the aerobic phase to one reactor. One set of parallel run experiments was performed with oxic preculture conditions and another with anoxic preculture conditions and the length of diauxic lags was compared.

4.3.4 Analytic Methods

Samples were withdrawn from the reactor using a syringe connected to a plastic tube that extended through the cap to the bottom of the reactor. The sample line was flushed several times, and 30 mL was withdrawn. A portion (10 mL) of each sample was used to measure absorbance. Absorbance of the culture was measured using a spectrophotometer (Milton Roy Spectronic 21D) at 550 nm using a 1.25 cm path length.

4.3.5 Experimental Results

The results of experiments showed two things clearly. Oxic preculture conditions (Figure 4.32) experiments had significantly longer diauxic lags than cultures that were revived anoxically (Figure 4.31). Also the diauxic lags were longer for cultures that had not been exposed to nitrate in the aerobic phase as seen from Figure 4.31. Presence of nitrate failed to influence the rate of aerobic growth in either experiment as observed in all the figures. These experiments support the hypothesis in models proposed by Liu et. al (1998 a, b).

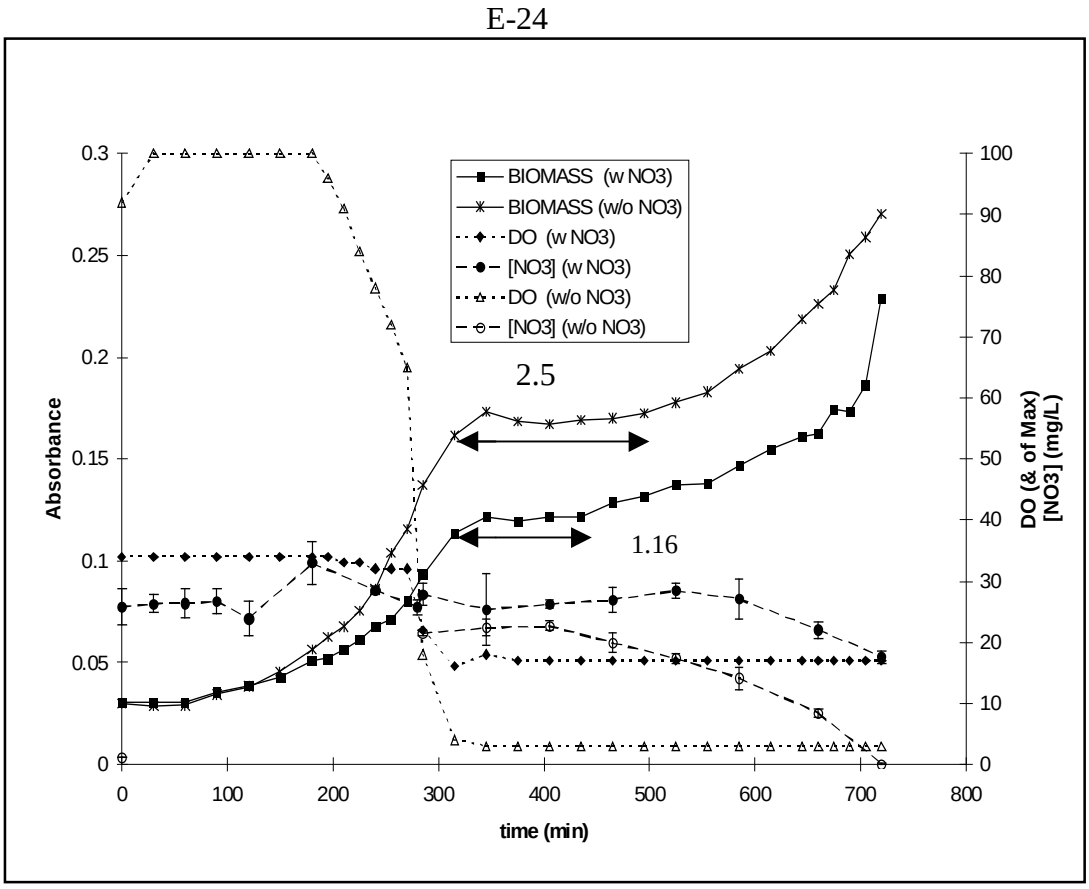

Figure 4.29. Experiment E-24. Comparison of biomass absorbance and dissolved oxygen levels against time. The symbols as in the chart legend represent pure culture absorbance exposed to different nitrate concentrations. The culture was revived anoxically.

E-25

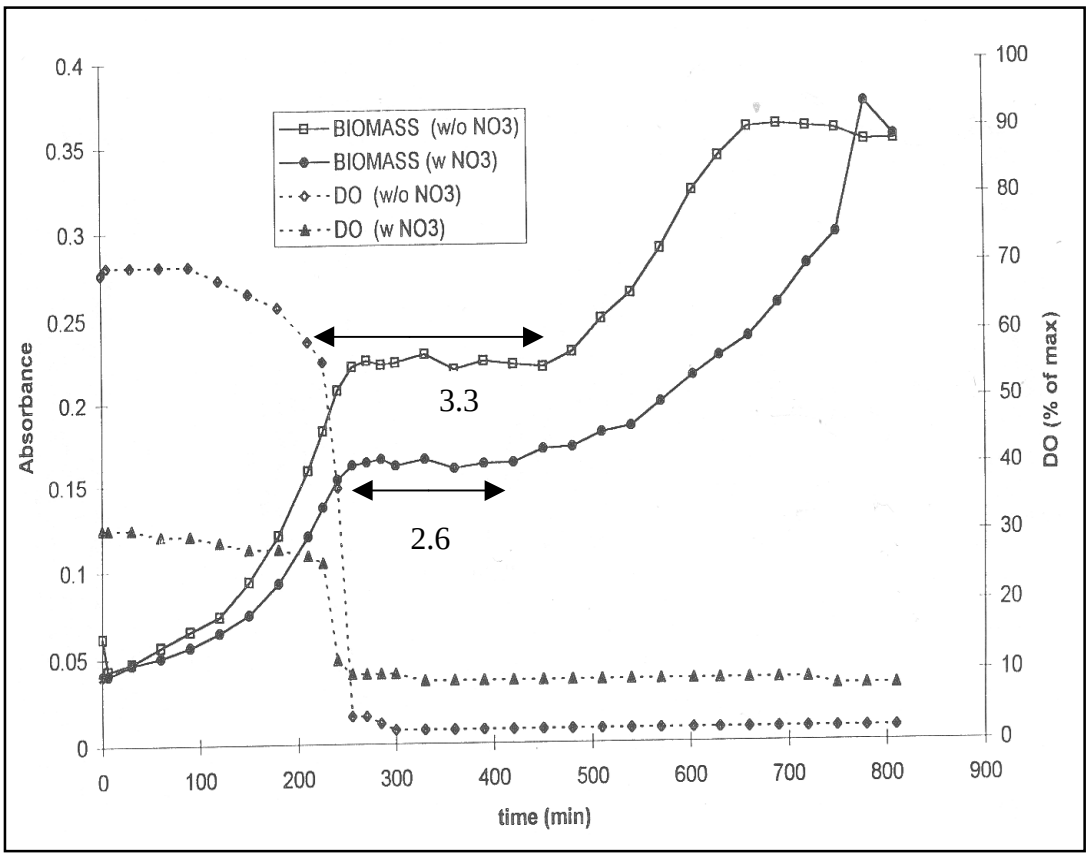

Figure 4.30. Experiment E-25. Comparison of biomass absorbance and dissolved oxygen levels against time. The symbols as in the chart legend represent pure culture absorbance exposed to different nitrate concentrations. The culture was revived anoxically.

E-26

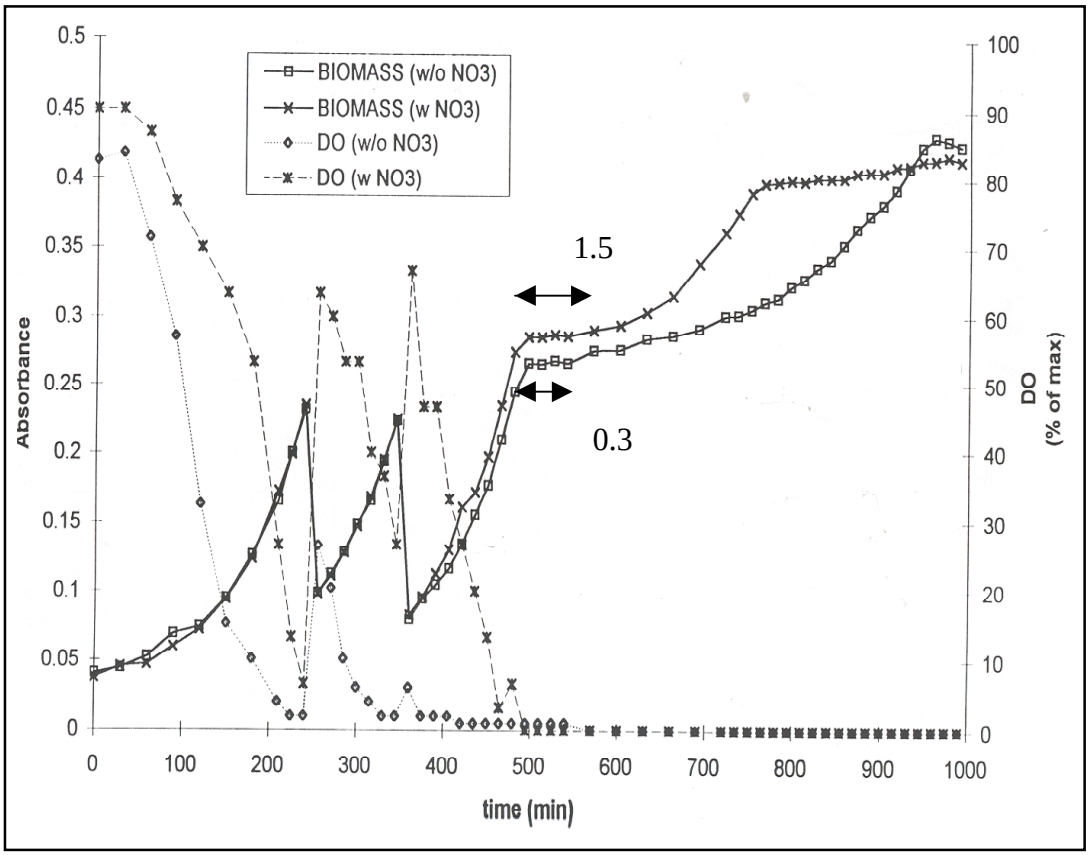

Figure 4.31. Experiment E-26. Comparison of biomass absorbance and dissolved oxygen levels against time. The symbols as in the chart legend represent pure culture absorbance exposed to different nitrate concentrations. The culture was revived anoxically.

E-27

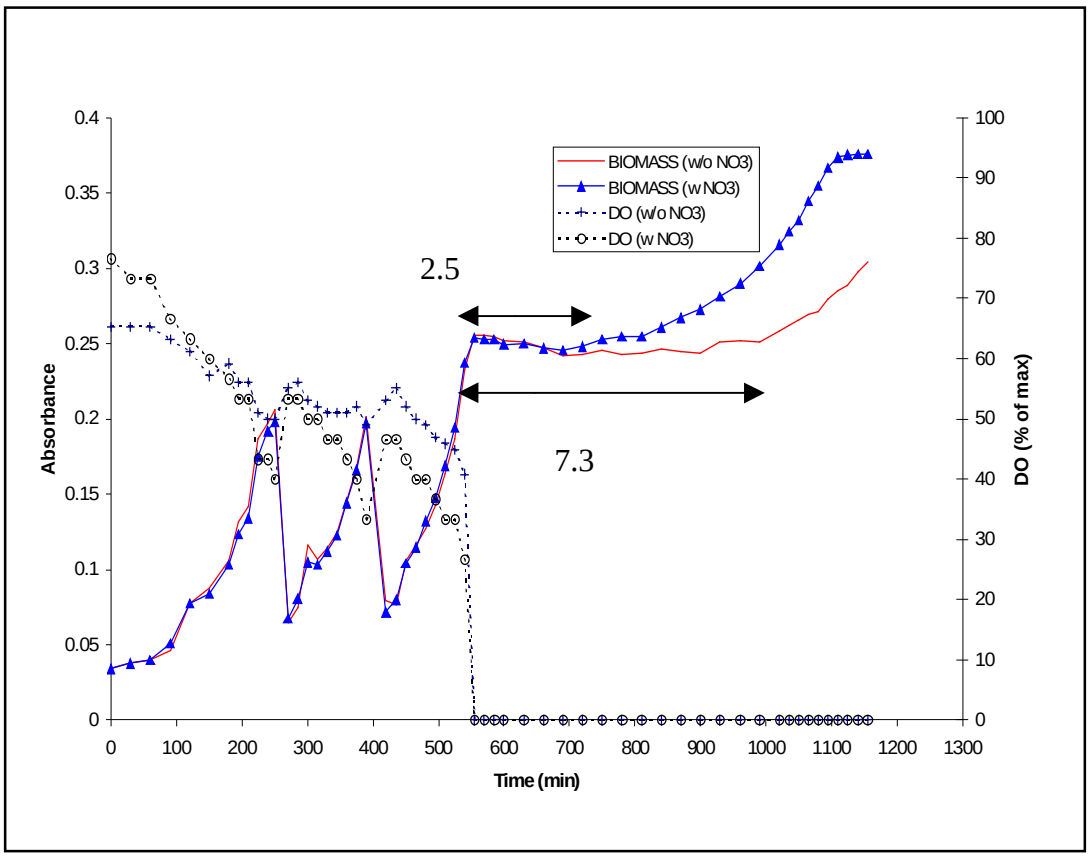

Figure 4.32. Experiment E-27. Comparison of biomass absorbance and dissolved oxygen levels against time. The symbols as in the chart legend represent pure culture absorbance exposed to different nitrate concentrations. The culture was revived in oxic conditions.

E-28

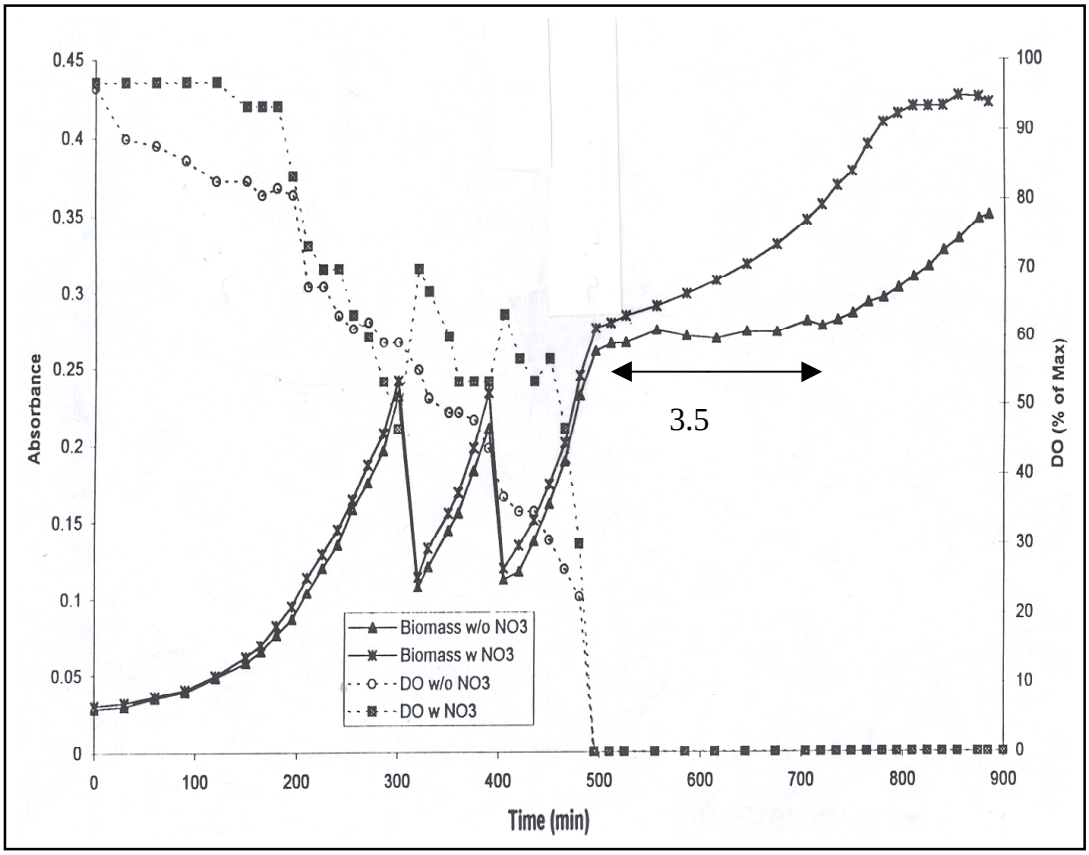

Figure 4.33. Experiment E-28. Comparison of biomass absorbance and dissolved oxygen levels against time. The symbols as in the chart legend represent pure culture absorbance exposed to different nitrate concentrations. The culture was revived anoxically.

CHAPTER 5
NEURAL NETWORKS

All the models developed so far have all been successful in providing detailed descriptions of the process kinetics and reflect state of the art understanding of processes such as denitrification and nitrification. The hypothesis used to justify the occurrence of a diauxic lag remains to be verified experimentally by tracking enzyme activity during a typical experiment. In contrast to the conventional models there is the black box modeling technique, which predicts the value of a variable given the historic values of itself (and perhaps others variables) but gives little insight into the process kinetics or the governing equations in the model. A neural network is capable of good performance even if the data have considerable non-linearity. Another of its significant advantages is that it is able to discover patterns in the data. In summary, a neural network can probably solve effectively problems that cannot be solved by traditional modeling or statistical methods. The choice of an appropriate network and a practical algorithm is required for the network to give the desired performance. In the present study a neural network is used to predict the duration of the diauxic lag given certain parameters such as the biomass concentrations in terms of absorbance, reviving phase of the culture, dissolved oxygen concentrations and nitrate concentrations in the aerobic phase and length of the aerobic phase in hours.

5.1 Algorithm Used

5.1.1 Back Propagation Algorithm

The back propagation network is probably the best known and widely used among all the types of neural networks systems. A typical back propagation network is as depicted in Figure 5.1. Essentially a back propagation network has an input layer, output layer and one or more hidden layers. The inter -connections between the input and hidden layers and the hidden and output layers are termed ‘weights’. Like most other neural network systems, input patterns are presented to the network and the network is trained to learn the corresponding output pattern .The number of input parameters in one input pattern determines the number of nodes in the input layer. Similarly the number of output nodes is the number of variables the neural network is required to predict. In the present study, we are interested in predicting the duration of the diauxie in hours. Hence the neural network has only one output node, being the length of the diauxic lag in hours. Both the number of nodes in the hidden layer and the number of hidden layers are not specified. Though some theoretical guidance exists to determine the number of hidden layers and hidden nodes, they are usually varied and the performance of the network recorded for each combination. Finally the combination which gives the best performance is chosen.

Rumelhart (1986) first proposed the basic back propagation algorithm. The name ‘back propagation’ comes from the fact that the error (gradient) of the hidden units is derived from propagating backward the error associated with output units. The first step of the back propagation algorithm is weight initialization where the weights are set to small random numbers. In the second step an input pattern is presented to the neural network and the output neuron activation’s (values at the output nodes) are calculated.

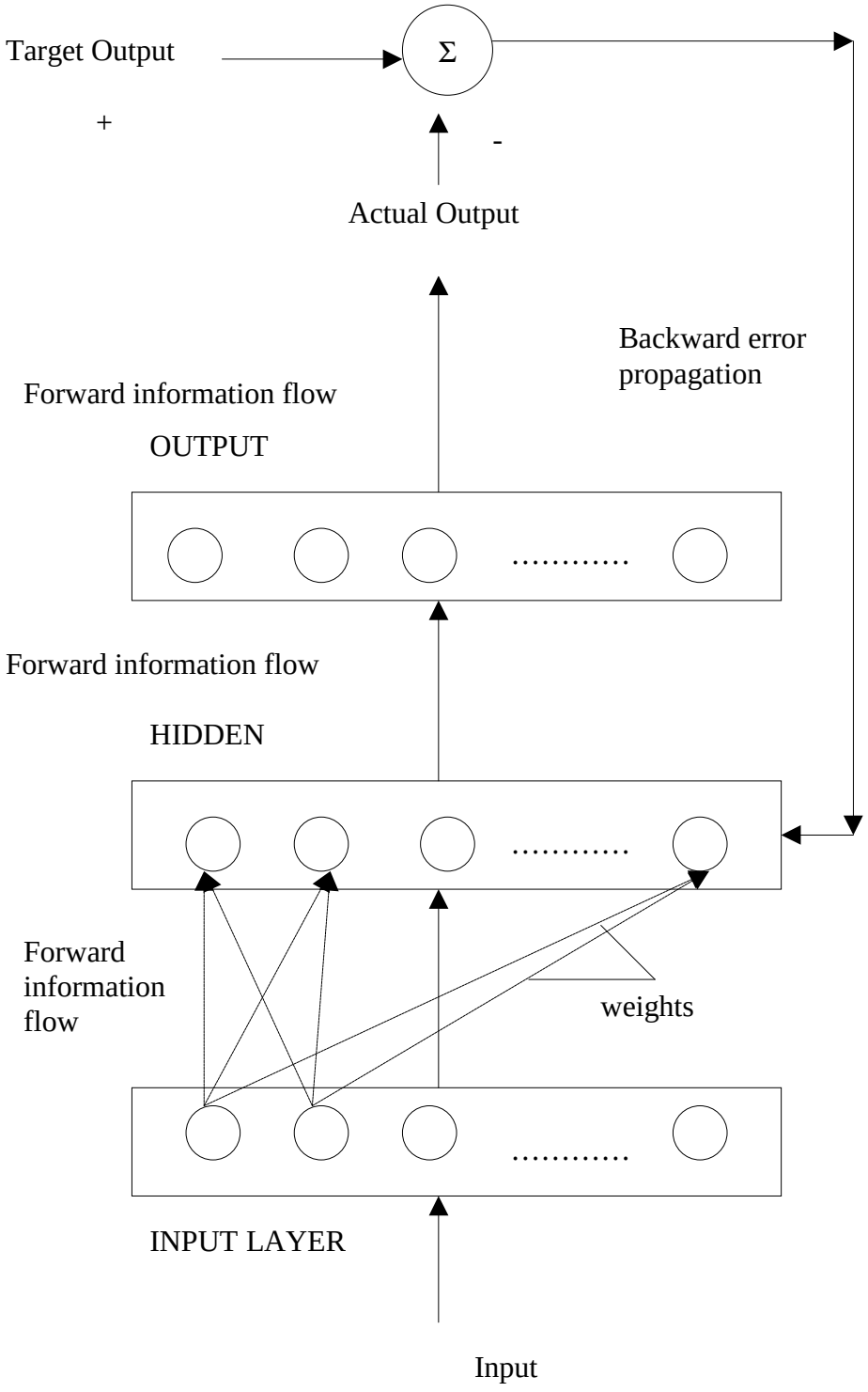

Figure 5.1. Backpropagation network

The third step is weight updating, where the weights are adjusted (backwards from the output to hidden layers recursively) to reduce the error. The second and third steps are repeated for each training pattern (input and corresponding output pattern). The number of such distinct training patterns presented to the network is called epoch size where an epoch is one pass of the above three steps for all the training patterns. The error measure used here is mean square error in the output activations. The mean square error for a single pass is the square of the difference between the attained and desired output activation for the output neuron. The epoch error is computed as the average of errors in training presentations within that epoch. Mathematically, if we were processing training pattern p, where the desired output activation was t_p and the actual attained activation was o_p then error for that single representation is given by

$$E_p = (t_p - o_p)^2 \tag{5-1}$$

If there were m such presentations in an epoch, the epoch error is given by

$$E = \frac{1}{m}\sum_{p=0}^{m-1} E_p \tag{5-2}$$

Rumelhart (1986) describes the equations governing the back propagation algorithm in great detail. Although the back propagation algorithm is simple and easy to implement, its success crucially depends on user defined parameters such as learning rate and momentum constant. Hence in many situations it lands up having poor convergence rates. Conjugate gradient search algorithms aim at minimizing some of these disadvantages.

5.1.2 Training by Conjugate Gradients

From an optimization point of view, learning in a neural network is equivalent to minimizing a global error function, which is a multivariate function that depends on the

weights in the network. Suppose we approximate the global error function to a quadratic function of the form

$$f(\mathbf{x}) = c - \mathbf{b}.\mathbf{x} + \frac{1}{2}\mathbf{x}.\mathbf{A}.\mathbf{x} \qquad (5\text{-}3)$$

where, $\mathbf{x}$ is the weight vector

The function is minimized when its gradient

$$\nabla f = \mathbf{A}.\mathbf{x} - \mathbf{b}\,\mathbf{x} \qquad (5\text{-}4)$$

is zero. The minimization is carried out by generating a succession of search directions $\mathbf{h}_k$ and improved minimizer's $\mathbf{x}_k$ (weight vectors). At each stage a quantity α_k (step size) is also is also found that minimizes $f(\mathbf{x}_k + \alpha_k \mathbf{h}_k)$, and $\mathbf{x}_{k+1}$ is set equal to the new point $\mathbf{x}_k + \alpha_k * \mathbf{h}_k$. The search direction vector h_k and the weight vector $\mathbf{x}_k$ are built in such a way that $\mathbf{x}_{k+1}$ is also the minimizer of the function f over all the vector spaces of directions already taken namely $\{\mathbf{h}_1, \mathbf{h}_2, \ldots \mathbf{h}_k\}$. Therefore in N iterations we arrive at the minimum over the entire vector space. The search direction vector $\mathbf{h}_{k+1}$ is given by the following equation

$$\mathbf{h}_{k+1} = \mathbf{g}_{k+1} + \gamma_k \mathbf{h}_k \qquad (5\text{-}5)$$

The Polak-Ribiere algorithm defines the scalar γ_k as follows

$$\gamma_k = \frac{(g_{k+1} - g_k).g_{k+1}}{g_k.g_k} \qquad (5\text{-}6)$$

where $\mathbf{g}_k$ is the negative gradient of f at some point $\mathbf{P}_k$ (i.e.)

$$\mathbf{g}_k = -\nabla f(\mathbf{P}_k) \qquad (5\text{-}7)$$

If we proceeded from $\mathbf{P}_k$ along the direction $\mathbf{h}_k$ to the local minima of f located at point $\mathbf{P}_{k+1}$ then $\mathbf{g}_{k+1}$ can be written as

$$\mathbf{g}_{k+1} = -\nabla f(\mathbf{P}_{k+1}) \qquad (5\text{-}8)$$

The above to logic can be implemented in two major stages recursively:

Stage 1: To find three points such that middle point is less than the first point.

The steps of the algorithm include:

(1) Save the weights as they come into the conjugate gradient module and compute the negative gradient of the weight vector $\mathbf{g}_k$ at point $\mathbf{P}_k$. Let $\mathbf{P}_k$ be the first of the three points we are trying to determine.

(2) Set the intial direction vector $\mathbf{h}_k$ equal to $\mathbf{g}_k$ if k =0. If k>0 compute $\mathbf{h}_k$ using equations (5) and (6).

(3) Find a second point $\mathbf{P}_{k+1}$ in the direction $\mathbf{h}_k$ such that $f(\mathbf{P}_{k+1}) < f(\mathbf{P}_k)$.

(4) Estimate a third point using the golden ration rule and compute the value of the error function at that point. The value of the error function at this third point need not be less than the second point.

We now have three points that define an interval. Since the error function is approximated to a quadratic equation, we can fit the three points in a parabola.

Stage 2: To refine this interval containing the minima until within satisfactory limits of accuracy and try to locate the local minimum

Let the first point be $\mathbf{P}_1$, its error e_1, second point be $\mathbf{P}_2$ and its error e_2 and so on. We take a ‘step’ in the negative gradient direction from $\mathbf{P}_2$ along the parabola and compute the value of the function at that point.

The following cases arise:

(1) If the function value at $\mathbf{P}_3$ is less than that at $\mathbf{P}_2$ and the 'step' is between $\mathbf{P}_2$ and $\mathbf{P}_3$: The function value at this newly stepped out point is computed and compared to e_3. If the function value is less than e_3 then the minimum is an internal point (between $\mathbf{P}_2$ and $\mathbf{P}_3$) and we are done. In this case $\mathbf{P}_1$ and $\mathbf{P}_2$ are updated along with their function values as follows: $\mathbf{P}_2$ becomes $\mathbf{P}_1$ and the minimum becomes $\mathbf{P}_2$.

(2) If the function value at $\mathbf{P}_3$ is less than that at $\mathbf{P}_2$ and the 'step' is beyond $\mathbf{P}_3$ but within the maximum step: $\mathbf{P}_3$ is updated along with its function value to 'step' and the function value at this newly stepped out point.

(3) If the function value at $\mathbf{P}_3$ is less than that at $\mathbf{P}_2$ and if the new point was above an arbitrary limit beyond $\mathbf{P}_3$ then we re-estimate the new point by taking a 'step' of the maximum size and returning to one of the cases above. If the new point were anywhere else then it is not desired and hence we use the golden ratio rule to step outside to a new point.

(4) If the function value at $\mathbf{P}_2$ is less than that at $\mathbf{P}_3$ and the new point ('step') is between $\mathbf{P}_2$ and $\mathbf{P}_3$: In this case $\mathbf{P}_1$ and $\mathbf{P}_2$ are updated along with their function values as follows: $\mathbf{P}_1$ becomes $\mathbf{P}_2$ and $\mathbf{P}_2$ becomes new point 'step'.

(5) If the function value at $\mathbf{P}_2$ is less than that at $\mathbf{P}_3$ and the new point ('step') is between $\mathbf{P}_1$ and $\mathbf{P}_2$: In this case $\mathbf{P}_2$ and $\mathbf{P}_3$ are updated along with their function values as follows: $\mathbf{P}_3$ becomes $\mathbf{P}_2$ and $\mathbf{P}_2$ becomes new point 'step'.

(6) If the new point were anywhere else then it is not desired and hence we use the golden ratio rule to step outside to a new point.

The conjugate gradient algorithm though similar to the back propagation algorithm with momentum differs from it in two ways. One, the step size is not fixed. Two, the momentum term γ varies in an optimal way rather than being fixed throughout.

5.1.3 Simulated Annealing

Annealing is a term from metallurgy. When the atoms in a metal are aligned randomly the metal is brittle more likely to get fractured. Hence when a metal is heated to very high temperatures (the atoms are completely random) and cooled rapidly it is more likely that the atoms settle down in random unstable state. On the other hand of the metal were cooled gradually, the atoms tend to fall into patterns that are relatively stable for that temperature. The same idea is used in optimization. The independent variables are randomly perturbed (weights in the case of a neural network) while keeping track of the best (lowest error) function value for each randomized set of variables. A high standard deviation for the random number generator is used. After many such tries the set that produced the best function value is used as the center for perturbation for the next temperature. The temperature (standard deviation) is decreased and new tries are performed.

5.1.4 Interleaved Simulated Annealing and Conjugate Gradient Algorithm

In the present study, the annealing parameters namely starting and stopping temperatures, which represent standard deviations are set to high and low values respectively initially. The temperature is reduced by a factor of c each time where c, is given by the relation

$$c = e^{\frac{\ln(stop\ /\ start)}{n-1}} \qquad (5\text{-}9)$$

Where start and stop are the starting and the stopping standard deviations n the number of temperatures. The starting weights are estimated by using the simulated annealing algorithm. The conjugate gradient algorithm then finds the local minima rapidly. Once there, simulated annealing casts about and trying to escape to a lower point. This alternation is continued until we are unable to escape from the local minima. Another point to note is that a limit has been set on the size of weights so that extremely large activation levels can be avoided. Should there be no limit on the size of the weights then any updating of the weights may not have any effect, as the weights may be either extremely large or small, hence the limit.

5.2 Neural Network Model for Low DO Experiments

5.2.1 Training the Network

A set of eighteen experiments (E-7 to E-23) was spilt into two sets – training and test data. Table 5.1 gives the data used to train the neural network model to predict the duration of the length of the diauxic lag in hours. Inputs to the neural network include biomass in terms of absorbance at the start of the experiment, duration of the aeration phase in hours and concentration of dissolved oxygen in mg/l (as in Figure 5.2). All the training data was normalized and then passed to the network. The number of nodes in the hidden layer was varied and the mean squared errors recorded (Figure 5.3). The mean square error was the lowest when the number of nodes in the hidden layer was three. The weights after training were saved and were used to test the network. Figure 5.4 shows the results when the training data was passed back to the neural network to verify if the network had learnt all the experimental data presented to it.

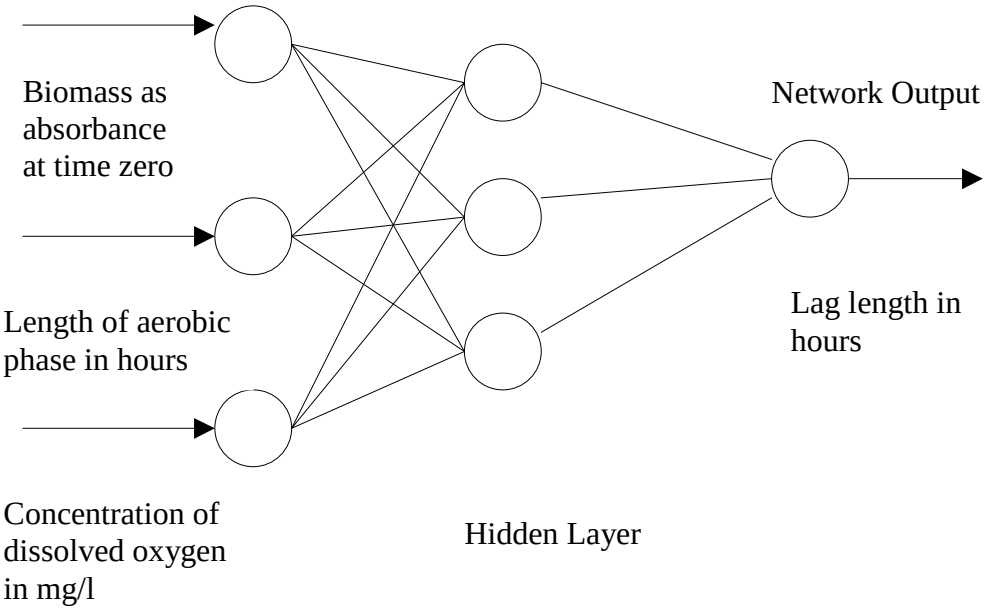

Figure 5.2: Neural network used to predict the duration of the diauxic lag for low DO experiments

Table 5.1. Training data for neural network model for low DO experiments

	Inputs to Network			Desired Output
Experiment Number	Length of Aerobic Phase (hrs)	Biomass in terms of absorbance at time zero	DO Concentration (mg/l)	Length of diauxic lag (hrs)
E-7	4.250	0.062	8.7 mg/L	2.100
E-7	4.250	0.068	.01 mg/L	0.930
E-8	4.250	0.080	8.7 mg/L	2.800
E-8	4.250	0.080	.01 mg/L	1.300
E-11	4.750	0.052	8.7 mg/L	1.300
E-11	4.750	0.052	.07 mg/L	0.000
E-12	5.250	0.045	8.7 mg/L	6.800
E-12	5.250	0.045	.09 mg/L	1.200
E-13	4.750	0.049	8.7 mg/L	4.900
E-13	4.750	0.051	.09 mg/L	4.200
E-14	5.000	0.047	8.7 mg/L	2.600
E-14	5.000	0.047	.09 mg/L	2.400
E-17	3.167	0.130	8.7 mg/L	3.200
E-17	3.167	0.129	.17 mg/L	1.700
E-18	4.417	0.054	8.7 mg/L	2.800
E-18	4.417	0.054	.17 mg/L	2.800
E-19	3.417	0.067	8.7 mg/L	1.800
E-19	3.417	0.067	.35 mg/L	0.840
E-21	3.833	0.069	8.7 mg/L	3.500
E-21	3.833	0.070	.70 mg/L	0.730
E-22	3.500	0.074	8.7 mg/L	0.580
E-22	3.500	0.076	.70 mg/L	0.430
E-23	3.333	0.077	8.7 mg/L	1.400
E-23	3.333	0.082	.70 mg/L	1.100

5.2.2 Testing the Network

Table 5.2 gives the set of data used to test the network with the weights found after training. Figure 5.5 shows the results of passing the test data to the trained neural network.

Table 5.2. Test data for neural network model for low DO experiments

	Inputs to Network			Desired Output
Experiment Number	Length of Aerobic Phase (hrs)	Biomass in terms of absorbance at time zero	DO Concentration (mg/l)	Length of diauxic lag (hrs)
E-9	4.750	0.052	8.7 mg/L	3.000
E-9	4.750	0.052	.04 mg/L	0.950
E-10	7.750	0.037	8.7 mg/L	7.600
E-10	7.750	0.037	.07 mg/L	4.500
E-15	5.000	0.050	8.7 mg/L	1.200
E-15	5.000	0.050	.09 mg/L	0.850
E-16	4.000	0.065	8.7 mg/L	4.200
E-16	4.000	0.065	.17 mg/L	0.880
E-20	3.417	0.099	8.7 mg/L	1.600
E-20	3.417	0.098	.35 mg/L	1.200

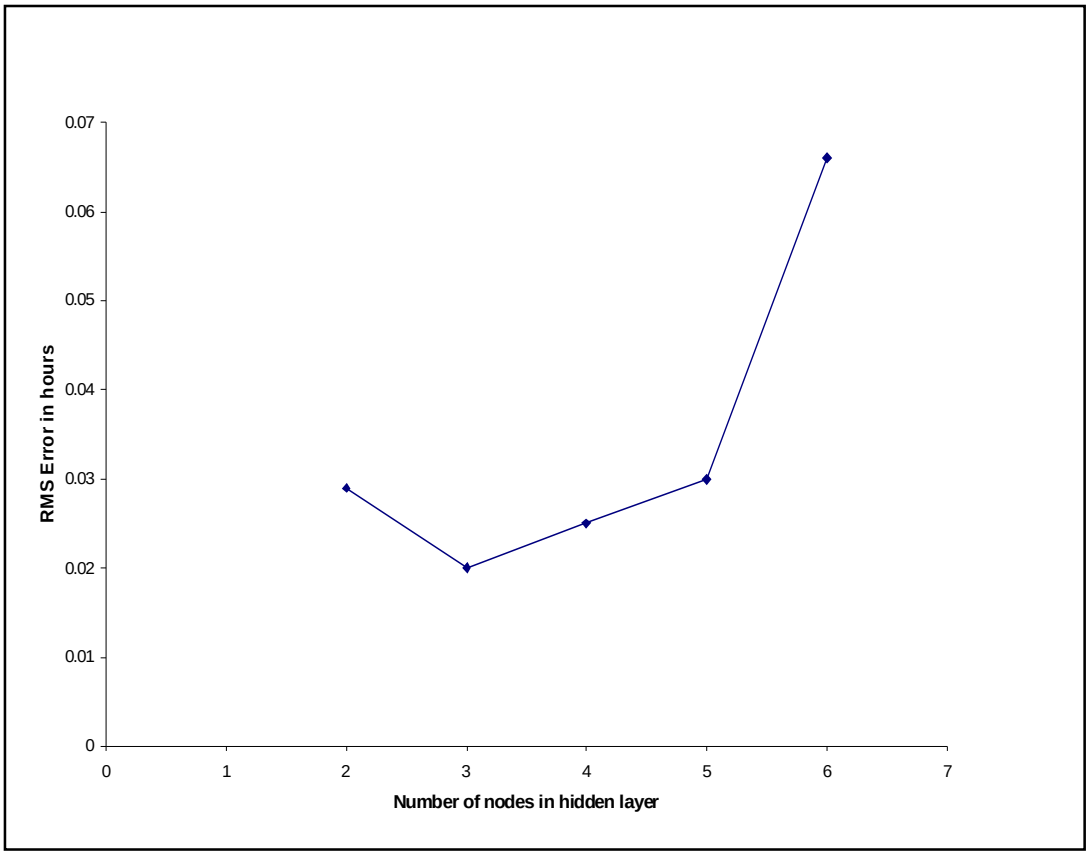

Figure 5.3. Graph showing the variation of root mean square error with the number of nodes in the hidden layer for neural network for low DO experiments

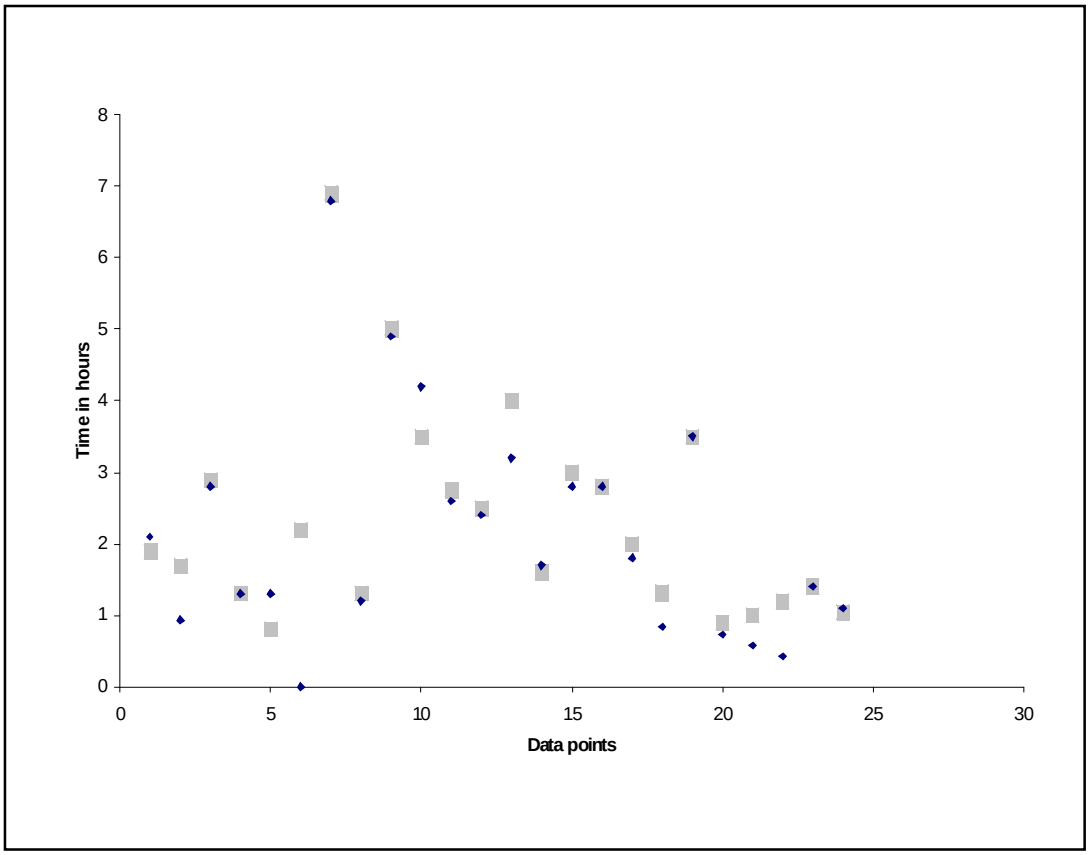

Figure 5.4. Comparison of the output from the neural network and the desired lag length when the training data was passed back to the trained network, for low DO experiments. The following symbols represent the data points in the graph:

Lag Length predicted by the network

Desired Output lag length

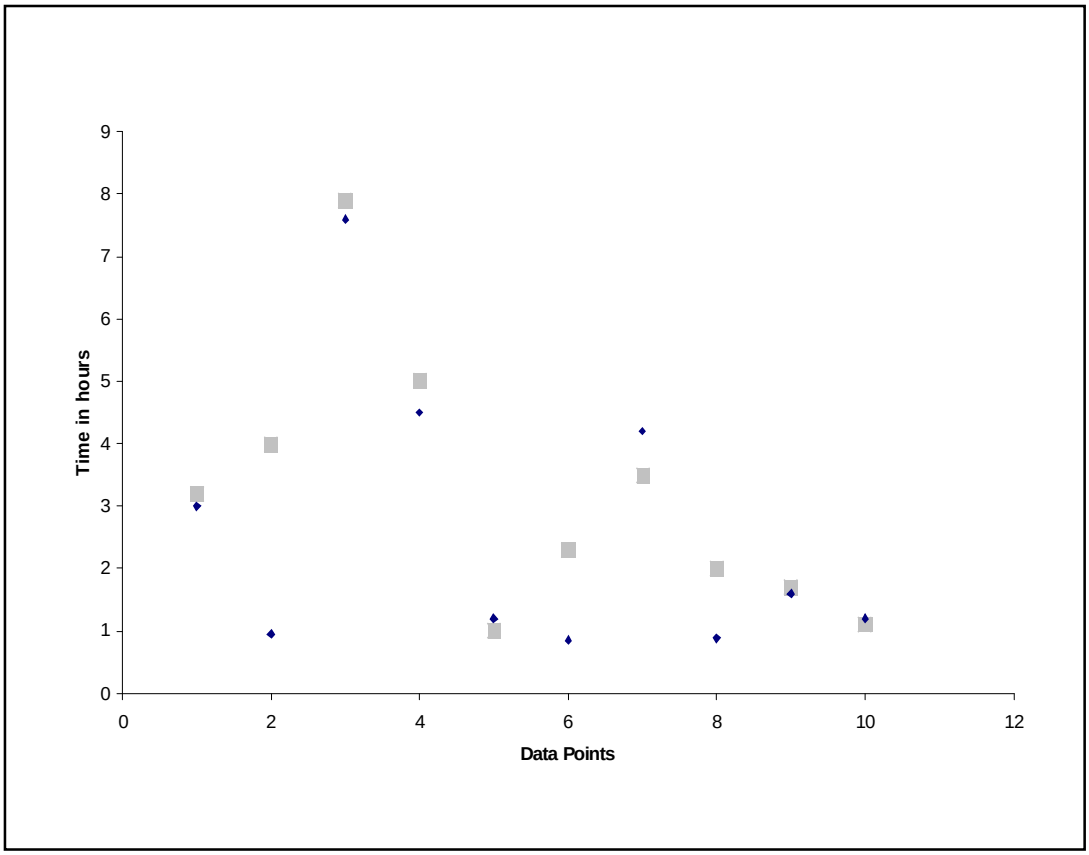

Figure 5.5. Comparison of the output from the neural network and the desired lag length when the test data was passed back to the trained network, for low DO experiments. The following symbols represent the data points in the graph:

▪ Lag Length predicted by the network

◆ Desired Output lag length

5.3 Neural Network Model Preculture Experiments

5.3.1 Training the Network

A set of nine experiments (E-3 to E-6 and E-24 to E-28) was split into two sets – training and test data. Table 5.3 gives the data used to train the neural network model to predict the duration of the length of the diauxic lag in hours. In all these experiments the dissolved oxygen concentration was maintained at 8.7mg/L through the aerobic phase and therefore was not an input to the neural network. Biomass in terms of absorbance at the start of the experiment, duration of the aeration phase in hours and concentration of nitrate in the aerobic phase, reviving phase of the culture were the inputs to the network (Figure 5.6). An oxic reviving phase transalated to an input of zero to the network while an anoxic reviving phase was denoted by an input value of one. All the other inputs were normalized and then passed to the network. The number of nodes in the hidden layer was chosen to be three as that gave the lowest mean square error (Figure 5.7). The weights after training were saved and were used to test the network. Figure 5.8 shows the results when the training data was passed back to the neural network to verify if the network had learnt all the experimental data presented to it.

5.3.2 Testing the Network

Table 5.4 gives the set of data used to test the network with the weights found after training. Figure 5.9 shows the results of passing the test data to the trained neural network.

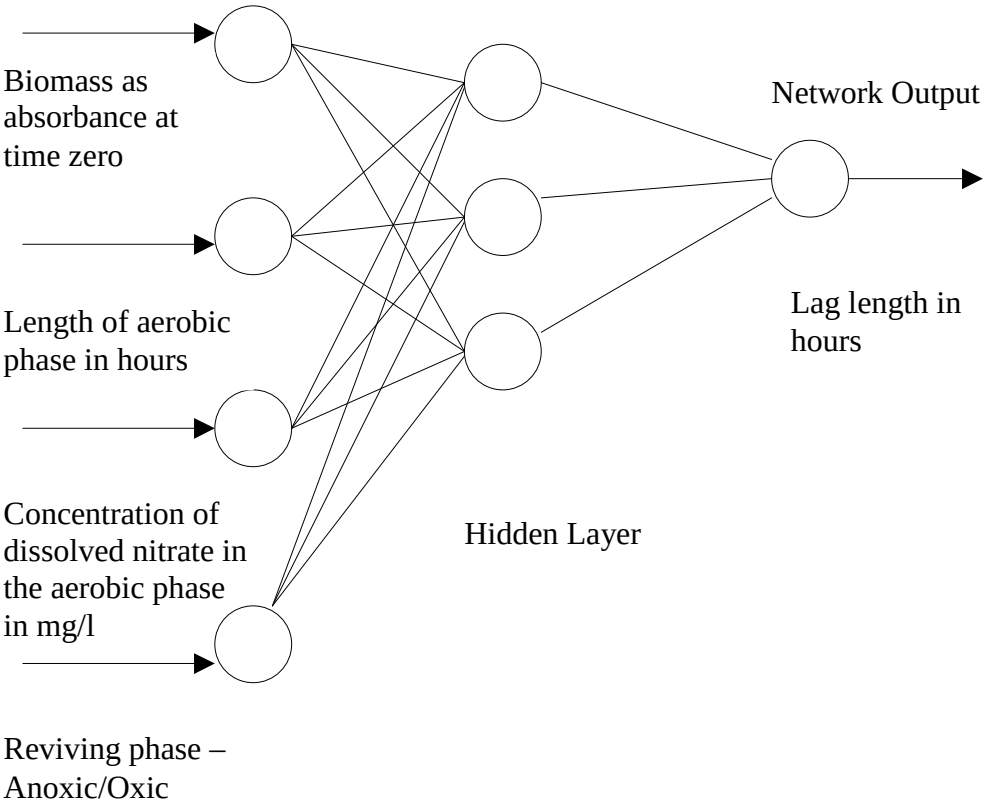

Figure 5.6: Neural network used to predict the duration of the diauxic lag for preculture experiments

Table 5.3. Training data for neural network model for preculture experiments

	Inputs to Network				Desired Output
Experiment Number	Length of Aerobic Phase (hrs)	Reviving phase of the culture	Biomass in terms of absorbance at time zero	Concentration of nitrate in the aerobic phase (g/l)	Length of diauxic lag (hrs)
E-24	5.833	Anoxic	0.030	0	2.500
E-24	5.833	Anoxic	0.030	40	1.167
E-26	8.167	Anoxic	0.040	0	1.500
E-26	8.167	Anoxic	0.040	40	0.333
E-27	9.167	Oxic	0.040	0	7.333
E-27	9.167	Oxic	0.040	40	2.500
E-28	8.333	Anoxic	0.030	0	3.500
E-28	8.333	Anoxic	0.030	40	0.000
E-5	2.500	Oxic	0.035	40	9.333
E-4	1.667	Oxic	0.030	40	5.833

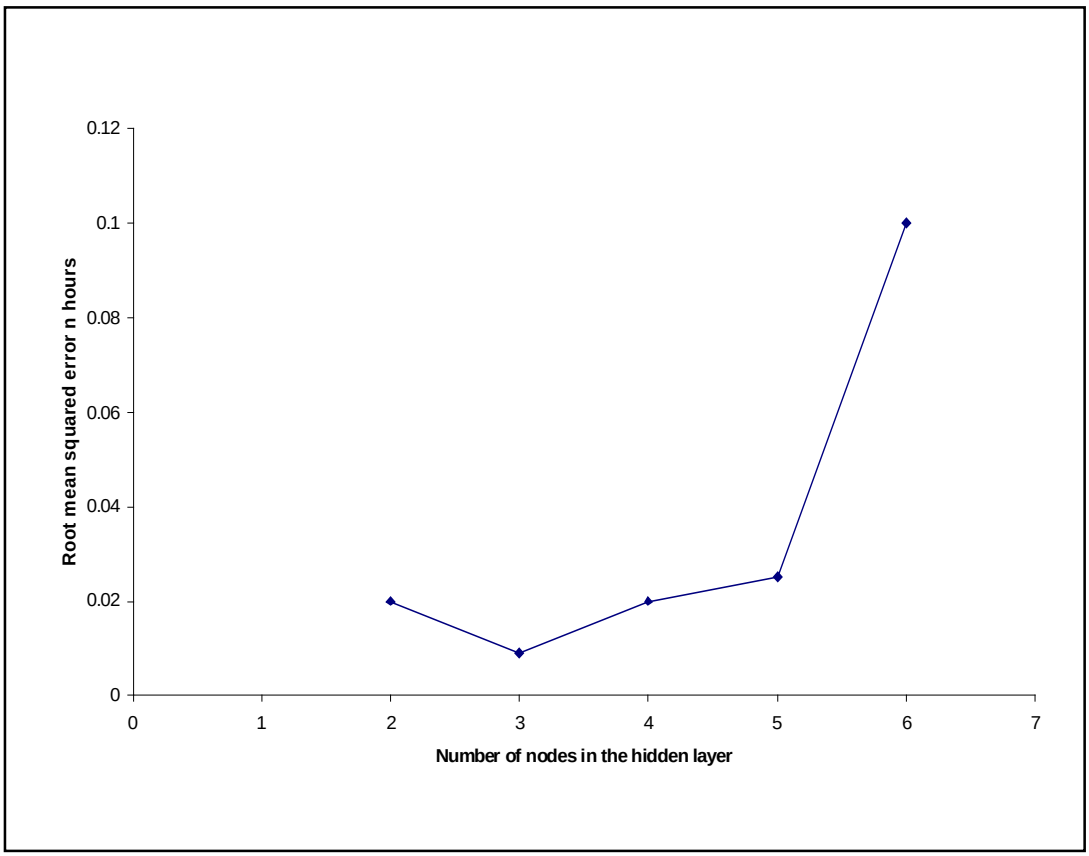

Figure 5.7. Graph showing the variation of root mean square error with the number of nodes in the hidden layer for neural network for preculture experiments

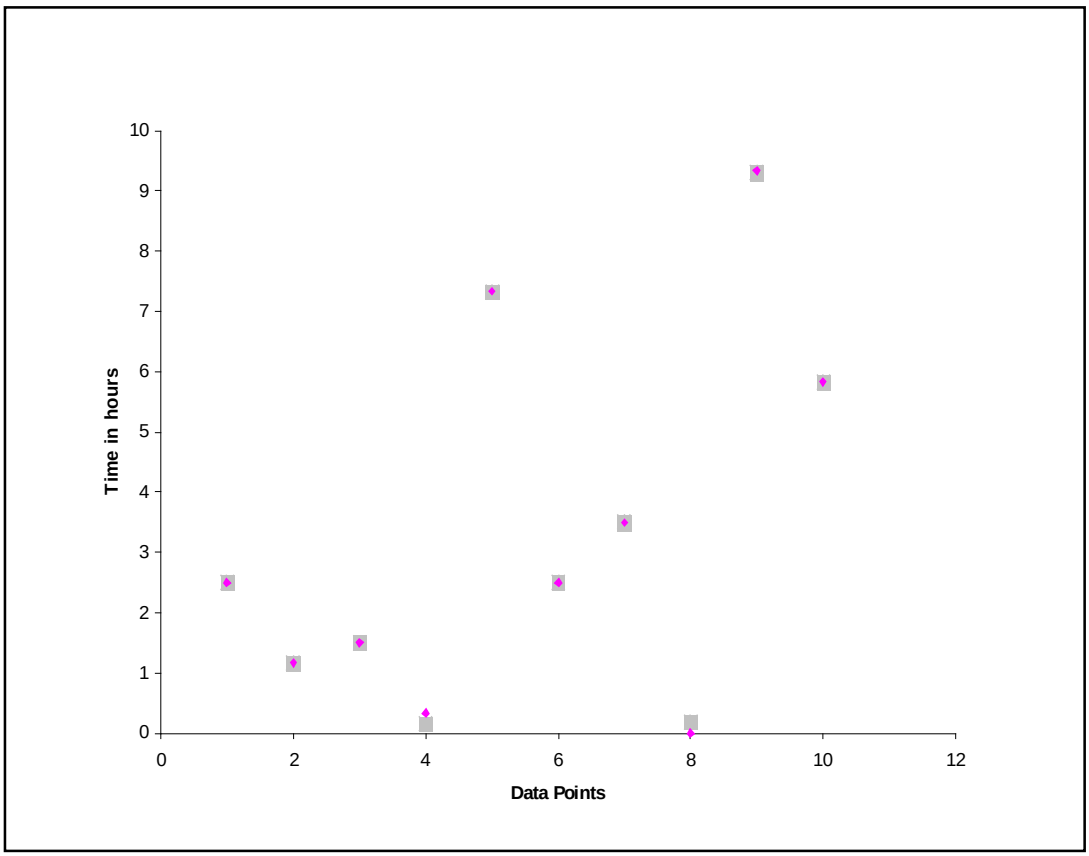

Figure 5.8. Comparison of the output from the neural network and the desired lag length when the training data was passed back to the trained network, for preculture experiments. The following symbols represent the data points in the graph:

- Lag Length predicted by the network
- Desired Output lag length

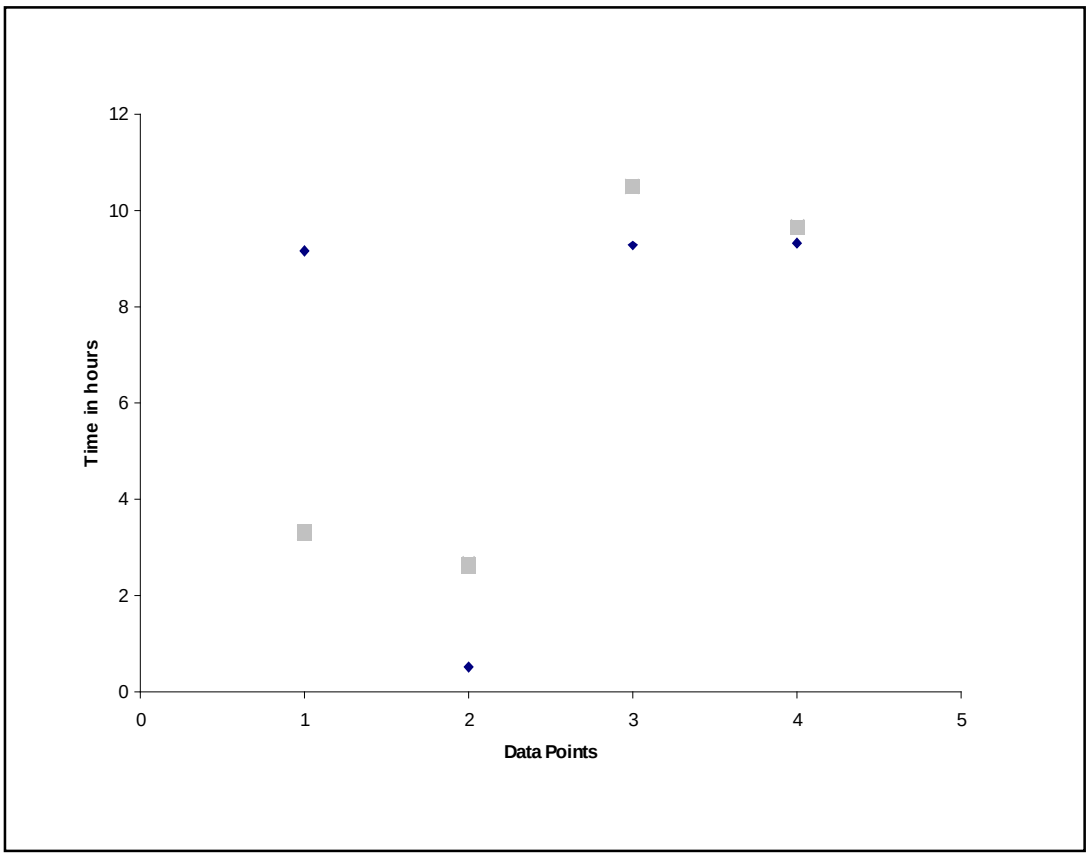

Figure 5.9. Comparison of the output from the neural network and the desired lag length when the test data was passed back to the trained network, for preculture experiments. The following symbols represent the data points in the graph:

Desired Output lag length

Lag Length predicted by the network

Table 5.4. Test data for neural network model for preculture experiments

	Inputs to Network				Desired Output
Experiment Number	Length of Aerobic Phase (hrs)	Reviving phase of the culture	Biomass in terms of absorbance at time zero	Concentration of nitrate in the aerobic phase (g/l)	Length of diauxic lag (hrs)
E-25	4.167	Anoxic	0.040	0	3.333
E-25	4.167	Anoxic	0.040	40	2.667
E-6	2.000	Oxic	0.035	40	10.500
E-3	1.750	Oxic	0.040	40	9.667

5.4 Discussion of Results

The neural network used to predict the diauxic lag lengths for low DO experiments had a larger set of training data than the network used to predict the lag length for preculture experiments. A larger test set of data was useful in that it presented a broader range of data to the network but it did not help in improving the performance of the network due the large variation in experimental data with practically the same input variables. The lowest root mean square error calculated for the training data was 0.02 hours. This can be attributed to the nature of the training data. However the network is able to predict the diauxic lag length with considerable accuracy (Figure 5.5) and predicted shorter diauxies for low DO concentrations compared to high DO concentrations. The network used to train the preculture experimental data had a very small training set size. The lowest root mean square error for the training data set of this network was 0.008 hours with three nodes in the hidden layer. Figure 5.9 shows that the network predicts higher lag lengths for experiments with oxic reviving phase. It could also predict higher lag lengths for bacteria that were not exposed to nitrate in the aerobic phase.

5.5 Hybrid Model

The complete hybrid model uses the material balance model for both the aerobic and anoxic growth phases and the neural network to predict the diauxic lag. The equation governing the aerobic growth with constant specific growth rate is:

$$X_B(t) = X_B(0)\, e^{\mu_O t} \quad (10)$$

Where $X_B(t)$ is the biomass concentration at time t

$X_B(0)$ is the biomass concentration at time zero

And μ_O is the specific growth rate in the aerobic phase

An analogous expression for biomass concentration in the anoxic phase assuming non-limiting nitrate concentrations is given by:

$$X_B(t) = X_B(t_0)\, e^{\mu_N (t-t_0)} \quad (11)$$

Where μ_N is the specific growth rate in the anoxic phase

and t_0 the time at the end of the diauxic lag when exponential growth resumes (anoxic growth curve).

The specific growth (oxic and anoxic) rates used in the model are from Lisbon (2001). Figure 5.10 shows the comparison of the growth curves as predicted by the hybrid model and experimental values for high dissolved oxygen concentrations in the aerobic phase for experiment E-21. In this case the specific growth rates (both oxic and anoxic) of this experiment and the average specific growth rates agree closely. Hence we can see growth curves predicted by the model closely match with the actual experimental data. Figure 5.11 shows a comparison of the growth curves as predicted by the hybrid model and experimental values for low dissolved oxygen concentrations in the aerobic phase for experiment E-21.

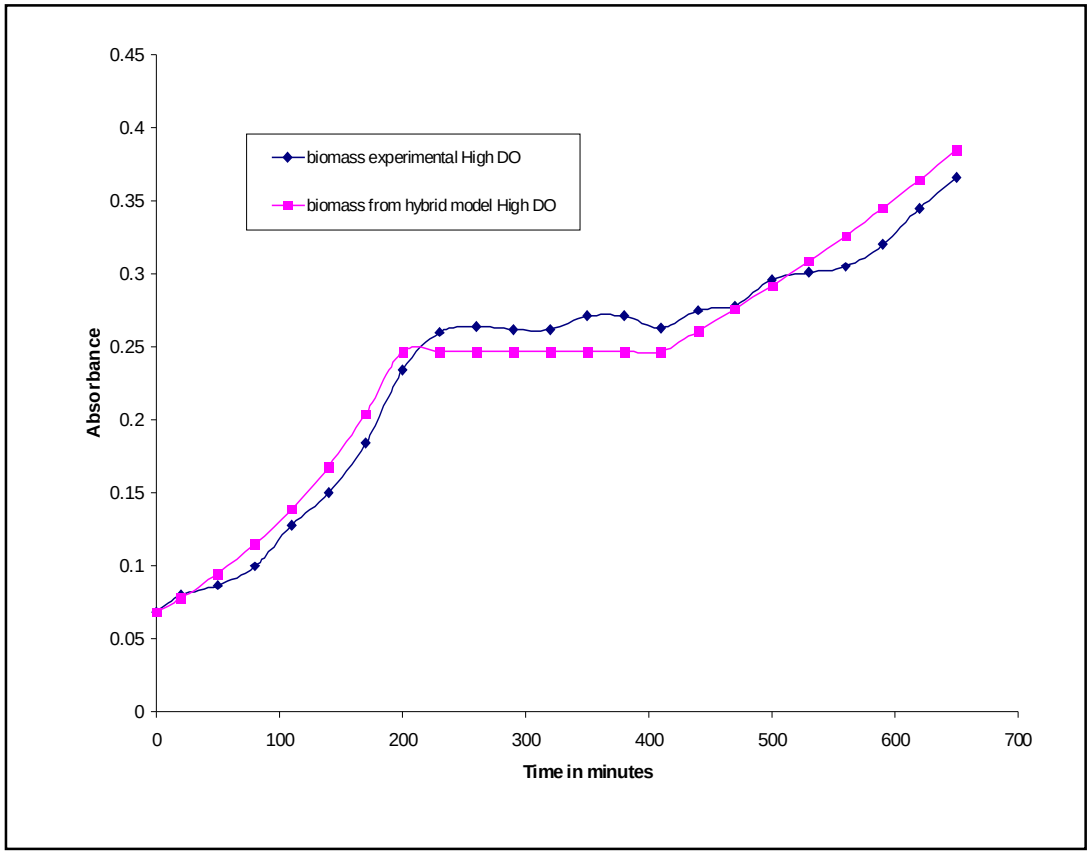

Figure 5.10. Comparison of the growth curves as predicted by the hybrid model and experimental values for high dissolved oxygen concentrations in the aerobic phase for experiment E-21

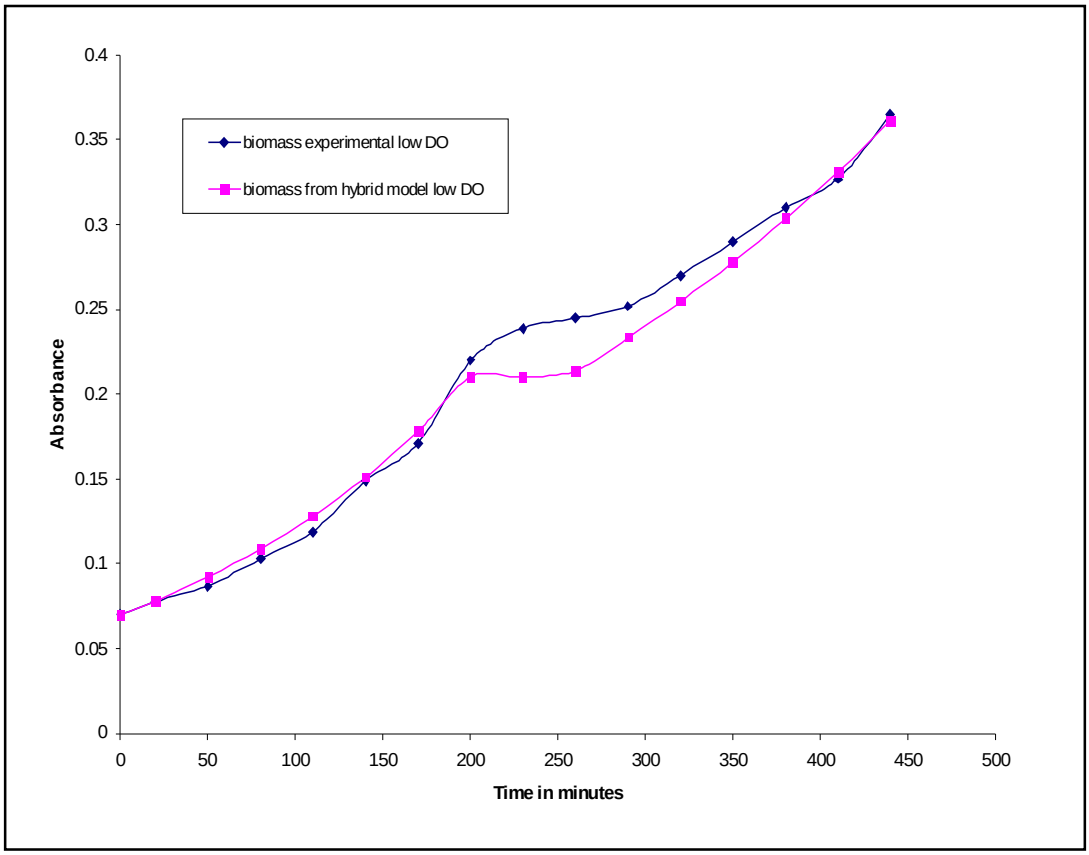

Figure 5.11. Comparison of the growth curves as predicted by the hybrid model and the actual experimental values for low dissolved oxygen (0.7mg/L) concentrations in the aerobic phase for experiment E-21

In experiment E-14 the model prediction doesn't closely agree with the experimental growth curves. This could be attributed several reasons. Firstly, the average specific growth rates are higher than the specific growth rates of this particular experiment. Secondly, the present hybrid model doesn't account for any diauxic lag at the beginning of the aerobic phase. Figure 5.12 shows the comparison of the growth curves as predicted by the hybrid model and experimental values for high dissolved oxygen concentrations in the aerobic phase for experiment E-14. Although the model captures the lag accurately it is not able to capture the aerobic and anoxic growth curves. Figure 5.13 shows the comparison of the growth curves as predicted by the hybrid model and experimental values for low dissolved oxygen concentrations in the aerobic phase for experiment E-14.

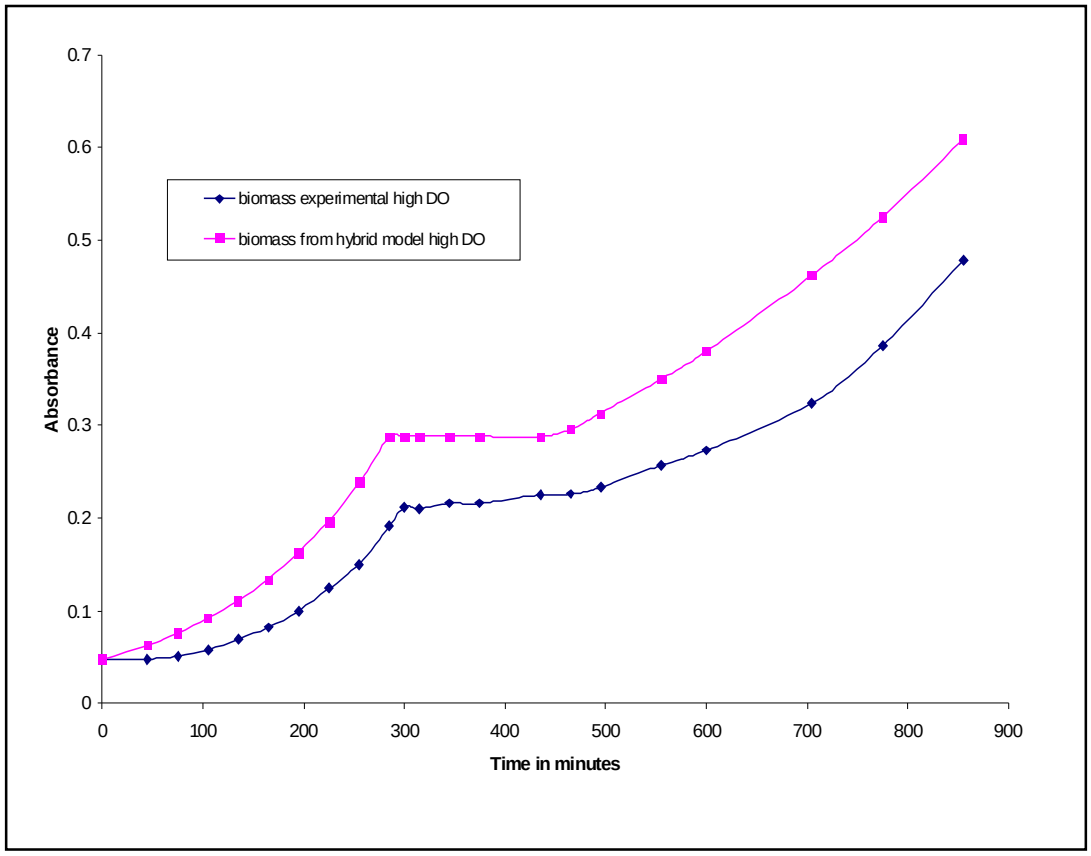

Figure 5.12 Comparison of the growth curves as predicted by the hybrid model and experimental values for high dissolved oxygen concentrations in the aerobic phase for experiment E-14

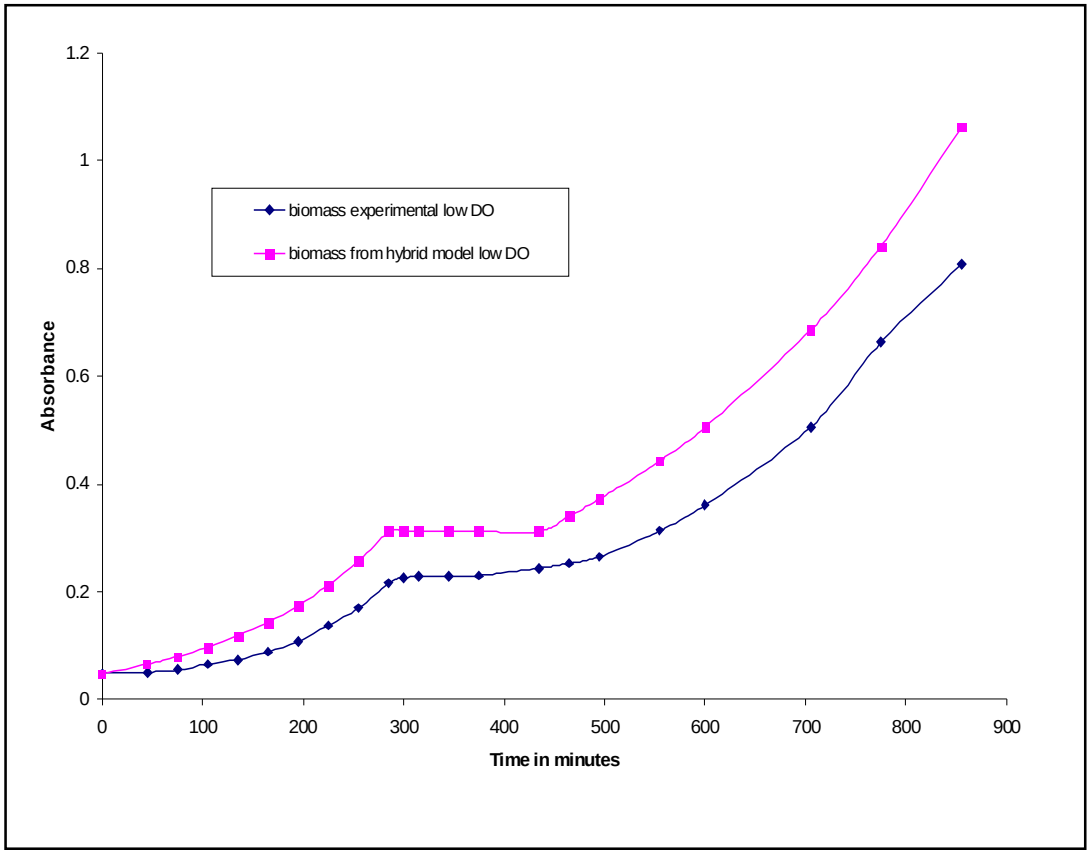

Figure 5.13 Comparison of the growth curves as predicted by the hybrid model and experimental values for low dissolved oxygen concentrations (0.09 mg/L) in the aerobic phase for experiment E-14

CHAPTER 6
CONCLUSIONS AND FUTURE WORK

This research has shown that a neural network model can predict the length of the diauxic lag given certain parameters as inputs. Although the network does not provide any insight into process dynamics or governing equations it certainly is very powerful as it can learn experimental data very quickly. In a typical nitrogen removal plant the entire history of data can be used to train the neural network. Estimation of the length of diauxic lag can have significant economic advantages in treatment plants.

Considerable experimental work needs to be done to expand the size of the data set available for training. A comprehensive network that takes in all parameters such as biomass in terms of absorbance, length of the aeration phase, dissolved oxygen concentrations, nitrate concentrations in aerobic phase to predict the duration of the diauxic lag can be developed. It might also be interesting to replace the duration of the aeration phase and the biomass at time zero with the ratio of the biomass at the end of the aeration phase to the biomass at time zero as an input. This network can then be integrated with the simple Monod type models for both the aerobic and anoxic phases to give a complete hybrid model.

Nitrate reductase enzyme activity through the course of an experiment also remains an unresolved problem. Possible improvisations in the enzyme assay such as freezing the whole cell samples in liquid nitrogen to stop cell activity once withdrawn from the reactor could give more accurate results. A reliable assay for nitrate reductase

and being able to track enzyme activity through the course of an experiment would help a major piece of the puzzle fall into place.

APPENDIX
PROGRAM LISTING

The following program accepts from the user the following information:
Number of nodes in the Input Layer
Number of nodes in the Hidden Layer
Training data file name with extension
Test data file name with extension
Number of data points

The program uses Simulated Annealing coupled with conjugate gradient search to find the point of minima and trains the network for the given training data. Once the network has been trained the test data is passed to the neural network and the results are written to file. Also the weights from the input to hidden layer and hidden to output layer are written to file.

Predefined constants and variable names used:

Variable/Constant name	What it stands for
MAXDATA	Maximum number of data points
MAXINP	Maximum number of input nodes
MAXHID	Maximum number of hidden nodes
STARTTEMP	Starting temperature for the simulated annealing
STOPTEMP	Stopping temperature for the simulated annealing
NTEMPS	Number of iterations to find the best seed value
Wmax	Maximum value of the weights
Wmin	Minimum value of the weights

PROGRAM LISTING

```
// NEURAL NETWORKS CODE - FOR VARIABLE NUMBER OF INPUT NODES
AND SINGLE OUTPUT NODE

// Standard Libraries included

# include <iostream.h>
# include <stdlib.h>
# include <time.h>
# include <ctype.h>
```

```
# include <math.h>
# include <string.h>
# include <stdio.h>

// Constants for Network Architecture

# define MAXDATA 30
# define MAXINP      30
# define MAXHID     30

// Constants for Simulated Annealing

# define GOLDENRATIO 1.618034

// Global variables predefined

float EP =1e-40;
float STARTTEMP = 2;
float STOPTEMP   = 0.2;
int NTEMPS = 2;
float wmax= 5.0;
float wmin= -5.0;
float a =0.9;

// Variables used in the code

int testdata;
int noofdata, inpnodes, hidnodes;
float inpdata[MAXDATA][MAXINP], maxi[MAXINP], mini[MAXINP],
inphidw[MAXINP][MAXHID], hidoutw[MAXHID], desop[MAXDATA];
float hid[MAXHID];
float newihw[MAXINP][MAXHID],
newhow[MAXHID],savihw[MAXINP][MAXHID], savhow[MAXHID];
float deriihw[MAXINP][MAXHID],
derihow[MAXHID],fderiihw[MAXINP][MAXHID], fderihow[MAXHID];
float olddihw[MAXINP][MAXHID], olddhow[MAXHID];
float test[MAXDATA][MAXINP], maxtestdata[MAXINP], mintestdata[MAXINP];

float nw;
float a1,a2,a3;
float nn1,nn2,nn3,enn1,enn2,enn3;
float t1, t2,denom, step, diff, step_err, rms,max_step;
float temp, tempmult;
float nn, op, dho, dhi;
float e,ee, er, error,eee;
```

```
// File variables

FILE *iptr, *optr;
char inpfile[20];
float fvalue;

int i,j,k;
int flag, flagg, giveup;
int seed, bestseed;

//  Function Prototypes

float errorcalfn0();
float errorcalfn1();
float werrorcalfn();
float rnd();

main ()
{

// Accept from user the number of input data file with extension data points,
// Number of input nodes, number of test data points, and hidden nodes.

cout << " \n Neural Networks Model of the Diauxic lag \n" ;

cout << "\n Enter the Name of the Input Data File with Extension : ";
cin >> inpfile;

cout << " \n Enter the Number of Data Points : " ;
cin >> noofdata;

cout << " \n Enter the Number of Input Nodes : ";
cin >> inpnodes;

cout << " \n Enter the Number of Test Data Points : " ;
cin >> testdata;

cout << " \n Enter the Number of Nodes in Hidden Layer : ";
cin >> hidnodes;

// Add a bias to the number of Input and Hidden layer

i= inpnodes+1;
j= hidnodes+1;
```

```
// Read the training data from the data file

iptr = fopen(inpfile, "r");

// Set the bias in the input data to one

for (i=0; i<noofdata;i++)
inpdata[i][0]=1;

// Reading the input data from file into the array

for (i=0; i<noofdata;i++)
 for (j=1; j<=inpnodes;j++)
 {
   fscanf(iptr,"%f",&fvalue);
   inpdata[i][j]=fvalue;
   printf("%f \t",inpdata[i][j]);
 }

// Close the file

fclose(iptr);

// Read the desired output data from user entered data name file with extension

cout << "\n Enter the name of the desired output data file with extension : ";
cin >> inpfile;
iptr = fopen(inpfile, "r");

for (i=0; i<noofdata;i++)
{
          fscanf(iptr,"%f",&fvalue);
   desop[i]=fvalue;
   printf("%f \t",desop[i]);
}

fclose(iptr);

// Accept test data file name from user and read data from file

cout << "\n Enter the name of the test data file with extension : ";
cin >> inpfile;
iptr = fopen(inpfile, "r");
for (i=0; i<testdata;i++)
for (j=1; j<=inpnodes;j++)
{
```

```
            fscanf(iptr,"%f",&fvalue);
   test[i][j]=fvalue;
   printf("%f \t",test[i][j]);
}
fclose(iptr);

// Find the Maximum each vector of the input data

for (j=1; j<=inpnodes;j++)
{
maxi[j]= mini[j]=0;
}

for (j=1; j<=inpnodes;j++)
{
maxi[j]=inpdata[0][j];
for (i=0;i<noofdata;i++)
{
if (inpdata[i][j]>maxi[j])
maxi[j]=inpdata[i][j];
}
}

// Find the Minimum each vector of the input data

for (j=1; j<=inpnodes;j++)
{
mini[j]=inpdata[0][j];
for (i=0;i<noofdata;i++)
{
if (inpdata[i][j]<mini[j])
mini[j]=inpdata[i][j];
}
}

// Scaling the Input data

printf("\n");
for (i=1; i<=inpnodes;i++)
for (j=0; j<noofdata;j++)
{
inpdata[j][i]=(inpdata[j][i]-mini[i])/(maxi[i]-mini[i]);
}

printf("\n scaled values : \n");
for (i=0; i<noofdata;i++)
```

```
for (j=1; j<=inpnodes;j++)
{
printf("%f \t",inpdata[i][j]);
}

// Scaling the Output data

float mindesop, maxdesop;
mindesop=maxdesop=desop[0];
for (i=0; i<noofdata;i++)
{
if (mindesop>desop[i]) mindesop=desop[i];
if (maxdesop<desop[i]) maxdesop=desop[i];
}

for (i=0; i<noofdata;i++)
{
desop[i]= (desop[i]-mindesop)/(maxdesop-mindesop);
}

// To find the maximum each vector of the test data

for (j=1; j<=inpnodes;j++)
{
maxtestdata[j]= mintestdata[j]=0;
}

for (j=1; j<=inpnodes;j++)
{
maxtestdata[j]=test[0][j];
for (i=0;i<testdata;i++)
{
if (test[i][j]>maxtestdata[j])
maxtestdata[j]=test[i][j];
}
}

// To find the minimum each vector of the test data

for (j=1; j<=inpnodes;j++)
{
mintestdata[j]=test[0][j];
for (i=0;i<testdata;i++)
{
if (test[i][j]<mintestdata[j])
mintestdata[j]=test[i][j];
```

```
}
}

// Scaling the test data

printf("\n");
for (i=1; i<=inpnodes;i++)
for (j=0; j<testdata;j++)
{
test[j][i]=(test[j][i]-mini[i])/(maxi[i]-mini[i]);
}

printf("\n scaled values : \n");
for (i=0; i<testdata;i++)
for (j=1; j<=inpnodes;j++)
{
printf("%f \t",test[i][j]);
}

time_t BeginTime, EndTime;
time(&BeginTime);

// Initialization of the weights in the Input-Hidden layer

for(i=1; i<=hidnodes;i++)
for(j=0; j<=inpnodes;j++)
inphidw[j][i]=0;

// Initialization of the weights in the Hidden-Output layer

for(j=0; j<=hidnodes;j++)
hidoutw[j]=0;

// Initial estimation of the error

error = errorcalfn0();

// Simulated Annealing

// Number of iterations to find the best seed

nw= 30*(5*hidnodes+1);

do
{
```

```
flag=0;

// Starting temperature of the simulated annealing

temp=STARTTEMP;

//

tempmult=exp(log(STARTTEMP/STOPTEMP) /(NTEMPS-1));

for(int itemp=0; itemp<NTEMPS;itemp++)
{

flagg=0;

for(k=1;k<=nw;k++)
{

// Set the seed value

seed=k;

// Seed the random number generator

srand((unsigned)seed);

// Set the new hidden output node weights to zero

for(j=0;j<=hidnodes;j++)
newhow[j]=0.0;

// Set the new input hidden node weights to zero

for(j=1;j<=hidnodes;j++)
for(int o=0;o<=inpnodes;o++)
{
newihw[o][j]=0.0;
}

// Evaluate the weights

for(j=0;j<=hidnodes;j++)
{
newhow[j]=hidoutw[j]+temp*rnd();
}
```

```
printf("\n");

for(j=1;j<=hidnodes;j++)
for(int o=0;o<=inpnodes;o++)
{
newihw[o][j]=inphidw[o][j]+temp*rnd();
}

// Check to see if the weight values are within bounds

for(j=0;j<=hidnodes;j++)
{
if (newhow[j]>wmax) newhow[j]=wmax;
if (newhow[j]<wmin) newhow[j]=wmin;
}
for(j=1;j<=hidnodes;j++)
for(int o=0;o<=inpnodes;o++)
{
if (newihw[o][j]>wmax) newihw[o][j]=wmax;
if (newihw[o][j]<wmin) newihw[o][j]=wmin;
}

// Calculate the error with these weights

er=errorcalfn1();

// If the error has improved then this is the best seed found so far

if (er<error)
{
flagg=1;
bestseed=seed;
e=er;
}

} // k loop ends here

// If there was any improvement in error then update the weights with this random
number and seed

if(flagg==1)
{
flag=1;

// Seed the random number generator
```

```
srand(bestseed);

// Weight Updation

for(j=0;j<=hidnodes;j++)
hidoutw[j]=hidoutw[j]+temp*rnd();

for(j=1;j<=hidnodes;j++)
for(int o=0;o<=inpnodes;o++)
inphidw[o][j]=inphidw[o][j]+temp*rnd();

// Check to see if the weight values are within bounds

for(j=0;j<=hidnodes;j++)
{
if (hidoutw[j]>wmax) hidoutw[j]=wmax;
if (hidoutw[j]<wmin) hidoutw[j]=wmin;
}
for(j=1;j<=hidnodes;j++)
for(int o=0;o<=inpnodes;o++)
{
if (inphidw[o][j]>wmax) inphidw[o][j]=wmax;
if (inphidw[o][j]<wmin) inphidw[o][j]=wmin;
}

// Calculate the error with the weights and save it

e=errorcalfn0();

// Reset the random number generator

srand(bestseed/2+999);

} // end if the if flagg (ie) if there was any improvement

// Update the temp value

temp*=tempmult;

} // itemp loop ends here

// If there was an improvement in the error then calculate the error derivatives

if (flag==1)
{
```

```
// Initialize the derivatives to zero

for(j=0;j<=hidnodes;j++)
{
fderihow[j]=0;
derihow[j]=0;
}

for(j=1;j<=hidnodes;j++)
for(int o=0;o<=inpnodes;o++)
{
fderiihw[o][j]=0;
deriihw[o][j]=0;
}

// Testing to see if this new point of reduced error is a local minima

do
{

// Saving the old derivative values

for(j=0;j<=hidnodes;j++)
{
olddhow[j]=derihow[j];
derihow[j]=0;
}

for(j=1;j<=hidnodes;j++)
for(int o=0;o<=inpnodes;o++)
{
olddihw[o][j]=deriihw[o][j];
deriihw[o][j]=0;
}

// New Gradient Calculation for the entire data set

// Computing the values at the hidden layer

for(i=0;i<noofdata;i++)
{
hid[0]=1;

// Computing the values at the hidden layer

for (k=1;k<=hidnodes;k++)
```

```
{
for(j=0;j<=inpnodes;j++)
{
hid[k]=hid[k]+inpdata[i][j]*inphidw[j][k];
}
if (hid[k]<-100) hid[k]=-100;
hid[k]=1.0/(1.0+exp(-hid[k]));
}

// Computing the values at the output layer

op=dho=0;
for(k=0;k<=hidnodes;k++)
{
op=op + hid[k]*hidoutw[k];
}
if (op<-100) op=-100;
op=1.0/(1.0+exp(-op));

// Error at the output layer to be back-propagated

dho=(1.0-op)*(op)*(desop[i]-op);

// Derivate of the weights from hidden to output layer

for(k=0;k<=hidnodes;k++)
{
derihow[k]+=hid[k]*dho;
}

// Derivative of the weights from input to hidden layer

for(j=1;j<=hidnodes;j++)
{
dhi=hid[j]*(1-hid[j])*dho*hidoutw[j];
for(int o=0;o<=inpnodes;o++)
deriihw[o][j]+=dhi*inpdata[i][o];
}

} // i loop ends here

// Conjugate Gradient Calculation

for(k=0;k<=hidnodes;k++)
{
a1 += olddhow[k]*olddhow[k];
```

```
a2 += derihow[k]* derihow[k];
a3 += derihow[k]* olddhow[k];
}

for(j=1;j<=hidnodes;j++)
for(int o=0;o<=inpnodes;o++)
{
a1 += olddihw[o][j]*olddihw[o][j];
a2 += deriihw[o][j]*deriihw[o][j];
a3 += deriihw[o][j]*olddihw[o][j];
}

if (a1!=0)
a= (a2-a3)/a1;
else
a=0;

// Gradient Calculation

for(k=0;k<=hidnodes;k++)
{
fderihow[k]=derihow[k]+ a*fderihow[k];
}

for(j=1;j<=hidnodes;j++)
for(int o=0;o<=inpnodes;o++)
{
fderiihw[o][j]=deriihw[o][j]+ a*fderiihw[o][j];
}

// Save the old weights for backup

for(k=0;k<=hidnodes;k++)
{
savhow[k]=hidoutw[k];
}

for(j=1;j<=hidnodes;j++)
for(int o=0;o<=inpnodes;o++)
{
savihw[o][j]=inphidw[o][j];
}

nn=5;

// Calculate the error for these updated weights
```

```
do
{
nn=nn/2;
eee= werrorcalfn();
} while (eee>e);

nn1=0.0;
nn2=nn;
enn1=e;
enn2=eee;
nn3=nn2+GOLDENRATIO*nn;
enn3=werrorcalfn();

// Parabolic Fit to estimate the Local Minima

while (enn3<enn2)
{

t1=(nn2-nn1)*(enn2-enn3);
t2= (nn2-nn3)*(enn2-enn1);
denom=2.0*(t2-t1);

if ((fabs( denom ) < EP) && (denom>0.0))
{denom=EP;}
else {denom=-EP;}

// Step calculation and max step to see that we don't jump too far

step = nn2 + ((nn2-nn1)*t1 - (nn2-nn3)*t2)/denom;
max_step=nn2+200.0*(nn3-nn2);

// If its between nn1 and nn2
// Then nn3  shifts to nn2
// And nn2 is the intermediate value step

if ((nn2-step)*(step-nn1)>0.0)
{
// calculate the error
step_err= werrorcalfn();
nn3=nn2;
nn2=step;
enn3=enn2;
enn2=step_err;
goto NEXTTEST;
}
```

```
// if its between nn2 and nn3

else if ((nn2-step) * (step-nn3) >0.0)
{
step_err= werrorcalfn();

// nn1  shifts to nn2
// and nn2 is the intermediate value step

if (step_err<enn3)
{
nn1=nn2;
nn2=step;
enn1=enn2;
enn2=step_err;
goto NEXTTEST;
}

// the point is to the left of nn3
// shift nn3 to step

else if (step_err>enn2)
{
nn3=step;
enn3=step_err;
goto NEXTTEST;
}

// if it is out of the range simply apply the golden ratio rule

else
{
step=nn3+GOLDENRATIO*(nn3-nn2);
step_err = werrorcalfn();
}

}

// if the step value is to the right of nn3

else if ((nn3-step) * (step-max_step)>0.0)
{
step_err= werrorcalfn();

// shift nn2 to nn3 and nn3 to step
```

```
if (step_err<enn3)
{
nn2=nn3;
nn3=step;
step=nn3+GOLDENRATIO*(nn3-nn2);
enn2=enn3;
enn3=step_err;
step_err=werrorcalfn();
}

}

// step may be even beyond max step

else if ((step-max_step) * (max_step-nn3)>=0.0)
{
step=max_step;
step_err= werrorcalfn();

if (step_err<enn3)
{
nn2=nn3;
nn3=step;
step=nn3+GOLDENRATIO*(nn3-nn2);
enn2=enn3;
enn3=step_err;
step_err=werrorcalfn();
}

}

// use golden ratio to update the step values

else
{
step= nn3+ GOLDENRATIO*(nn3-nn2);
step_err=werrorcalfn();
}

nn1=nn2;
nn2=nn3;
nn3=step;
enn1=enn2;
enn2=enn3;
enn3=step_err;
```

```
}


// Code jumps here if we have made one improvisation

NEXTTEST:
giveup=0;

do
{
t1=(nn2-nn1)*(enn2-enn3);
t2=(nn2-nn3)*(enn2-enn1);
denom=2.0*(t2-t1);

if (fabs( denom ) < EP)
{
if (giveup==1) { giveup=2;}
if (giveup==0) { giveup=1;}

if (denom>0.0)
denom=EP;
else denom=-EP;
}

// Narrow down the search for minima until the error reduces below the threshold
required

step=nn2 + ((nn2-nn1)*t1 - (nn2-nn3)*t2)/denom;
step_err=werrorcalfn();

if ((nn2-step) * (step-nn1) >0.0)
{
nn3=nn2;
nn2=step;
enn3 =enn2;
enn2=step_err;
}
else if ((nn2-step) * (step-nn3) >0.0)
{
nn1=nn2;
nn2=step;
enn1=enn2;
enn2=step_err;
}
else break;
```

```
if (giveup==2) break;

} while (fabs(nn3-nn1)>0.00001);

eee=werrorcalfn();
printf(" Error (eee) : %f \n",eee);
diff = e-eee;
printf("diff : %f \n ",diff);

e=eee;
} while (fabs(eee) > 0.000001);
}

STARTTEMP=2;
STOPTEMP=2;
NTEMPS=0;

} while (flag==1);

// Clocks the time taken for the training

time (&EndTime);

printf("Time Elapsed in seconds : %lu \n ", EndTime-BeginTime);
printf("Sum of Error Squared : %f \n ", eee);

rms = sqrt(eee/noofdata);
printf("Unscaled Root Mean Squared Error : %f \n ", rms);

// Writing the final weights to file

optr= fopen("weights.dat", "w");

for(k=0;k<=hidnodes;k++)
{
fprintf(optr, "%f \t " , hidoutw[k]);
}
fprintf(optr, "\n ");

for(j=1;j<=hidnodes;j++)
for(int o=0;o<=inpnodes;o++)
{
fprintf(optr, "%f \t " ,inphidw[o][j]);
}
```

```
fprintf(optr, "Unscaled Root Mean Squared Error : %f \n ", rms);

// Writing the results of passing back the training data to file

for(i=0;i<noofdata;i++)
{
hid[0]=1;
for (k=1;k<=hidnodes;k++)
{
for(j=0;j<=inpnodes;j++)
{
hid[k]=hid[k]+inpdata[i][j]*inphidw[j][k];
}
if (hid[k]<-100) hid[k]=-100;
hid[k]=1.0/(1.0+exp(-hid[k]));
}

op=0;
for(k=0;k<=hidnodes;k++)
{
op=op + hid[k]*hidoutw[k];
}
if (op<-100) op=-100;
op=1.0/(1.0+exp(-op));
op=op*(maxdesop-mindesop)+(mindesop);
fprintf(optr, "%f \n " ,op);
}

fprintf(optr, "Unscaled Root Mean Squared Error : %f \n ", rms);

// Evaluation of network performance for the test data

for(i=0;i<testdata;i++)
{
hid[0]=1;
for (k=1;k<=hidnodes;k++)
{
for(j=0;j<=inpnodes;j++)
{
hid[k]=hid[k]+test[i][j]*inphidw[j][k];
}
if (hid[k]<-100) hid[k]=-100;
hid[k]=1.0/(1.0+exp(-hid[k]));
}

op=0;
```

```
for(k=0;k<=hidnodes;k++)
{
op=op + hid[k]*hidoutw[k];
}
if (op<-100) op=-100;
op=1.0/(1.0+exp(-op));
op=op*(maxdesop-mindesop)+(mindesop);
fprintf(optr, "%f \n " ,op);
}

fprintf(optr, "Unscaled Root Mean Squared Error : %f \n ", rms);

fclose(optr);

} //end of main



// Function Errorcal to calculate the error with the present set of weights

float errorcalfn0()
{
int ii,jj,kk;
float fn0ee=0,op=0,fn0eee=0;
for (kk=1;kk<=hidnodes;kk++)
hid[kk]=0.0;

for (ii=0; ii<noofdata;ii++)
{
hid[0]=1;
for (kk=1;kk<=hidnodes;kk++)
{
for(jj=0;jj<=inpnodes;jj++)
{
hid[kk]=hid[kk]+inpdata[ii][jj]*inphidw[jj][kk];
}
if (hid[kk]<-100) hid[kk]=-100;
hid[kk]=1.0/(1.0+exp(-hid[kk]));
}

op=0;
for(kk=0;kk<=hidnodes;kk++)
{
op=op + hid[kk]*hidoutw[kk];
}
if (op<-100) op=-100;
```

```
op=1.0/(1.0+exp(-op));

fn0ee=0;
fn0ee=(desop[ii]-op)*(desop[ii]-op);
fn0eee+=fn0ee;
}

return fn0eee;
}

// Function same as above with the new weights

float errorcalfn1()
{
int ii,jj,kk;
float fn1ee=0,fn1eee=0,op=0;

for (kk=1;kk<=hidnodes;kk++)
hid[kk]=0.0;

for (ii=0; ii<noofdata;ii++)
{
hid[0]=1;
for (kk=1;kk<=hidnodes;kk++)
{
for(jj=0;jj<=inpnodes;jj++)
{
hid[kk]=hid[kk]+inpdata[ii][jj]*newihw[jj][kk];
}
if (hid[kk]<-100) hid[kk]=-100;
hid[kk]=1.0/(1.0+exp(-hid[kk]));
}

op=0;
for(kk=0;kk<=hidnodes;kk++)
{
op=op + hid[kk]*newhow[kk];
}
if (op<-100) op=-100;
op=1.0/(1.0+exp(-op));

fn1ee=0;
fn1ee=(desop[ii]-op)*(desop[ii]-op);
fn1eee+=fn1ee;
}
```

```
return fn1eee;
}



// Function to calculate the error in the conjugate gradient module

float werrorcalfn()
{

int ii,jj,kk,oo;
float wee=0,weee=0;

for(kk=0;kk<=hidnodes;kk++)
{
hidoutw[kk]=savhow[kk]+ nn*fderihow[kk];
}

for(jj=1;jj<=hidnodes;jj++)
for(int oo=0;oo<=inpnodes;oo++)
{
inphidw[oo][jj]=savihw[oo][jj]+ nn*fderiihw[oo][jj];
}

for (ii=0; ii<noofdata;ii++)
{
hid[0]=1;
for (kk=1;kk<=hidnodes;kk++)
{
for(jj=0;jj<=inpnodes;jj++)
{
hid[kk]=hid[kk]+inpdata[ii][jj]*inphidw[jj][kk];
}
if (hid[kk]<-100) hid[kk]=-100;
hid[kk]=1.0/(1.0+exp(-hid[kk]));
}

op=0;
for(kk=0;kk<=hidnodes;kk++)
{
op=op + hid[kk]*hidoutw[kk];
}
if (op<-100) op=-100;
op=1.0/(1.0+exp(-op));

wee=0;
```

```
wee=(desop[ii]-op)*(desop[ii]-op);
weee+=wee;
}

return weee;
}

// Random number generator

float rnd()
{
time_t t;
srand((unsigned) time(&t));
float rnd=0.0;
float RANDMAX=pow(2,15)-1.0;
rnd=((float)rand()+ (float) rand() -(float) rand()- (float) rand())/(2.0* (float)RANDMAX)
* 3.464101615;
return (rnd);
}
```

LIST OF REFERENCES

Aida T., Hata S., and Kusonoki H. (1984) Temporary Low Oxygen Conditions for the Formation of Nitrate Reductase and Nitrous Oxide Reductase by Denitrifying *Pseudomonas* sp. G59, *Canadian Journal of Microbiology*, **32**, 543-547.

Baloo S. and Ramkrishna D. (1991) Metabolic Regulation in Bacterial Continuous Cultures: II, *Biotechnology and Bioengineering*, **38**, 1353-1363.

Dodd J. R. and Bone H.(1975), Nitrate Reduction by Denitrifying Bacteria in Single and Two Stage Continous Flow, *Water Res.*, **9**, 323-328.

Häck M. and Köhne M. (1999) Estimation of Wastewater Process Parameters using Neural Networks, *Water Science and Technology*, **33**, 101-115.

Hamilton W. A. and Dawes E. A. (1959) A Diauxic Effect with *Pseudomonas aeruginos. The Biochemical Journal*, **71**, 25P-26P.

Henze M., Grady C.P.L., Gujer W., Marais G. V. R., and Matsuo T. (1987) Activated Sludge Model No. 1. *IAWPRC Scient. Tech. Rep. No. 1*. IAWPRC London, U.K.

Henze M., Gujer W., Mino T., Matsuo T. and Wentzel M.C. (1995) Activated Sludge Model No. 2. *IAWPRC Scient. Tech. Rep. No. 3.* IAWPRC London, U.K.

Hurd C. L. Berges J. A., Osborne J., and Harrison P. J. (1995) Optimization and Characterization of the Enzyme for Fucus Gardneri (Phaeophtyta) *Journal of Pharmacology*, **31**, 835.

Kamara A., Bernard O., Genovesi A., Dochain D., Benhammou A., Steyer J.P., (2000) Hybrid Modelling of Anaerobic Wastewater Treatment Processes, *Water Science & Technology*, **43**, 43–50.

Kodama T., Shimada K., and Mori T. (1969) Studies on Anaerobic Biphasic Growth of a Denitrifying Bacterium *Pseudomonas stutzeri*, *Plant & Cell physiology*, **10**, 855-865.

Koike I. and Hattori A. (1975) Growth yield of a Denitrifying Bacterium, *Pseudomonas denitrificans*, under Aerobic and Denitrifying Conditions, *Journal of General Microbiology*, **88,** 1-10.

Komapala D.S., Ramakrishna D., Jansen B.B., and Tsao G.T. (1986) Investigation of Bacterial Growth on Mixed Substrates: Experimental Evaluation of Cybernetic Models, *Biotechnology and Bioengineering,* **28**, 1044-1055

Kornaros M. and Lybertos G. (1998) Kinetic Modelling of *Pseudomonas denitrificans* Growth and Denitrification Under Aerobic, Anoxic, and Transient Operating Conditions, *Water Environment Research*, **32**, 6, 1912-1922.

Kornaros M., Zafiri C., and Lybertos G. (1996) Kinetics of denitrication by *Pseudomonas denitrificans* under Growth Conditions Limited by Carbon and/or Nitrate or Nitrite, *Water Environment Research*, **68**, 5, 934-945.

Korner H. and Zumft W. G. (1989) Expression of Denitrification Enzymes in Response to the Dissolved Oxygen Level and Respiratory Substrate in Continous Culture of *Pseudomonas stutzer*, *Applied and Environmental Microbiology* **55**, 7, 1670-1676.

Krul J. M. and Veeningen R. (1977) The Synthesis of the Dissimilatory Nitrate Reductase Under Aerobic Conditions In a Number of Denitrifying Bacteria Isolated from Activated Sludge and Drinking Water, *Water Research*, **11**, 39-43.

Lee I. H., Fredrickson A. G., and Tsuchiya H. M. (1974) Diauxic Growth of *Propionibacterim shermanii, Applied Microbiology*, **11**, 39-43.

Li M. F. (1994) *Neural Networks in Computer Intelligence*, McGraw Hill, Inc., New York.

Lisbon K., McKean M., Shekar S., Svoronos S., and Koopman B. (2001) Diauxic Lag of *Pseudomonas denitrificans* in Transition from Oxic to Anoxic Growth: Effect of Dissolved Oxygen Concentration, *Journal of Environmental Engineering* (Under publication).

Liu P., Potter T., Svoronos S. A., and Koopman B. (1995) Hybrid Model of Nitrogen Dynamics in a Periodic Wastewater Treatment Process, Presented at *1995 AIChE Annual Meeting*, Miami Beach, FL.

Liu P., Zhan G., Svoronos S. A., and Koopman B. (1996) Cybernetic Approach to Modelling Denitrification in Activated Sludge, Presented at *1996 AIChE National Meeting*, Chicago.

Liu P., Zhan G., Svoronos S. A., and Koopman B. (1998a) Diauxic Lag from Changing Electron Acceptors in Activated Sludge Treatment, *Water Research* 32, **11**, 3452-3460.

Liu P., Svoronos S. A., and Koopman B. (1998b) Experimental and Modeling Study of Diauxic Lag of *Pseudomonas denitrificans* Switching from Oxic to Anoxic Conditions, *Biotechnology and Bioengineering*, **60**, 6, 649-655.

Marshall R. O., Dishburger H. J., MacVicar R., and Hallmark, G. D. (1953) Studies on the Effect of Aeration on Nitrate Reduction by Pseudomonas Species using N^{15}, *Journal of Bacteriology*, **64**, 254-258.

Masters T. (1993) *Practical Neural Network Recipies in C++*, Academic Press, New York.

Monod J. (1942) Recherches sur la Croissance des Cultures Bacteriennes, *Actualites Scientifique et Industrielles*, **911**, 1-215.

Monod J. (1947) The Phenomenon of Enzymatic Adaptation and Its Bearings on Problems of Genetic and Cellular Differentiation, *Growth*, **11**, 223-289.

Monod J. (1949) The Growth of Bacterial Cultures, *Annual Review of Microbiology*, **3,** 371-394.

Payne W. J. (1981) *Denitrification*, Wiley, New York.

Payne W. J. (1983) Bacterial Denitrification: Asset of Defect? *Bioscience*, **33**, 5, 319-325.

Ramakrishna D. (1982) A Cybernetic Perspective of Microbial Growth in Foundations of Biochemical Engineering, in *Kinetics and Thermodynamics in Biological Systems*, Papoutsakis E. I., Stephanopolous G. T., and Blanch H. W., Eds American Chemical Society, Washington, D.C., 161-178.

Ramkrishna D., Kompala D. S., and Tsao G. T. (1984) Cybernetic Modeling of Microbial Populations, in *Frontiers of Chemical Reaction Eng.*, Doriaswamy L. K., Eds. Wiley Eastern Limted, New Delhi.

Ramkrishna D., Kompala D. S., and Tsao G. T. (1987) Are Mircobes Optimal Strategists? *Biotechnology Process*, **3**, 3, 121-126.

Ramakrishna D., Ramkrishna R. and Konopka A.E.(1995) Cybernetic Modelling of Growth in Mixed, Substitutable Substrate Environments. Preferential and Simultaneous Utilization, Presented at 1995 *AIChE National Meeting*, Miami Beach.

Sadana A. and Raju R. R. (1990) Stability Index for Enzymes Deactivating by Different Mechanisms, *Journal of Biotechnol.*, **13**, 327-335.

Schulp J. A. and Stouthamer A. H. (1970) The Influence of Oxygen, Glucose and Nitrate upon the Formation of Nitrate Reductase and the Respiratory System in *Bacillus licheniformis, Journal of General Microbiolgy*, **64**, 195-203.

Simpkin T. J. and Boyle W. C. (1988) The Lack of Repression By Oxygen of the Denitrifying Enzymes in Activated Sludge, *Water Research*, **22**, 2, 201-206.

Standing C. N., Fredrickson A. G., and Tsuchiya H. M (1972) Batch and Continous-Culture Transients for Two Substrate Systems, *Applied* Microbiology, **23**, 2, 354-359.

Steinberg N. A., Blum J. S., Hochestein L., and Oremland R. S. (1992) Nitrate Is a Preferred Electron Acceptor for Growth of Freshwater Selenate-Respiring Bacteria, *Applied and Environment Microbiology*, **58**, 426-428.

Stouthamer A. H. (1980) Bioenergetic studies on Paracoccus denitrificans, *Trends in Biochemical Sciences*, **5**, 164-166.

Straight J. V. and Ramakrishna D. (1991) Complex Growth Dynamics in Batch Cutltures: Experiments and Cybernetic Models, *Biotechnol. Bioeng*., **37**, 895-909.

Straight J. V. and Ramakrishna D. (1994) Cybernetic Modelling and Regulation of Metabolic Pathways. Growth on Complimentary Nutrients, *Biotechnol*. *Prog*. **10**, 574-587.

Tay J. H. and Zhang X. (1999) Neural Fuzzy Modeling of Anaerobic Biological Wastewater Treatment Systems, *Journal of Environmental Engineering*, **125**, 1149-1159.

Zhao H., Issacs S. H., Soeberg H., and Kummel M. (1994) A Novel Control Stratergy for Improved Nitrogen Removal in an Alternating Activated Sludge Process-Part I. Process Analysis, *Water Research*, **28**, 521-534.

Zhao H., Isaacs S.H., Spielberg H. and Kummel M., (1994) Novel Control Strategy for Improved Nitrogen Removal in an Alternating Activated Sludge Process-Part II. Control Development, *Water Research*, **28**, 535-542.

Zhao H., Hao O.J. and McAvoy J. T., (1999) Approaches to Modeling Nutrient Dynamics: ASM2, Simplified Model and Neural Nets, *Water Science and Technology*,**39**, 227-234.

BIOGRAPHICAL SKETCH

Sangeetha Shekar was born on June 20th, 1977, in Madras, India. She received her bachelor's degree in chemical engineering from Birla Institute of Technology and Sciences, Pilani, India. In 1998, she was accepted to the University of Florida to pursue a Master of Science. She currently is pursuing a second master's in computer and information sciences and engineering.